



CZECH TECHNICAL UNIVERSITY IN PRAGUE  
Faculty of Nuclear Sciences and Physical Engineering



# Scaling and estimating for GIG-distributed data

## Škálování a odhadování pro GIG-distribuovaná data

Master's Thesis

Author: **Bc. Anežka Lhotáková**  
Supervisor: **Doc. Mgr. Milan Krbálek, Ph.D.**  
Academic year: 2022/2023

## ZADÁNÍ DIPLOMOVÉ PRÁCE

Student: Bc. Anežka Lhotáková  
Studijní program: Aplikované matematicko-stochastické metody  
Název práce (česky): Škálování a odhadování pro GIG-distribuovaná data  
Název práce (anglicky): Scaling and estimating for GIG-distributed data

### Pokyny pro vypracování:

- 1) Studujte obecné teoretické vlastnosti balančních částicových systémů s repulzivním generátorem.
- 2) Úplně a kompaktně vyřešte škálovací úlohu pro GIG rozdělení splňující podmínku škálovatelnosti.
- 3) Reformulujte a řešte škálovací úlohu pro případ, kdy parametry nesplňují standardní podmínku škálovatelnosti.
- 4) Navrhněte a testujte stabilizační proceduru pro odhadování parametrů GIG-distribuovaných dat.
- 5) Zkoumejte vliv kontaminace dat na účinnost klasických a asistovaných odhadovacích metod.

Doporučená literatura:

- 1) B. Jorgensen, Statistical Properties of the Generalized Inverse Gaussian Distribution, Lecture Notes in Statistics 9, New York: Springer-Verlag, 1982.
- 2) M. Krbálek, F. Šeba, M. Krbálková, Super-random states in vehicular traffic — Detection & explanation, Physica A 585, 2022, 126418.
- 3) A. Lhotáková, M. Krbálek, Scaling of the Generalized Inverse Gaussian distribution, Proceedings of SPMS 2020/2021, Chlum u Třeboně 2020, Malá Skála 2021, 2021
- 4) B. Efron, Bootstrap Methods: Another Look at the Jackknife, The Annals of Statistics 7 (1), 1979, 1-26.
- 5) O. Kollert, M. Krbálek, T. Hobza, M. Krbálková, Statistical rigidity of vehicular streams—theory versus reality, Journal of Physics Communications 3, 2019, 035020.

Jméno a pracoviště vedoucího diplomové práce:

Doc. Mgr. Milan Krbálek, Ph.D.

Katedra matematiky, Fakulta jaderná a fyzikálně inženýrská, České vysoké učení technické v Praze, Trojanova 13, 120 00 Praha 2

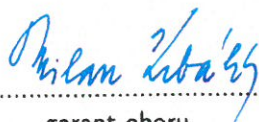
Jméno a pracoviště konzultanta:

Datum zadání diplomové práce: 28.2.2022


Datum odevzdání diplomové práce: 5.1.2023

Doba platnosti zadání je dva roky od data zadání.

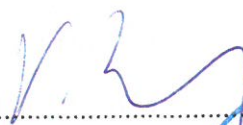
V Praze dne 28.02.2022



garant oboru



vedoucí katedry



děkan



*Acknowledgment:*

I would like to thank my supervisor Doc. Mgr. Milan Krbálek, Ph.D. for his willingness, professionalism, language proofreading, diligence, and also his positive attitude that kept me motivated. I would also like to thank my family and those closest to me for their moral support and interest.

*Author's declaration:*

I declare that this Master's Thesis is entirely my own work and I have listed all the used sources in the bibliography.

Prague, May 2, 2023

Anežka Lhotáková

A handwritten signature in black ink, appearing to be 'Anežka Lhotáková', written in a cursive style.

*Název práce:*

## **Škálování a odhadování pro GIG-distribuovaná data**

*Autor:* Bc. Anežka Lhotáková

*Program:* Aplikované matematicko-stochastické metody

*Druh práce:* Diplomová práce

*Vedoucí práce:* Doc. Mgr. Milan Krbálek, Ph.D., České vysoké učení technické v Praze, Fakulta jaderná a fyzikálně inženýrská, Katedra matematiky

*Abstrakt:* Tato práce se zabývá výzkumem vlastností Zobecněného inverzního Gaussova (GIG) rozdělení. V první části je představena teorie balančních částicových systémů, která ve spojení s teorií termodynamického dopravního plynu umožňuje definici balančních částicových systémů s repulzivním, resp. smíšeným generátorem. Práce dále představuje vlastnosti GIG distribuce a úzce se zaměřuje na problematiku jeho škálování. V závislosti na konfiguraci parametrů jsou představeny dvě možné varianty, jak lze ke škálování této distribuce přistupovat. Ve druhé části práce je na základě vlastností GIG rozdělení formulována stabilizační procedura pro bodové odhadovací metody parametrů a její vliv na chybu odhadovací metody je statisticky testován provedením experimentu, který je navrhnut podle tzv.  $2^k$ -faktoriál návrhu.

*Klíčová slova:* balanční částicový systém, balancovaná hustota, bodové odhady parametrů, modelování dopravy, stochastická kompresibilita, škálování, termodynamický dopravní plyn, Zobecněné inverzní Gaussovo rozdělení (GIG),  $2^k$ -faktoriál návrh

*Title:*

## **Scaling and estimating for GIG-distributed data**

*Author:* Bc. Anežka Lhotáková

*Abstract:* This thesis provides the research of properties of the Generalized Inverse Gaussian (GIG) distribution. In the first part, the theory of balanced particle systems is introduced, which, in conjunction with the theory of thermodynamic traffic gas, allows the definition of balanced particle systems with a repulsive or composite generator. This thesis also discusses the properties of the GIG distribution and closely focuses on the issue of its scaling. Depending on the configuration of the parameters, two possible approaches are presented for the task of this distribution's scaling. In the second part of the thesis, based on the properties of the GIG distribution, a stabilization procedure is formulated for point estimation methods of parameters. Its effect on the estimation method error is statistically tested by conducting an experiment designed according to the so-called  $2^k$  factorial design.

*Key words:* balanced density, balanced particle system, Generalized Inverse Gaussian distribution (GIG), parameter estimation, scaling, stochastic compressibility, thermodynamic traffic gas, traffic modeling,  $2^k$  factorial design

# Contents

<b>Introduction</b>	<b>7</b>
<b>1 Balanced particle system with repulsive generator</b>	<b>9</b>
1.1 Balanced densities . . . . .	9
1.2 Balanced particle system . . . . .	10
1.3 Thermodynamic traffic gas . . . . .	14
1.3.1 Interaction potentials and total energy of the system . . . . .	15
1.3.2 Distribution of clearances . . . . .	18
1.4 Balanced particle system with repulsive generator and its properties . . . . .	20
<b>2 Generalized Inverse Gaussian distribution</b>	<b>24</b>
2.1 Balanced properties . . . . .	25
2.2 General moments . . . . .	26
2.3 Relationships between parameters . . . . .	27
2.4 Scaling . . . . .	28
2.4.1 Scaling via the parameter $\lambda$ . . . . .	29
2.4.2 Scaling via the parameter $\beta$ . . . . .	35
2.4.3 Summary of scaling results . . . . .	39
2.5 Compressibility of systems generated by GIG distribution . . . . .	41
<b>3 Estimation of GIG-distributed data</b>	<b>42</b>
3.1 Methods for point estimation of parameters . . . . .	42
3.1.1 Method of Moments (MM) . . . . .	42
3.1.2 Minimum Distance Estimator (MDE) . . . . .	43
3.1.3 Maximum Likelihood Estimator (MLE) . . . . .	44
3.1.4 Proposal for improving estimation methods . . . . .	45
3.2 Testing of estimation methods . . . . .	46
3.2.1 Experiment design . . . . .	46
3.2.2 Evaluation of the experiment . . . . .	48
3.2.3 Summary of estimation methods testing . . . . .	60
<b>Conclusion</b>	<b>61</b>
<b>Appendix</b>	<b>63</b>

# Introduction

Compared to other scientific disciplines, traffic modeling is a relatively young field. When asked who invented the first automobile, the answers seem to vary depending on what the reader considers as a vehicle. One of the earliest historical records goes back to the second half of the 17th century, when Ferdinand Verbiest designed the first steam-powered carriage, which was, however, only a toy for the Kangxi Emperor. It would not fit a driver, and it is not even known if the design resulted in real construction. The fathers of the automobile industry are often considered Carl Benz and Gottlieb Daimler, who at the end of the 19th century introduced three- and four-wheeled cars powered by internal combustion engines. Since then, the automotive industry has developed dynamically and, thanks to its comfort and accessibility, has become part of our everyday lives. And just as the number of drivers has grown and transportation networks have expanded, so has evolved the field of traffic modeling, which describes driver's behavior and studies traffic flow characteristics.

As a significant tool in the theory of traffic modeling, the thermodynamic traffic gas is utilized to transfer information about the force interaction that helps capture the driver's behavior onto a mathematically formulated model. The mathematical perspective allows scalability of the problem in terms of generalization (such as transferring the model to the unit circle, unifying the weights of vehicles, transitioning from distances between car bumpers to distances between particles, etc.). If we further focus on the study of particle distribution in such a model, we obtain the Generalized Inverse Gaussian distribution (GIG), whose properties, particularly its scaling, are yet not fully explored.

In the practical part of the thesis, we aim to test classical parameter estimation methods for GIG-distributed data. As part of this testing, we propose a suggestion for possible improvement of the estimation in the form of assistance, which takes into account the discovered properties of the GIG distribution.

Before the beginning of the research, let us unite the notation. It is possible, that the definitions of the terms may slightly vary depending on the scientific field or literature, or might be unknown to the reader. Therefore, we consider it necessary to briefly summarize and unify the notation and definitions of the specific terms (see Table 1).

Notation	Description	Note
$\mathbb{R}$	set of real numbers	
$\mathbb{N}$	set of natural numbers	
$\text{Dom}(f)$	domain of the function $f$	Let $f(x) : X \rightarrow Y$ . Then $\text{Dom}(f) = \{x \in X : f(x) \in \mathbb{R}\}$ .
$\text{Ran}(f)$	range of the function $f$	Let $f(x) : X \rightarrow Y$ . Then $\text{Ran}(f) = f(\text{Dom}(f))$ .
$\mathcal{L}(\mathbb{S})$	class of integrable functions on the set $\mathbb{S}$	$f(x) \in \mathcal{L}(\mathbb{S}) \Leftrightarrow \int_{\mathbb{S}} f(x) dx$ exists and is finite
$\mathcal{C}^n(\mathbb{S})$	class of continuous functions of order $n$ on the set $\mathbb{S}$	$f(x) \in \mathcal{C}^n(\mathbb{S}) \Leftrightarrow \forall s \in \mathbb{S} : \lim_{x \rightarrow s} \frac{d^n f}{dx^n}(x) = \frac{d^n f}{dx^n}(s)$
$\mathcal{PC}(\mathbb{S})$	class of piecewise continuous functions on the set $\mathbb{S}$	The function $f(x)$ has finitely many points of discontinuity, is continuous from the left on the set $\mathbb{S}$ , and all discontinuities are finite jumps, i.e. $\lim_{x \rightarrow s_+} f(x) - \lim_{x \rightarrow s_-} f(x) \in \mathbb{R}$ .
$\text{supp}(f)$	support of the function $f$	Let $f : X \rightarrow \mathbb{R}$ . Then $\text{supp}(f) = \{x \in X : f(x) \neq 0\}$ .
$\mathcal{U}_\varepsilon^*(a)$	$\varepsilon$ -reduced neighborhood of the point $a$	Let $a \in \mathbb{R}, \varepsilon \in \mathbb{R}^+$ . Then $\mathcal{U}_\varepsilon^*(a) = \{x \in \mathbb{R} : 0 <  a - x  < \varepsilon\}$
$(f \star g)(x)$	convolution of the functions $f$ and $g$	$(f \star g)(x) = \int_{\mathbb{R}} f(y)g(x - y)dy$
$\Theta(x)$	Heaviside step function	$\Theta(x) = \begin{cases} 1 & \text{for } x > 0, \\ 0 & \text{for } x \leq 0. \end{cases}$
$\delta(x)$	Dirac function	Formal definition (see [6]): Let $\varphi(x)$ denote a test function. Then $(\delta, \varphi(x)) = \varphi(0)$ . Informal definition: $\delta(x) = \begin{cases} +\infty & \text{for } x = 0, \\ 0 & \text{otherwise.} \end{cases}$
$\Gamma(x)$	Gamma function	$\Gamma(x) = \int_0^{+\infty} y^{x-1} e^{-y} dy$
$\mu_n(f)$	$n$ -th general moment of the function $f$	Let $f : \mathbb{R} \rightarrow \mathbb{R}$ and $x^n f(x) \in \mathcal{L}(\mathbb{R})$ . Then $\mu_n(f) = \int_{\mathbb{R}} x^n f(x) dx$ .
$\text{E}[X]$	expected value of a random variable	Let $X$ be a random variable with distribution $f(x)$ and $x f(x) \in \mathcal{L}(\mathbb{R})$ . Then $\text{E}[X] = \int_{\mathbb{R}} x f(x) dx$ .
$\text{VAR}[X]$	variance of a random variable	Let $X$ be a random variable with distribution $f(x)$ and $x f(x), x^2 f(x) \in \mathcal{L}(\mathbb{R})$ . Then $\text{VAR}[X] = \text{E}[X^2] - \text{E}[X]^2$ .
$\mathcal{L}[f(x)](s)$	Laplace transform	$\mathcal{L}[f(x)](s) = \int_0^{+\infty} f(x) e^{-sx} dx$

Table 1: Overview of the notation used.



# Chapter 1

## Balanced particle system with repulsive generator

After introducing basic definitions and concepts, we can delve into the topics of this thesis. Modeling of traffic flow is closely related to the theory of thermodynamic traffic gas. The aim of this chapter is to familiarize the reader with the basic ideas of balance particle systems and their connection to the aforementioned thermodynamic traffic gas. Research conducted in this field demonstrates the suitability of linking these disciplines, and the culmination of this mutual complementation is the theory centered around the Generalized Inverse Gaussian distribution, which is the main subject of investigation in this master's thesis.

### 1.1 Balanced densities

In this section, we will introduce the concept of balanced densities, which will serve as a cornerstone in the construction of the theory associated with balancing particle systems. As will be shown, this particular class of densities proves itself to be very suitable for solving mathematical traffic modeling problems.

**Definition 1.1** (Balanced density). Balanced density is a function  $f(x) : \mathbb{R} \rightarrow \mathbb{R}$ , which fulfills following axioms:

1. completeness:  $\text{Dom}(f) = \mathbb{R}$
2. non-negativity:  $\text{Ran}(f) \subset \mathbb{R}_0^+$
3. integrability:  $f(x) \in \mathcal{L}(\mathbb{R})$
4. piecewise continuity:  $f(x) \in \mathcal{PC}(\mathbb{R})$
5. positive support:  $\text{supp}(f) \subset \mathbb{R}_0^+$
6. balancing tail: Such  $\varkappa \in \mathbb{R}$  exists, that

$$\alpha > \varkappa \Rightarrow \lim_{x \rightarrow +\infty} f(x)e^{\alpha x} = +\infty,$$

$$\alpha < \varkappa \Rightarrow \lim_{x \rightarrow +\infty} f(x)e^{\alpha x} = 0.$$

The number  $\varkappa$  defined by the last axiom of balancing tail is known as balancing index of a function  $f(x)$  and is denoted by  $\text{inb}(f)$ .

If the function  $f(x)$  satisfies the aforementioned definition, we declare it as a balanced density and denote it as  $f(x) \in \mathcal{B}$ . It should be noted that axioms 1-4 define a general density, and if we add the normalization requirement in the form of

$$\int_{\mathbb{R}} f(x) dx = 1,$$

we obtain a balanced probability density, or in the case of axioms 1-4, a probability density. Thanks to previous research [9] or [10], we already know that for specific choices of parameters, well-known densities such as Gamma, Exponential, and Erlang distributions are also balanced densities. The following table contains the formulas of these distributions in the form that satisfies the definition of balanced densities:

distribution name	$f(x)$	parametrization	$\text{inb}(f)$
Exponential	$\Theta(x)Ae^{-\lambda x}$	$A > 0, \lambda > 0$	$\lambda$
Erlang	$\Theta(x)Ax^n e^{-\lambda x}$	$A > 0, n \in \mathbb{N}, \lambda > 0$	$\lambda$
Gamma	$\Theta(x)Ax^\alpha e^{-\lambda x}$	$A > 0, \alpha \in \mathbb{R}, \lambda > 0$	$\lambda$
GIG	$\Theta(x)Ax^\alpha e^{-\lambda x} e^{-\frac{\beta}{x}}$	$A > 0, \alpha \in \mathbb{R}, \beta > 0, \lambda > 0$	$\lambda$
Superhyperbolic	$\Theta(x)Ax^\alpha e^{-\lambda x} e^{-\frac{\beta}{x^\varepsilon}}$	$A > 0, \alpha \in \mathbb{R}, \beta > 0, \lambda > 0, \varepsilon > 1$	$\lambda$

The penultimate mentioned density is the so-called Generalized Inverse Gaussian (GIG) distribution. We will pay special attention to this distribution because, as the goal of this work, we will find that it brings valuable insights into the study of traffic flow. All the mentioned distributions have the same balance index  $\text{inb}(f) = \lambda$ . The value of this index can be derived from the definition, or by using the so-called balance criterion, according to which the function  $f(x) : \mathbb{R} \rightarrow \mathbb{R}$  has a balanced tail if and only if

$$\varkappa = - \lim_{x \rightarrow +\infty} \frac{\ln(f(x))}{x} \in (0, +\infty).$$

This criterion represents a necessary and sufficient condition for satisfying the 6th balance axiom. One of the advantages of this class of densities is that every balanced density  $f(x) \in \mathcal{B}$  has all the general moments, i.e.,

$$\forall k \in \mathbb{N}_0 : \mu_k(f(x)) = \int_{\mathbb{R}} x^k f(x) dx \in \mathbb{R}.$$

The sequence of these general moments  $(\mu_k(f(x)))_{k=0}^{+\infty}$  is called the moment code of the density  $f(x)$ . If the balanced density  $f(x)$  is scaled, i.e.,  $\mu_0 = \mu_1 = 1$ , we denote this fact as  $f(x) \in \mathcal{B}_{11}$ . In other words, a random variable  $X$  with distribution  $f(x) \in \mathcal{B}_{11}$  has an expected value of  $\mathbb{E}[X] = 1$ .

## 1.2 Balanced particle system

Now that we have introduced the class of balanced densities, i.e., the class of functions that satisfy the axioms from Definition 1.1, we can move on to explaining the concept of balanced particle systems. In these systems, we work with three basic concepts: multi-headways  $\mathcal{X}$ , headways  $\mathcal{R}$ , and interval frequencies  $\mathcal{N}_L$ . To define them, let's consider a system of dimensionless particles allocated on a line, with a reference particle located at the origin. Then, by headways  $\mathcal{R}_0, \mathcal{R}_1, \dots$ , we mean the distances between neighboring particles, and by multi-headways  $\mathcal{X}_i$ , we mean the distance of the  $i$ -th particle from

the reference particle. We impose an additional requirement on the headways, namely that  $\mathcal{R}_0, \mathcal{R}_1, \dots$  are independent random variables with the same distribution  $h(x)$ , i.e.

$$\mathcal{R}_0, \mathcal{R}_1, \dots \sim h(x).$$

This property of random variables is commonly abbreviated as i.i.d., which stands for *independent identically distributed*. The distribution  $h(x)$  that characterizes the distribution of headways is called the generator of the particle system. For a better understanding of the concepts of multi-headways and headways, the reader can refer to Figure 1.1.

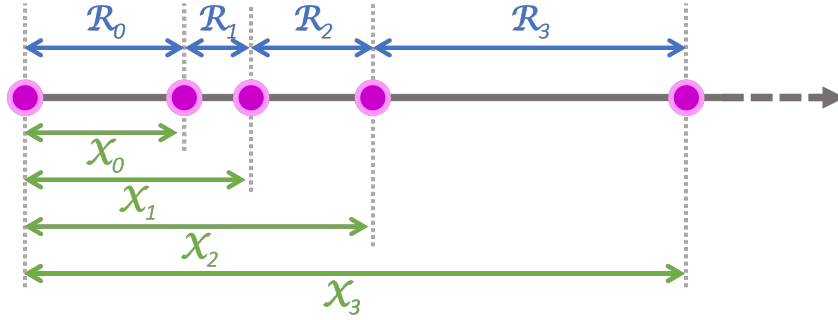


Figure 1.1: An example of the definition of headways  $\mathcal{R}_0, \mathcal{R}_1, \mathcal{R}_2, \mathcal{R}_3$  and multi-headways  $\mathcal{X}_0, \mathcal{X}_1, \mathcal{X}_2, \mathcal{X}_3$  on a line.

The headways  $\mathcal{R}_0, \mathcal{R}_1, \dots$  and multi-headways  $\mathcal{X}_k$  are random variables, and they are related by the following equation

$$\mathcal{X}_k = \sum_{j=0}^k \mathcal{R}_j.$$

Since the headways  $\mathcal{R}_0, \mathcal{R}_1, \dots$  are independent random variables with the same distribution  $h(x) \in \mathcal{B}$ , we know from the theorem on the probability density function of independent random variables (see [9]) that for the distribution  $f_{X+Y}$  of the sum of two independent variables  $X \sim f_X(x)$  and  $Y \sim f_Y(y)$ , the following equation holds

$$f_{X+Y}(z) = (f_X \star f_Y)(z) = \int_{\mathbb{R}} f_X(x) f_Y(z-x) dx, \quad (1.1)$$

and therefore, for the distribution of the multi-headways  $\mathcal{X}_k$ , we have

$$\mathcal{X}_k = \sum_{j=0}^k \mathcal{R}_j = \mathcal{R}_0 + \mathcal{R}_1 + \dots + \mathcal{R}_k \stackrel{(1.1)}{\sim} (h \star h \star \dots \star h)(z) := \star_{j=0}^k h(x).$$

From the knowledge of the sequence of random variables  $\mathcal{R}_0, \mathcal{R}_1, \dots$  and their generator  $h(x)$ , we can now introduce the definition of a balanced particle system.

**Definition 1.2.** A balanced particle system is defined as a sequence of multi-headways  $(\mathcal{X}_k)_{k=0}^{+\infty}$  denoted by the formula  $\mathcal{X}_k = \sum_{j=0}^k \mathcal{R}_j$ , satisfying the following axioms:

1. Independence axiom: The sequence  $(\mathcal{R}_j)_{j=0}^{+\infty}$  is a sequence of non-negative, absolutely continuous, identically distributed, and independent random variables.

2. **Balanced generator axiom:** The probability density function  $h(x)$  of the random variable  $\mathcal{R}_0$  (referred to as the generator of the balanced particle system) belongs to the class of balanced densities, i.e.,  $h(x) \in \mathcal{B}$ .

Moreover, if the generator  $h(x) \in \mathcal{B}_{11}$ , i.e., if  $\mathbf{E}[\mathcal{R}_0] = \mathbf{E}[\mathcal{R}_1] = \dots = 1$ , then this balanced particle system is referred to as scaled.

A slightly different perspective can be used to describe the particle system on the line using discrete random variables called interval frequencies  $\mathcal{N}_L$ , which quantify the number of particles occurring in the interval  $(0, L)$  of length  $L \in \mathbb{R}^+$  with respect to a reference particle. The description of these particles is based on probabilities  $\mathbf{P}[\mathcal{N}_L = k]$ , i.e., the probabilities that exactly  $k$  particles occur in the interval  $(0, L)$ . If these probabilities are known for all  $k \in \mathbb{N}_0$ , then it constitutes a complete statistical description, and it is evident that

$$\sum_{k=0}^{+\infty} \mathbf{P}[\mathcal{N}_L = k] = 1.$$

One can establish connections between interval frequencies, as defined above, and the previous concepts of headways and multi-headways. For example, the probability  $\mathbf{P}[\mathcal{N}_L = 0]$ , which represents the probability that there are no particles in the interval of length  $L$ , can be computed using the knowledge of the headways generator  $\mathcal{R}_0 \sim h(x)$  as follows

$$\mathbf{P}[\mathcal{N}_L = 0] = \mathbf{P}[\mathcal{R}_0 \geq L] = 1 - \mathbf{P}[\mathcal{R}_0 < L] = 1 - \int_{-\infty}^L h(z) dz. \quad (1.2)$$

Analogously, one can derive the probability  $\mathbf{P}[\mathcal{N}_L = k]$  using the multi-headways generator

$$\mathcal{X}_k \sim \star_{j=0}^k h(x) := g_k(x),$$

as follows

$$\begin{aligned} \mathbf{P}[\mathcal{N}_L = k] &= \mathbf{P}[\mathcal{X}_{k-1} < L \wedge \mathcal{X}_k \geq L] = \mathbf{P}[(\mathcal{X}_{k-1} < L) \cap (\mathcal{X}_k < L)^c] = \\ &= \mathbf{P}[(\mathcal{X}_{k-1} < L) \setminus (\mathcal{X}_k < L)] = \mathbf{P}[\mathcal{X}_{k-1} < L] - \mathbf{P}[\mathcal{X}_k < L] = \\ &= \int_{-\infty}^L g_{k-1}(z) dz - \int_{-\infty}^L g_k(z) dz \end{aligned} \quad (1.3)$$

If we want to determine the generator based on interval frequencies, we can obtain similar equations for the headways generator  $h(x)$  from equations (1.2) and (1.3)

$$h(x) \stackrel{(1.2)}{=} -\Theta(x) \frac{d}{dx} \mathbf{P}[\mathcal{N}_x = 0]$$

and for the multi-headways generator  $g_k(x) = \star_{j=0}^k h(x)$

$$g_k(x) \stackrel{(1.3)}{=} -\Theta(x) \sum_{j=0}^k \frac{d}{dx} \mathbf{P}[\mathcal{N}_x = j].$$

Let's mention two basic particle systems that will help the reader connect the established concepts. The first system to be introduced is the Dirac particle system characterized by equidistantly arranged particles, where the headways satisfy  $\mathcal{R}_0 = \mathcal{R}_1 = \dots = \ell$ , where  $\ell > 0$  is an optional parameter representing the distance between particles. As derived in [9], for this system, the headways, multi-headways, and interval frequencies are determined as follows

- $\mathcal{R}_i \sim \delta(x - \ell)$ ,  $i = 0, 1, 2, \dots$ ,
- $\mathcal{X}_k \sim \delta(x - \ell(k + 1))$ ,
- $P[\mathcal{N}_L = k] = \Theta(L - k\ell)(1 - \Theta(L - \ell(k + 1)))$ .

The second basic system is the Poisson particle system, whose interval frequencies are characterized by a Poisson distribution with parameter  $\lambda > 0$ . For more detailed calculations, we again encourage the reader to refer to [9], from which we know that this system is characterized as follows

- $\mathcal{R}_i \sim \Theta(x)\lambda e^{-\lambda x}$ ,  $i = 0, 1, 2, \dots$ ,
- $\mathcal{X}_k \sim \Theta(x)\frac{\lambda^{k+1}}{k!}x^k e^{-\lambda x}$ ,
- $P[\mathcal{N}_L = k] = \frac{(\lambda L)^k}{k!}e^{-\lambda L}$ .

The balance particle system can also be described through other related characteristics such as

- expected value of headways  $E[\mathcal{R}_i] = \int_{\mathbb{R}} xh(x)dx$ ,
- expected value of multi-headways  $E[\mathcal{X}_k] = \int_{\mathbb{R}} xg_k(x)dx$ ,
- trend function  $\omega(L) = E[\mathcal{N}_L] = \sum_{k=0}^{+\infty} kP[\mathcal{N}_L = k]$ ,
- cluster function  $r(x) = \sum_{k=0}^{+\infty} g_k(x)$ ,

which are referred to as first-order characteristics, or alternatively through

- variance of headways  $\text{VAR}[\mathcal{R}_i] = E[\mathcal{R}_i - E[\mathcal{R}_i]]^2 = E[\mathcal{R}_i^2] - E[\mathcal{R}_i]^2$ ,
- variance of multi-headways  $\text{VAR}[\mathcal{X}_k] = E[\mathcal{X}_k - E[\mathcal{X}_k]]^2 = E[\mathcal{X}_k^2] - E[\mathcal{X}_k]^2$ ,
- second moment of interval frequency  $E[\mathcal{N}_L^2] = \sum_{k=0}^{+\infty} k^2P[\mathcal{N}_L = k]$ ,
- variance of frequencies  $\square(L) = E[\mathcal{N}_L - E[\mathcal{N}_L]]^2 = E[\mathcal{N}_L - \omega(L)]^2$ ,
- stochastic rigidity  $\Delta(L) = E[\mathcal{N}_L - L]^2 = E[\mathcal{N}_L^2] - 2LE[\mathcal{N}_L] + L^2$ ,

collectively referred to as second-order characteristics. Let's focus on the newly introduced concept of stochastic rigidity. Although stochastic rigidity is very similar to frequency variance, the advantage of its definition is that it does not require the knowledge of the expected value of particles in an interval of a given length. At the same time, for systems where  $E[\mathcal{N}_L] = L$ , the concepts of stochastic rigidity and frequency variance are clearly equivalent.

Deriving the form of stochastic rigidity for the aforementioned Dirac and Poisson particle systems is not complicated. Let's consider both of these particle systems in their scaled forms. In the case of the Dirac system, the situation is straightforward. Since it is an equidistant arrangement of particles, the number of particles in an interval of length  $L$  is always the same, hence the variance is zero, and thus for stochastic rigidity we have

$$\Delta_D(L) = 0.$$

In the case of the scaled Poisson particle system, it is no longer sufficient to rely solely on discussion, but based on a calculation, which can be found at the end of the thesis in the Appendix, one can arrive at the result

$$\Delta_P(L) \stackrel{(3.7)}{=} L.$$

The advantage of balanced particle systems is that it is always possible to find the exact value of stochastic rigidity, although it can still be a computationally demanding task with complicated results. A way to deal with this difficulty was introduced in the [14]. In this work, it was shown that in a balanced particle system, stochastic rigidity quickly approaches a linear asymptote and can be approximated by the equation

$$\Delta(L) \approx \chi L + \delta,$$

where  $\chi$  is a parameter called stochastic compressibility and  $\delta$  is a parameter referred to as deflection. In addition to the approximation of stochastic rigidity, the [14] also establishes a relationship between compressibility  $\chi$  and the moments of the headways generator  $h(x)$

$$\chi = \mu_2(h(x)) - \mu_1^2(h(x)) = \mathbb{E}[\mathcal{R}_i^2] - \mathbb{E}[\mathcal{R}_i]^2 = \text{VAR}[\mathcal{R}_i]. \quad (1.4)$$

In other words, in a balanced particle system with the generator  $h(x)$ , stochastic compressibility is equal to the variance of neighboring headways. Based on the value of stochastic compressibility, we define three categories<sup>1</sup> for balanced particle systems in the following definition:

**Definition 1.3.** A scaled balanced particle system with compressibility  $\chi$  is called

- sub-compressible if  $\chi < 1$ ,
- uni-compressible if  $\chi = 1$ ,
- super-compressible if  $\chi > 1$ .

Returning to the previously discussed Dirac and Poisson particle systems, the compressibility of the Dirac system is  $\chi_D = 0$ , thus it is a sub-compressible particle system, while the Poisson particle system with  $\chi_P = 1$  represents an uni-compressible system.

### 1.3 Thermodynamic traffic gas

Let us now deviate from the theory of balance systems and simultaneously acquaint ourselves with the thermodynamic traffic gas. In this thesis, we consider the simplified version of traffic flow, in which we simulate one-way flow on a single-lane road without intersections, entrances, or exits using a particle gas with  $N \in \mathbb{N}$  particles distributed on a one-dimensional curve in 2D space. It is a system with a fixed number of particles  $N \in \mathbb{N}_0$ , which are ordered by position and cannot change their order. For each  $i$ -th particle,  $i = 1, \dots, N$ , we can track its position  $x_i$  and instantaneous velocity  $v_i$ . If we impose periodic conditions for the input and output of particles from the observed interval of length  $L$  in the form of

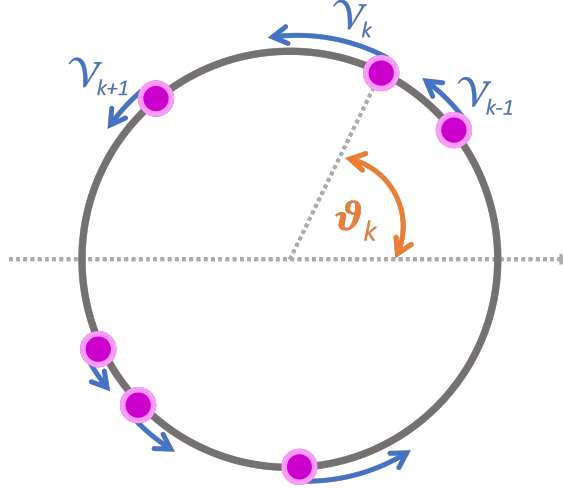
$$x_{k+N}(\tau) = x_k(\tau) + L, \quad v_{k+N}(\tau) = v_k(\tau), \quad k = 1, \dots, N,$$

then we obtain a system on a line with periodic boundary conditions, and there is nothing preventing us from transitioning to a circle of length  $L$ . The particles can then be described by their angular components  $\vartheta_1, \dots, \vartheta_N$ , where  $\vartheta_{k+N}(\tau) = \vartheta_k(\tau) + 2\pi$ . In such a system (see Figure 1.2), we define the distance between the  $k$ -th and  $i$ -th particles as

$$r_{ik} = \frac{L}{2\pi} \arccos(\cos(\vartheta_i - \vartheta_k)).$$

With this, the basic framework of the thermodynamic traffic gas model was introduced. Now we can proceed to the exploration of its properties that describe the behavior of its particles.

<sup>1</sup>In older literature, particle systems were classified based on stochastic rigidity as sub-poissonian, poissonian, and super-poissonian. However, due to the irregular behavior that stochastic rigidity can exhibit at the origin of the coordinate system, this classification was not very suitable, and the classification through the Definition 1.3, as presented above, is being gradually adopted.

Figure 1.2: Particle gas on a circle of length  $L$ .

### 1.3.1 Interaction potentials and total energy of the system

One of the differences of the field of traffic modeling compared to classical scientific fields is the significant influence of socio-dynamic interactions. It is not surprising that the driver's brain plays a significant role in traffic flow modeling. This factor can be introduced into the system through a force that depends on the distance between vehicles, with the force weakening as the distance increases. Conversely, when the distance between vehicles decreases, this force should have a strong repulsive nature, reflecting the behavior of a driver preventing collisions. We are interested in forces  $F(r) : \mathbb{R} \rightarrow \mathbb{R}$  that characterize

- behavior preventing collision and overtaking:  $\lim_{r \rightarrow 0_+} F(r) = +\infty$ ,
- weakening or disappearance of interaction for large distances:  $\lim_{r \rightarrow +\infty} F(r) = 0$ ,
- smoothness of traffic:  $F(r) \in \mathcal{C}^1(\mathbb{R}^+)$ .

These conditions correspond, for example, to the class of forces

$$F(r) = \frac{1}{r^\gamma}, \quad \gamma \in (0, +\infty). \quad (1.5)$$

However, we are usually accustomed to working with the corresponding potential instead of the force, which is related to the force by the relationship  $\vec{F} = -\text{grad}\varphi(r)$ , i.e., in our one-dimensional case

$$F(r) = -\frac{d\varphi}{dr} \Leftrightarrow \varphi(r) = -\int_0^r F(t)dt + \text{const.} \stackrel{(1.5)}{=} -\int_0^r \frac{1}{t^\gamma} dt + \text{const.} \quad (1.6)$$

Depending on the value of parameter  $\gamma$ , we obtain a set of potentials as solutions to (1.6), which are listed in Table 1.1.

$\varphi(r)$	$\gamma$	name of the potential
$\frac{1}{\gamma-1}r^{1-\gamma}$	(0, 1)	power potential
$-\ln(r)$	1	logarithmic potential
$\frac{1}{\gamma-1}r^{1-\gamma}$	(1, 2)	sub-hyperbolic potential
$\frac{1}{\gamma-1}r^{1-\gamma}$	2	hyperbolic potential
$\frac{1}{\gamma-1}r^{1-\gamma}$	$> 2$	super-hyperbolic potential

Table 1.1: Table of potentials given by the class of forces (1.5).

In the context of interactions, it is also desirable to describe their range. If we again compare particles to drivers, a driver can be influenced by vehicles immediately in front of and behind him, as well as drivers in front of their neighbor. Let  $\mathbb{I}_k$  denote the set of indices of particles with which the  $k$ -th particle interacts. Depending on the cardinality of this set, we classify the ranges of potentials into the following four categories:

- long-ranged:  $\mathbb{I}_k = \{1, 2, \dots, N\} \setminus \{k\}$ ,
- short-ranged:  $\mathbb{I}_k = \{k-1, k+1\}$ ,
- local-ranged:  $\mathbb{I}_k = \{i = 1, 2, \dots, N : x_i \in \mathcal{U}_\varepsilon^*(x_k)\}$ ,
- medium-ranged:  $\mathbb{I}_k = \{k-m, k+m : m \in \hat{s}\}$ , where  $s \in \mathbb{N} \wedge 1 < s \ll N$ .

The potential associated with the  $k$ -th particle is given by the equation  $\varphi_k(r) = \sum_{i \in \mathbb{I}_k} \varphi_{ki}(r)$ , where  $\varphi_{ki}(r)$  is the two-body potential describing the interaction between the  $i$ -th and  $k$ -th particles. Based on the knowledge of the potential, we can proceed with the calculation of the Hamiltonian for the entire system of particles. Let  $\vec{v} = (v_1, \dots, v_N)$  be the vector of instantaneous velocities and

$$\mathbb{R} = \begin{bmatrix} r_{11} & r_{12} & \dots & r_{1N} \\ r_{21} & r_{22} & \dots & r_{2N} \\ \vdots & \vdots & \ddots & \vdots \\ r_{N1} & r_{N2} & \dots & r_{NN} \end{bmatrix} = \begin{bmatrix} 0 & r_{12} & \dots & r_{1N} \\ r_{21} & 0 & \dots & r_{2N} \\ \vdots & \vdots & \ddots & \vdots \\ r_{N1} & r_{N2} & \dots & 0 \end{bmatrix}$$

as the symmetric real matrix of distances between all particles in the system. The total potential energy of the  $N$ -particle ensemble is given by

$$\mathbb{U}(\mathbb{R}) = \sum_{k=1}^N \varphi_k = \sum_{k=1}^N \sum_{i \in \mathbb{I}_k} \varphi_{ki}(r_{ik}).$$

If we restrict ourselves to homogeneous systems, i.e., systems in which particles have the same mass  $m$ , same interaction rules (potential  $\varphi$ ) and the same optimal velocity  $w$ , then  $\varphi_{ki}(r) = \varphi(r)$  and the potential energy  $\mathbb{U}$  takes the form

$$\mathbb{U}(\mathbb{R}) = \sum_{k=1}^N \sum_{i \in \mathbb{I}_k} \varphi(r_{ik}).$$

We can calculate the kinetic energy for a homogeneous system similarly, without loss of generality, let's set  $m = 1$ . Then the kinetic energy is given by

$$\mathbb{T}(\vec{v}) = \sum_{k=1}^N \frac{1}{2} (v_k - w)^2$$



and the total Hamiltonian of the system is therefore

$$\mathbf{H} = \mathbf{H}(\vec{v}, \mathbb{R}) = \mathbf{T}(\vec{v}) + \mathbf{U}(\mathbb{R}) = \sum_{k=1}^N \frac{1}{2}(v_k - w)^2 + \sum_{k=1}^N \sum_{i \in \mathbb{I}_k} \varphi(r_{ik}).$$

Let's denote  $r_k = r_{k,k-1}$  for simplicity, then specifically for short-ranged gas, the Hamiltonian of the system is given by

$$\mathbf{H}(\vec{v}, \vec{r}) = \sum_{k=1}^N \frac{1}{2}(v_k - w)^2 + \sum_{k=1}^N \varphi(r_k), \quad (1.7)$$

or for the circular variant

$$\mathbf{H}(\vec{v}, \vec{\vartheta}) = \sum_{k=1}^N \frac{1}{2}(v_k - w)^2 + \sum_{k=1}^N \varphi(\vartheta_k - \vartheta_{k-1}).$$

The stationary state of this deterministic system, i.e., the state where the total energy of the system stabilizes at a constant value and does not change further in time, occurs in this deterministic variant when all vehicles have a velocity equal to  $w$  and are equidistantly arranged

$$v_1 = \dots = v_N = w \quad \wedge \quad r_1 = \dots = r_N = \frac{L}{N}.$$

In the language of probability, this state can be expressed using Dirac's function

$$\forall k \in \mathbb{N} : \mathcal{V}_k \sim \delta(v_k - w) \quad \wedge \quad \forall k \in \mathbb{N} : \mathcal{R}_k \sim \delta\left(r_k - \frac{L}{N}\right).$$

However, for our purposes, it will be inevitable to consider a stochastic version of the system instead of the deterministic one. In the stochastic approach, it is not possible to determine the speed or position of a particle deterministically at a given time  $t$ . Instead, we are provided with a probability of the variable's value. The system will then be described by the joint probability density

$$\mathbf{P}(\vec{v}, \vec{r}) = \mathbf{P}(v_1(t), \dots, v_N(t), r_1(t), \dots, r_N(t))$$

and its stationary state is given by the equation

$$\frac{\partial \mathbf{P}}{\partial t}(\vec{v}, \vec{r}) = 0.$$

The transition between the deterministic and stochastic versions can be performed using standard procedures of physics, where the aforementioned thermodynamic system is placed into a so-called thermal reservoir with a thermodynamic temperature  $T$ . This reservoir interacts with the system of particles in such a way that its randomly moving micro-particles disrupt the original deterministic arrangement of the gas. For the purposes of traffic modeling, we do not directly observe the temperature of the reservoir  $T$ , but rather the stochastic resistivity of the system given by

$$\beta_T = \frac{1}{\mathbf{k}_B T}, \quad (1.8)$$

which can be understood as a measure of the system's resistance to the influence of the thermal reservoir. The constant  $\mathbf{k}_B$ , in this case, denotes the Boltzmann constant. Based on the value of the stochastic resistivity (1.8), we classify the states of the particle gas into three categories:

$\beta_T = 0$ : states with the maximum degree of fluctuation of individual quantities,

$\beta_T > 0$ : states with a reduced degree of fluctuation of individual quantities,

$\beta_T \rightarrow +\infty$ : deterministic states, where the degree of fluctuation is zero.

In traffic theory, the concept of stochastic resistivity is synonymous with the mental strain of drivers. This reflects the fact that the driver is required to evaluate an extensive range of data about the current state of their surroundings during driving and based on this data, decide on the movement of his/her vehicle.

Let's now return to the determination of the joint probability density in our system with the Hamiltonian (1.7) and the value of the thermodynamic temperature of the reservoir  $T$ . From the theory of thermodynamic gases, we know that the joint probability density is generally given by the formula

$$P(\vec{v}, \vec{r}) = \frac{1}{Z_N} e^{-\frac{H(\vec{v}, \vec{r})}{k_B T}},$$

where  $Z_N$  is the so-called partition sum calculated via the normalization condition

$$\int_{\mathbb{R}^{2N}} P(\vec{v}, \vec{r}) d(\vec{v}, \vec{r}) = 1.$$

If we focus on a short-range particle gas with  $N$  particles on a circular ring of length  $L$ , this joint probability density takes the form

$$P(\vec{v}, \vec{r}) = \Theta(\vec{r}) \frac{1}{Z_N(L)} e^{-\frac{H(\vec{v}, \vec{r})}{k_B T}} \delta\left(L - \sum_{k=1}^N r_k\right).$$

Substituting the found form of the Hamiltonian (1.7) for the short-ranged potential and denoting  $\beta_T = \frac{1}{k_B T}$ , we obtain the expression for the joint probability density of the short-ranged thermodynamic particle gas as

$$P(\vec{v}, \vec{r}) = \Theta(\vec{r}) \frac{1}{Z_N(L)} e^{-\frac{\beta_T}{2} \sum_{k=1}^N (v_k - \omega)^2} e^{-\beta_T \sum_{k=1}^N \varphi(r_k)} \delta\left(L - \sum_{k=1}^N r_k\right). \quad (1.9)$$

### 1.3.2 Distribution of clearances

We have now derived the joint probability density (1.9) for the instantaneous velocities  $\vec{v}$  of vehicles and distance between two vehicles  $\vec{r}$  in a system with a short-range general potential. At this point, the reader may observe certain parallels in the concepts that have been introduced in the section about balanced particle systems. Let us now focus on the study of how vehicles are distributed on the road, i.e., the individual distances  $\vec{r}$  between vehicles, which are referred to as clearances in traffic theory and as headways in balanced particle systems. It should be noted that, for further analysis, it is more convenient for us to study gaps between vehicles rather than their positions, as it makes it easier to interpret the influence of interaction forces or, for example, the aforementioned mental strain.

Our goal is to determine the statistical distribution of clearances in the stationary state. We consider clearances  $\mathcal{R}_1, \mathcal{R}_2, \dots, \mathcal{R}_N$  and seek their distribution  $\mathcal{R}_1 \sim g(r_1), \mathcal{R}_2 \sim g(r_2), \dots, \mathcal{R}_N \sim g(r_N)$ , where without loss of generality, it is sufficient to investigate only the distribution  $\mathcal{R}_1 \sim g(r_1)$ , as homogeneity

implies  $g(r_1) = g(r_2) = \dots = g(r_N)$ . From probability theory, it is known that by integrating expression (1.9) over all velocities  $v_1, \dots, v_N$ , we obtain the joint probability density for clearances as

$$P(\vec{r}) = \Theta(\vec{r}) \frac{1}{Z_N(L)} e^{-\beta_T \sum_{k=1}^N \varphi(r_k)} \delta\left(L - \sum_{k=1}^N r_k\right).$$

Let's calculate the value of the partition sum  $Z_N(L)$ , which represents the normalization factor, such that

$$\int_{\mathbb{R}^N} P(\vec{r}) d\vec{r} \stackrel{!}{=} 1.$$

Hence,

$$Z_N(L) = \int_{\mathbb{R}^N} \Theta(\vec{r}) e^{-\beta_T \sum_{k=1}^N \varphi(r_k)} \delta\left(L - \sum_{k=1}^N r_k\right) d(r_1, \dots, r_N). \quad (1.10)$$

We will proceed with this form for now. For the distribution  $g(r_1)$  of the variable  $\mathcal{R}_1$ , we have

$$\begin{aligned} g(r_1) &= \int_{\mathbb{R}^{N-1}} P(\vec{r}) d(r_2, r_3, \dots, r_N) = \\ &= \Theta(r_1) \frac{e^{\beta_T \varphi(r_1)}}{Z_N(L)} \underbrace{\int_{\mathbb{R}^{N-1}} \Theta(r_2, r_3, \dots, r_N) e^{-\beta_T \sum_{k=2}^N \varphi(r_k)} \delta\left(L - r_1 - \sum_{k=2}^N r_k\right) d(r_2, r_3, \dots, r_N)}_{\boxtimes}. \end{aligned}$$

If we take a closer look at the integral denoted by the symbol  $\boxtimes$ , which remains after rearranging the expression, we find that it is nothing else but a partition sum  $Z_{N-1}(L - r_1)$  of a system of  $N - 1$  particles distributed on a segment of length  $L - r_1$ . The distribution of the variable  $\mathcal{R}_1$  is therefore given by

$$g(r_1) = \Theta(r_1) \frac{Z_{N-1}(L - r_1)}{Z_N(L)} e^{-\beta_T \varphi(r_1)}.$$

Without loss of generality, we can then write

$$g(r) = \Theta(r) \frac{Z_{N-1}(L - r)}{Z_N(L)} e^{-\beta_T \varphi(r)}. \quad (1.11)$$

As shown in [9] or in the Appendix, the value of the partition sum  $Z_N(L)$  for such a system can be approximated by

$$Z_N(L) \stackrel{(3.15)}{\doteq} C \frac{F^N(\lambda) e^{\lambda L}}{\sqrt{N}}, \quad (1.12)$$

where  $C$  represents a general constant, independent of  $N$  and  $L$ ,  $\lambda$  is a stationary point to the equation (3.11), and  $F(s)$  denotes the Laplace transform of the function  $\Theta(r) e^{-\beta_T \varphi(r)}$ ,

$$F(s) = \mathcal{L}[\Theta(r) e^{-\beta_T \varphi(r)}](s).$$

Substituting the approximate value of the partition sum (1.12) into the derived density (1.11), we obtain the probability density

$$g(r|N) = \Theta(r) \frac{\sqrt{N}}{\sqrt{N-1}} F^{-1}(\lambda) e^{-\beta_T \varphi(r)} e^{-\lambda r}.$$

By taking the limit as the number of particles  $N$  goes to infinity, we arrive at the approximate relationship

$$g(r) = \lim_{N \rightarrow +\infty} g(r|N) = \Theta(r)F^{-1}(\lambda)e^{-\beta_T\varphi(r)}e^{-\lambda r}. \quad (1.13)$$

By applying a series of thoughts for the stationary point mentioned in [9] and Appendix, we then come to a conclusion that finding the value of  $F(\lambda)$  is the task of normalizing the density  $g(r)$ , and we can interpret it as the normalization constant  $A$  of the probability density

$$g(r) = \Theta(r)Ae^{-\beta_T\varphi(r)}e^{-\lambda r}, \quad (1.14)$$

where  $A \int_0^{+\infty} e^{-\beta_T\varphi(r)}e^{-\lambda r} dr = 1$ .

## 1.4 Balanced particle system with repulsive generator and its properties

Up to this point, we have devoted a substantial part of the text to explaining the desirable concepts to readers not familiar with traffic modeling theory, so that we can now meaningfully introduce the concept of balancing systems with a repulsive short-ranged potential.

In the previous section, we derived the form of the vehicle gap (clearance) distribution, which is given by equation (1.14), where  $\varphi(x)$  is a general potential. Let us now choose  $\varphi(x)$  in the form

$$\varphi(x) = \rho\psi(x) - \varkappa \ln x, \quad (1.15)$$

where  $\rho$  and  $\varkappa$  are parameters, and  $\psi(x)$  is a repulsive potential, such that its derivative  $G(x) = -\frac{d\psi(x)}{dx}$  satisfies conditions corresponding to driver behavior:

$$\lim_{x \rightarrow 0_+} G(x) = +\infty,$$

$$\lim_{x \rightarrow +\infty} G(x) = 0,$$

$$G(x) \in \mathcal{C}^1(\mathbb{R}^+).$$

Now, let's consider the following two situations depending on the values of parameters:

1.  $\rho > 0, \varkappa \geq 0$ ,
2.  $\rho > 0, \varkappa < 0$ .

We will now consider the first variant, where both parameters  $\rho$  and  $\varkappa$  are positive. It is easy to show the following facts for the potential  $\varphi(x)$  in the form of (1.15) and its corresponding force  $F(x) = -\frac{d\varphi(x)}{dx}$ :

$$\lim_{x \rightarrow 0_+} F(x) = \lim_{x \rightarrow 0_+} \rho \left( -\frac{d\psi(x)}{dx} \right) + \frac{\varkappa}{x} = \lim_{x \rightarrow 0_+} \rho G(x) + \frac{\varkappa}{x} = +\infty,$$

$$\lim_{x \rightarrow +\infty} F(x) = \lim_{x \rightarrow +\infty} \rho \left( -\frac{d\psi(x)}{dx} \right) + \frac{\varkappa}{x} = \lim_{x \rightarrow +\infty} \rho G(x) + \frac{\varkappa}{x} = 0,$$

$$G(x) \in \mathcal{C}^1(\mathbb{R}^+) \Rightarrow F(x) \in \mathcal{C}^1(\mathbb{R}^+).$$

Thus, with this choice of potential (1.15) with positive parameters  $\rho$  and  $\varkappa$ , we also obtain a repulsive potential. Substituting this into the derived distribution of gaps (1.14), we obtain the density

$$g(r) = \Theta(r)Ax^{\beta_T\varkappa}e^{-\beta_T\rho\psi(r)}e^{-\lambda r}.$$

Let's rename the parameters for clarity as  $\alpha := \kappa\beta_T$  and  $\beta := \rho\beta_T$ . We obtain the distribution in the following form:

$$g(r) = \Theta(r)Ax^\alpha e^{-\beta\psi(r)}e^{-\lambda r}, \quad (1.16)$$

which will be the starting point for our further considerations. The parameters  $\alpha \geq 0, \beta > 0, \lambda > 0$  of the distribution (1.16) are referred to as the *tension*, *intensity*, and *concentration*, respectively. Based on the calculations just performed, we can introduce the concept of a balanced repulsive particle system.

**Definition 1.4.** A balanced particle system with a repulsive generator is defined as a particle system whose generator is the function

$$g(x) = \Theta(x)Ax^\alpha e^{-\beta\psi(x)}e^{-\lambda x}, \quad (1.17)$$

where  $\alpha \geq 0, \beta > 0, \lambda > 0, A^{-1} = \int_0^{+\infty} x^\alpha e^{-\beta\psi(x)}e^{-\lambda x} dx$  is the normalization factor, and the potential  $\psi(x)$  satisfies the following conditions:

1.  $\psi(x) \in \mathcal{C}^1(0, +\infty)$ ,
2.  $\frac{d\psi(x)}{dx} < 0$  on the interval  $(0, +\infty)$ ,
3.  $\lim_{x \rightarrow +\infty} \psi(x) = 0$ ,
4.  $\lim_{x \rightarrow 0^+} \frac{d\psi(x)}{dx} = -\infty$ ,
5.  $\lim_{x \rightarrow +\infty} \frac{d\psi(x)}{dx} = 0$ .

As has already been verified in [13], the function (1.17) with the conditions imposed on the potential  $\psi(x)$  satisfies the axioms stated in Definition 1.1, i.e.,  $g(x) \in \mathcal{B}$ . The fact that it is a balanced particle system can also be verified through the balanced criterion, by computing the balanced index of the given generator  $g(x)$

$$\kappa = - \lim_{x \rightarrow +\infty} \frac{\ln(g(x))}{x} = \beta \lim_{x \rightarrow +\infty} \frac{\psi(x)}{x} + \lambda \stackrel{rH}{=} \beta \lim_{x \rightarrow +\infty} \frac{d\psi(x)}{dx} + \lambda = \lambda.$$

Since the balanced index is positive, the function  $g(x)$  satisfies the balanced axiom, confirming its affiliation in the class of balanced densities.

Thanks to the strict requirements that we impose on the potential of the repulsive particle system, this system is equipped with useful properties. To prove these properties, the following integral will be crucial for us

$$I_1 = \int_{\mathbb{R}} \beta x \psi'(x) g(x) dx.$$

Since second property in definition 1.4 specifies that  $\psi'(x) < 0$  in the interval  $(0, +\infty)$ , it is obvious that  $I_1 < 0$  for this integral as well. Let's perform the following adjustment

$$\begin{aligned} I_1 &\stackrel{(1.17)}{=} \int_0^{+\infty} A\beta\psi'(x)x^{\alpha+1}e^{-\beta\psi(x)}e^{-\lambda x}dx = \\ &= |per\ partes| = \left[-Ax^{\alpha+1}e^{-\beta\psi(x)}e^{-\lambda x}\right]_0^{+\infty} + A \int_0^{+\infty} (\alpha+1-\lambda x)x^\alpha e^{-\beta\psi(x)}e^{-\lambda x}dx = \\ &= (\alpha+1) \int_{\mathbb{R}} g(x)dx - \lambda \int_{\mathbb{R}} xg(x)dx = (\alpha+1)\mu_0 - \lambda\mu_1 < 0, \end{aligned}$$

where  $\mu_0$  and  $\mu_1$  denote the zeroth and first general moment of the density  $g(x)$ . Thus, a general inequality holds between these moments

$$\lambda\mu_1 > (\alpha + 1)\mu_0.$$

If  $g(x)$  is scaled, i.e.,  $\mu_0 = \mu_1 = 1$ , then for the parameters of the function  $g(x)$ , we obtain the relationship

$$\alpha + 1 < \lambda. \quad (1.18)$$

From this result, it can be observed, for example, that for a special case of a scaled repulsive particle system where  $\alpha = 0$ , the parameter  $\lambda$  is always greater than 1. The inequality between individual neighboring moments can even be shown for any  $k$ -th moment. Let's consider a modified version of the integral

$$I_k = \int_{\mathbb{R}} \beta x^k \psi'(x) g(x) dx < 0,$$

then by using integration per partes, we can arrive at a relationship defining the monotony between two consecutive moments

$$\lambda\mu_k > (\alpha + k)\mu_{k-1}.$$

We are able to show an even more general property of the moment code of the function (1.17), which arises from the non-negativity of the following integral

$$0 < A \int_0^{+\infty} (x-1)^2 x^{k+\alpha} e^{-\beta\psi(x)} e^{-\lambda x} dx = \int_{\mathbb{R}} x^{k+2} g(x) dx - 2 \int_{\mathbb{R}} x^{k+1} g(x) dx + \int_{\mathbb{R}} x^k g(x) dx = \mu_{k+2} - 2\mu_{k+1} + \mu_k.$$

This property, where  $\mu_{k+2} + \mu_k > 2\mu_{k+1}$ , is called the convexity of the moment code for a balanced particle system with a repulsive generator. We have thus demonstrated relationships that apply to individual moments. However, for the scaled balanced repulsive particle system, we are able to uncover the specific bound for its second moment  $\mu_2$ . Referring to the already proven convexity of the moment code, it is clear that from the relationship  $\mu_{k+2} + \mu_k > 2\mu_{k+1}$ , by substituting  $k = 0$ , we obtain the lower bound

$$\mu_2 + \mu_0 > 2\mu_1, \text{ thus for } \mu_0 = \mu_1 = 1 \text{ follows that } \mu_2 > 1.$$

When determining the upper bound, it is necessary to emphasize the following two inequalities

$$\begin{aligned} \forall \varepsilon > 0, \forall x \in (0, +\infty), \forall \lambda > 0: & \quad e^{-\lambda x} > e^{-(\lambda+\varepsilon)x}, \\ \forall \varepsilon > 0, \forall x \in (0, +\infty), \forall \beta > 0: & \quad e^{-\beta\psi(x)} > e^{-(\beta+\varepsilon)\psi(x)}, \end{aligned}$$

where for the first mentioned inequality, we can state that, thanks to the discovered relationship (1.18),  $\alpha + 1$  is the lowest possible value that  $\lambda$  can approach. Then for the second moment, the following estimate can be made

$$\mu_2 = \int_{\mathbb{R}} x^2 g(x) dx = \int_0^{+\infty} A x^{\alpha+2} e^{-\beta\psi(x)} e^{-\lambda x} dx < \lim_{\beta \rightarrow 0_+} \lim_{\lambda \rightarrow \alpha+1} \int_0^{+\infty} A x^{\alpha+2} e^{-\beta\psi(x)} e^{-\lambda x} dx.$$

Upon performing the limit transition  $\beta \rightarrow 0_+$  and  $\lambda \rightarrow \alpha + 1$ , the density  $A x^{\alpha+2} e^{-\beta\psi(x)} e^{-\lambda x}$  transforms into the form  $A x^{\alpha+2} e^{-(\alpha+1)x}$ . Thus, it corresponds to the Gamma distribution, for which the value of  $A$  can be easily computed from the normalization equation as  $A = \frac{(\alpha+1)^{\alpha+1}}{\Gamma(\alpha+1)}$ . By substitution, we obtain the result

$$\mu_2 < \frac{(\alpha+1)^{\alpha+1}}{\Gamma(\alpha+1)} \int_0^{+\infty} x^{\alpha+2} e^{-(\alpha+1)x} dx = \frac{(\alpha+1)^{\alpha+1}}{\Gamma(\alpha+1)} \frac{\Gamma(\alpha+3)^{\alpha+1}}{(\alpha+1)^{\alpha+3}} = 1 + \frac{1}{\alpha+1} \leq 2.$$

At first glance, this result may seem insignificant. However, when placed in the context of the theory of balanced particle systems, we have just shown that a scaled balanced particle system with a repulsive generator is always sub-compressible, as

$$\chi = \text{VAR}[\mathcal{R}] = \mu_2(g(x)) - \mu_1^2(g(x)) < 2 - 1 = 1.$$

Let us now return to the case when we choose the second option for the potential substitution (1.15), i.e.,  $\rho > 0$  and  $\varkappa < 0$ . It is apparent that in such a case,  $\varphi(x)$  does not inherit the repulsive characteristics from the potential  $\psi(x)$ . On the contrary, if we look at the situation from the perspective of forces

$$F(x) = \rho G(x) + \frac{\varkappa}{x},$$

then the second term of this function expresses attractive forces. By performing the same substitution as in the previous case, we can define a balanced particle system with a composite generator.

**Definition 1.5.** A balanced particle system with a composite generator is defined as a balanced particle system whose generator is a function

$$g(x) = \Theta(x)Ax^\alpha e^{-\beta\psi(x)} e^{-\lambda x},$$

where  $\alpha < 0, \beta > 0, \lambda > 0, A^{-1} = \int_0^{+\infty} x^\alpha e^{-\beta\psi(x)} e^{-\lambda x} dx$  is the normalization factor, and the potential  $\psi(x)$  satisfies the following conditions:

1.  $\psi(x) \in \mathcal{C}^1(0, +\infty)$ ,
2.  $\frac{d\psi(x)}{dx} < 0$  on the interval  $(0, +\infty)$ ,
3.  $\lim_{x \rightarrow +\infty} \psi(x) = 0$ ,
4.  $\lim_{x \rightarrow 0_+} \frac{d\psi(x)}{dx} = -\infty$ ,
5.  $\lim_{x \rightarrow +\infty} \frac{d\psi(x)}{dx} = 0$ .

## Chapter 2

# Generalized Inverse Gaussian distribution

In the previous chapter, we used mathematical and physical knowledge to derive that balance particle systems are suitable for the statistical description of headways between vehicles. Depending on the sign of the parameter  $\alpha$ , we derived a class of functions

$$\mathbb{F} = \{f(x) : f(x) = A\Theta(x)x^\alpha e^{-\beta\psi(x)} e^{-\lambda x} \wedge A > 0, \alpha \in \mathbb{R}, \beta > 0, \lambda > 0\},$$

which can be used to generate balance particle systems with repulsive or composite potential. Let's substitute a specific function for the general repulsive potential

$$\psi(x) = \frac{1}{x}.$$

Certainly, this function satisfies the requirements of a repulsive potential as defined in Definitions 1.4 and 1.5, since

1.  $\frac{1}{x} \in \mathcal{C}^1(0, +\infty)$ ,
2.  $\frac{d}{dx} \frac{1}{x} = -\frac{1}{x^2} < 0$  on the interval  $(0, +\infty)$ ,
3.  $\lim_{x \rightarrow +\infty} \frac{1}{x} = 0$ ,
4.  $\lim_{x \rightarrow 0_+} \frac{d}{dx} \frac{1}{x} = \lim_{x \rightarrow 0_+} -\frac{1}{x^2} = -\infty$ ,
5.  $\lim_{x \rightarrow +\infty} \frac{d}{dx} \frac{1}{x} = \lim_{x \rightarrow +\infty} -\frac{1}{x^2} = 0$ .

By making this choice of the potential function  $\psi(x)$ , we have obtained the Generalized Inverse Gaussian distribution (abbreviated as GIG), which we generally define using the following formula

$$g(x) = A\Theta(x)x^\alpha e^{-\frac{\beta}{x}} e^{-\lambda x}, \quad A > 0, \alpha \in \mathbb{R}, \beta > 0, \lambda > 0 \quad (2.1)$$

and in this work we reserve the notation  $g(x)$  for it. As mentioned in the previous text, we call the parameters  $A, \alpha, \beta, \lambda$  of this distribution normalization constant, tension, intensity, and concentration, respectively. In accordance with the previous text, we also note that for values of the parameter  $\alpha \geq 0$ , this distribution generates sub-compressible particle systems. Let us mention some basic characteristics of the GIG distribution that we will use advantageously in our computational considerations.



## 2.1 Balanced properties

We consider GIG distribution in the context of balanced particle systems, so it is appropriate to verify that this function actually satisfies the conditions of balance density. Detailed calculations were already performed in the bachelor's thesis [10]. Let us summarize the main arguments leading to the proof of axioms 1-6 in definition 1.1.

- Axioms 1 and 2 are trivially satisfied due to the Heaviside step function  $\Theta(x)$  included in the GIG distribution formula (2.1).
- In investigating the piecewise continuity for the parameters  $A > 0, \alpha \in \mathbb{R}, \beta > 0$  and  $\lambda > 0$ , the following values of limits are crucial

$$\begin{aligned}\lim_{x \rightarrow 0_-} g(x) &= 0, \\ \lim_{x \rightarrow 0_+} g(x) &= 0.\end{aligned}$$

Therefore, not only is GIG a piecewise continuous function  $g(x) \in \mathcal{PC}(\mathbb{R})$ , but it is also a continuous function  $g(x) \in \mathcal{C}(\mathbb{R})$ .

- To prove integrability, we use the fact that  $\int_{\mathbb{R}} g(x) dx = A \int_0^{+\infty} x^\alpha e^{-\lambda x} e^{-\frac{\beta}{x}} dx$  and the function  $x^\alpha e^{-\lambda x} e^{-\frac{\beta}{x}}$  is continuous on  $\mathbb{R}^+$ . Therefore, if its limits as  $x \rightarrow 0_+$  and  $x \rightarrow +\infty$  are finite and an integrable majorant can be found, then the integral of this function is certainly finite. The values of the limits are

$$\begin{aligned}\lim_{x \rightarrow 0_+} x^\alpha e^{-\lambda x} e^{-\frac{\beta}{x}} &= \begin{cases} 0 & \text{for } \alpha \neq 0, \\ 1 & \text{for } \alpha = 0, \end{cases} \\ \lim_{x \rightarrow +\infty} x^\alpha e^{-\lambda x} e^{-\frac{\beta}{x}} &= 0.\end{aligned}$$

The integrable majorant is a function that is Lebesgue integrable on the given interval and also upper bounds the absolute value of the examined function. In our case, we can choose the integrable majorant

$$m(x) : |g(x)| \leq m(x) \in \mathcal{L}(\mathbb{R}), \quad \forall x \in \text{Dom}(g)$$

depending on the parameter  $\alpha$  as

$$\begin{aligned}\alpha \leq 0 : m(x) &= C e^{-\lambda x}, \text{ where } C > 0 \text{ is a constant,} \\ \alpha > 0 : m(x) &= x^\alpha e^{-\lambda x}.\end{aligned}$$

Since the limits of the function  $x^\alpha e^{-\lambda x} e^{-\frac{\beta}{x}}$  are finite and we have found an integrable majorant, it follows from the aforementioned considerations that the function  $g(x)$  has a finite integral, i.e.  $g(x) \in \mathcal{L}(\mathbb{R})$ .

- The non-negativity of the support of  $\text{supp}(g)$  is again trivially satisfied owing to the Heaviside step function  $\Theta(x)$ .
- The last axiom regarding the balancing tail can be easily fulfilled by computing the balancing index  $\text{inb}(g)$  using the balance criterion

$$\text{inb}(g) = - \lim_{x \rightarrow +\infty} \frac{\ln(g(x))}{x} = - \lim_{x \rightarrow +\infty} \left[ \frac{\ln(A\Theta(x))}{x} - \frac{\beta}{x^2} - \lambda \right] = \lambda > 0.$$

## 2.2 General moments

Belonging to balanced densities guarantees the existence of all general moments for GIG, which is very convenient since it ensures, for example, the solvability of normalization equation. Let us consider  $X$  as a random variable  $X \sim g(x)$  in this text. The zeroth moment can be used to define the normalization equation for the GIG distribution

$$\mu_0(g) = \mathbb{E}[X] = \int_R g(x) dx \stackrel{!}{=} 1. \quad (2.2)$$

By solving this equation, we obtain the value of the normalization constant  $A = \frac{\left(\sqrt{\frac{\lambda}{\beta}}\right)^{\alpha+1}}{2\mathcal{K}_{\alpha+1}(2\sqrt{\beta\lambda})}$  and by substituting it, the normalized form of the Generalized Inverse Gaussian distribution is obtained

$$g_N(x) = \Theta(x) \frac{\left(\sqrt{\frac{\lambda}{\beta}}\right)^{\alpha+1}}{2\mathcal{K}_{\alpha+1}(2\sqrt{\beta\lambda})} x^\alpha e^{-\frac{\beta}{x}} e^{-\lambda x} \quad (2.3)$$

and we reserve the notation  $g_N(x)$  for it. The symbol  $\mathcal{K}_\alpha$  denotes the Macdonald function of order  $\alpha$ , also known as the modified Bessel function of the second kind, as it solves the modified Bessel ordinary differential equation known from [6] as

$$x^2 \mathcal{K}_\alpha''(x) + x \mathcal{K}_\alpha'(x) - (x^2 + \alpha^2) \mathcal{K}_\alpha(x) = 0$$

and has the following integral form

$$\mathcal{K}_\alpha(x) = \frac{2^{\alpha-1}}{x^\alpha} \int_0^{+\infty} y^{\alpha-1} e^{-y} e^{-\frac{x^2}{4y}} dy. \quad (2.4)$$

For the Macdonald function of order  $\alpha$ , where  $\alpha \in \mathbb{R}$ , the following useful relations hold

$$\begin{aligned} \mathcal{K}_{\alpha-1}(x) - \mathcal{K}_{\alpha+1}(x) &= -\frac{2\alpha}{x} \mathcal{K}_\alpha(x), \\ \mathcal{K}_\alpha(x) &= \mathcal{K}_{-\alpha}(x), \\ \mathcal{K}_\alpha'(x) &= -\mathcal{K}_{\alpha+1}(x) + \frac{\alpha}{x} \mathcal{K}_\alpha(x), \\ \mathcal{K}_{\alpha+1}'(x) &= -\mathcal{K}_\alpha(x) - \frac{\alpha+1}{x} \mathcal{K}_{\alpha+1}(x). \end{aligned} \quad (2.5)$$

At the same time, for small values of  $x$ , we know the approximation of this function from [18]:

$$x^\alpha \mathcal{K}_\alpha(x) \approx 2^{\alpha-1} \Gamma(\alpha) (2\alpha-1)^{\frac{1}{2}-\alpha} (2x+2\alpha-1)^{\alpha-\frac{1}{2}} e^{-x} = \frac{1}{2} 2^\alpha \Gamma(\alpha) \left[1 + \frac{2x}{2\alpha-1}\right]^{\alpha-\frac{1}{2}} e^{-x}. \quad (2.6)$$

This approximation holds for all values of  $\alpha \in \mathbb{R}^+$ , but let us mention that especially for  $\alpha = \frac{1}{2}$  it is appropriate to use the unadjusted expression of the approximation (2.6), which is of the form

$$x^{\frac{1}{2}} \mathcal{K}_{\frac{1}{2}}(x) \approx 2^{-\frac{1}{2}} \Gamma\left(\frac{1}{2}\right) e^{-x} = \sqrt{\frac{\pi}{2}} e^{-x}. \quad (2.7)$$

If we consider the normalized GIG distribution  $g_N(x)$ , then the first and second moments are equal to

$$\begin{aligned}\mu_1(g_N) &= \int_{\mathbb{R}} x g_N(x) dx = \sqrt{\frac{\beta}{\lambda}} \frac{\mathcal{K}_{\alpha+2}(2\sqrt{\beta\lambda})}{\mathcal{K}_{\alpha+1}(2\sqrt{\beta\lambda})}, \\ \mu_2(g_N) &= \int_{\mathbb{R}} x^2 g_N(x) dx = \frac{\beta}{\lambda} \frac{\mathcal{K}_{\alpha+3}(2\sqrt{\beta\lambda})}{\mathcal{K}_{\alpha+1}(2\sqrt{\beta\lambda})}.\end{aligned}$$

Note a certain pattern in the results of individual moments. It is not surprising that a formula can indeed be derived for any  $k$ -th moment ( $k \in \mathbb{N}$ ) for the normalized GIG:

$$\mu_k(g_N) = \frac{\left(\sqrt{\frac{\lambda}{\beta}}\right)^{\alpha+1}}{2\mathcal{K}_{\alpha+1}(2\sqrt{\beta\lambda})} \int_0^{+\infty} x^{\alpha+k} e^{-\frac{\beta}{x}} e^{-\lambda x} dx \stackrel{(2.4)}{=} \left(\frac{\beta}{\lambda}\right)^{\frac{k}{2}} \frac{\mathcal{K}_{\alpha+1+k}(2\sqrt{\beta\lambda})}{\mathcal{K}_{\alpha+1}(2\sqrt{\beta\lambda})}. \quad (2.8)$$

If we know the first and second moments of the normalized GIG distribution, we can calculate the variance:

$$\text{VAR}[X] = \mu_2(g_N) - \mu_1^2(g_N) = \frac{\beta}{\lambda} \left[ \frac{\mathcal{K}_{\alpha+3}(2\sqrt{\beta\lambda})}{\mathcal{K}_{\alpha+1}(2\sqrt{\beta\lambda})} - \frac{\mathcal{K}_{\alpha+2}^2(2\sqrt{\beta\lambda})}{\mathcal{K}_{\alpha+1}^2(2\sqrt{\beta\lambda})} \right].$$

### 2.3 Relationships between parameters

As part of further procedures, let us now prove two basic inequalities that hold between individual parameters of the scaled Generalized Inverse Gaussian distribution. For the scaled GIG, we have  $\mu_0(g_N) = \mu_1(g_N) = 1$ , hence

$$\mu_1(g_N) \stackrel{(2.8)}{=} \sqrt{\frac{\beta}{\lambda}} \frac{\mathcal{K}_{\alpha+2}(2\sqrt{\beta\lambda})}{\mathcal{K}_{\alpha+1}(2\sqrt{\beta\lambda})} = 1. \quad (2.9)$$

The first inequality we derive is based on the definition of variance. We have already discussed that the situation when  $\text{VAR}[X] = 0$  corresponds to an equidistant distribution of particles in particle systems. However, for the remaining systems, the variance must be positive, and therefore, we have

$$\begin{aligned}0 < \text{VAR}[X] &= \mu_2(g_N) - \mu_1^2(g_N) \stackrel{(2.8)}{=} \frac{\beta}{\lambda} \frac{\mathcal{K}_{\alpha+3}(2\sqrt{\beta\lambda})}{\mathcal{K}_{\alpha+1}(2\sqrt{\beta\lambda})} - 1 = \\ &\stackrel{(2.5)}{=} \frac{\beta}{\lambda} \frac{\mathcal{K}_{\alpha+1}(2\sqrt{\beta\lambda}) + \frac{2(\alpha+2)}{2\sqrt{\beta\lambda}} \mathcal{K}_{\alpha+2}(2\sqrt{\beta\lambda})}{\mathcal{K}_{\alpha+1}(2\sqrt{\beta\lambda})} - 1 = \\ &\stackrel{(2.9)}{=} \frac{\beta}{\lambda} + \frac{(\alpha+2)\mathcal{K}_{\alpha+1}(2\sqrt{\beta\lambda})}{\lambda\mathcal{K}_{\alpha+1}(2\sqrt{\beta\lambda})} - 1 = \\ &= \frac{\beta + \alpha + 2}{\lambda} - 1,\end{aligned} \quad (2.10)$$

thus, we have shown the first significant relationship between parameters of the scaled GIG distribution

$$\alpha + \beta - \lambda + 2 > 0. \quad (2.11)$$

The second inequality follows from the procedure we have already applied in previous chapters. Let us examine the value of the following integral

$$\mathbf{I} = - \int_0^{+\infty} A x^{\alpha-1} e^{-\frac{\beta}{x}} e^{-\lambda x} dx,$$

using the method of integration per partes, where we choose  $u = x^{\alpha+1} e^{-\lambda x}$  and  $v' = -\frac{1}{x^2} e^{-\frac{\beta}{x}}$ , and we understand constant  $A$  as the normalization constant calculated from (2.2). We obtain

$$\mathbb{I} = |\text{per partes}| = \frac{\alpha+1}{\beta} \underbrace{\int_0^{+\infty} A x^\alpha e^{-\frac{\beta}{x}} e^{-\lambda x} dx}_{\mu_0(g_N)=1} - \frac{\lambda}{\beta} \underbrace{\int_0^{+\infty} A x^{\alpha+1} e^{-\frac{\beta}{x}} e^{-\lambda x} dx}_{\mu_1(g_N)=1} = \frac{\alpha+1}{\beta} - \frac{\lambda}{\beta}.$$

Furthermore, let us show that this integral  $\mathbb{I}$  is less than  $-1$ , i.e.

$$\mathbb{I} = - \int_0^{+\infty} A x^{\alpha-1} e^{-\frac{\beta}{x}} e^{-\lambda x} dx = \frac{\alpha+1}{\beta} - \frac{\lambda}{\beta} < -1.$$

To do this, we use the following valid inequality

$$0 < A \int_0^{+\infty} (1-x)^2 x^{\alpha-1} e^{-\frac{\beta}{x}} e^{-\lambda x} dx = A \int_0^{+\infty} (x^{\alpha-1} - 2x^\alpha + x^{\alpha+1}) e^{-\frac{\beta}{x}} e^{-\lambda x} dx,$$

from which it follows that

$$- \underbrace{\int_0^{+\infty} A x^{\alpha-1} e^{-\frac{\beta}{x}} e^{-\lambda x} dx}_{\mathbb{I}} \leq \underbrace{\int_0^{+\infty} A x^{\alpha+1} e^{-\frac{\beta}{x}} e^{-\lambda x} dx}_{\mu_1(g_N)=1} - 2 \underbrace{\int_0^{+\infty} A x^\alpha e^{-\frac{\beta}{x}} e^{-\lambda x} dx}_{\mu_0(g_N)=1} = 1 - 2 = -1.$$

Thus, we have succeeded in showing the second significant inequality for the parameters of the scaled GIG in the form

$$\alpha + \beta - \lambda + 1 < 0. \quad (2.12)$$

## 2.4 Scaling

One of the biggest challenges of studying the properties of the GIG distribution is its scaling. Significant contributions to this task have been made by [10] and [18], whose findings will be presented here and built upon. Recall that scaling of a distribution requires the fulfillment of a set of two equations

$$\text{normalization equation: } \mu_0(g) \stackrel{!}{=} 1,$$

$$\text{scaling equation: } \mu_1(g_N) \stackrel{!}{=} 1.$$

The normalization equation has been solved in the previous text (2.2), yielding the normalized form of the GIG distribution (2.3), which we denote as  $g_N(x)$ . By expanding the form of the scaling equation

$$\mu_1(g_N) \stackrel{(2.8)}{=} \sqrt{\frac{\beta}{\lambda}} \frac{\mathcal{K}_{\alpha+2}(2\sqrt{\beta\lambda})}{\mathcal{K}_{\alpha+1}(2\sqrt{\beta\lambda})} \stackrel{!}{=} 1 \quad (2.13)$$

We see that we are not able to explicitly express any of the parameters as a scaling parameter. Except for one exception, when the scaling equation for  $\alpha = -\frac{3}{2}$  is of the form

$$\mu_1(g_N) = \sqrt{\frac{\beta}{\lambda}} \frac{\mathcal{K}_{\frac{1}{2}}(2\sqrt{\beta\lambda})}{\mathcal{K}_{-\frac{1}{2}}(2\sqrt{\beta\lambda})} \stackrel{(2.5)}{=} \sqrt{\frac{\beta}{\lambda}} \frac{\mathcal{K}_{\frac{1}{2}}(2\sqrt{\beta\lambda})}{\mathcal{K}_{\frac{1}{2}}(2\sqrt{\beta\lambda})} = \sqrt{\frac{\beta}{\lambda}} \stackrel{!}{=} 1.$$

It is apparent that the scaling parameter is a linear function of  $\lambda(\beta) = \beta$  when  $\alpha = -\frac{3}{2}$ . One way to deal with non-explicit results is to choose an approximate method and at least reveal the basic properties that the scaling parameter fulfills. Another question that arises in connection with scaling the Generalized Inverse Gaussian distribution is the existence of solutions to scaling equation (2.13). As mentioned before, the advantage of balanced densities is that all of their general moments exist, so the scaling equation will likely also be solvable. However, it depends on which parameter we define as the scaling parameter.

### 2.4.1 Scaling via the parameter $\lambda$

#### Existence of the scaling equation solution

Assume now that the scaling parameter of the Generalized Inverse Gaussian distribution is the parameter  $\lambda > 0$ . Then, we want to describe the behavior of the function  $\lambda(\alpha, \beta)$  implicitly defined by equation (2.13). For the purpose of theoretical explanations, let us introduce the function  $\Phi : \mathbb{R}^2 \rightarrow \mathbb{R}$  for a fixed parameter  $\alpha$  by the formula

$$\Phi(\beta, \lambda) = \sqrt{\frac{\beta}{\lambda} \frac{\mathcal{K}_{\alpha+2}(2\sqrt{\beta\lambda})}{\mathcal{K}_{\alpha+1}(2\sqrt{\beta\lambda})}} - 1.$$

If we find a suitable set  $\mathbb{B}$  of all possible choices of  $\beta$  for which the function  $\Phi(\beta, \lambda)$  satisfies

$$\Phi(\beta, \lambda) = 0, \tag{2.14}$$

then  $\Phi(\beta, \lambda)$  generates a unique implicit function  $\lambda(\beta)$ , i.e., there exists a solution to the scaling equation. Let us consider this function as a function of a single variable  $\Phi(\lambda)$  with the parameter  $\beta > 0$ . Thus, let us investigate the behavior of the function

$$\Phi(\lambda) = \sqrt{\frac{\beta}{\lambda} \frac{\mathcal{K}_{\alpha+2}(2\sqrt{\beta\lambda})}{\mathcal{K}_{\alpha+1}(2\sqrt{\beta\lambda})}} - 1.$$

The domain of the function and the range of values are  $\text{Dom}(\Phi) = (0, +\infty)$ ,  $\text{Ran}(\Phi) \subset (-1, +\infty)$ . We are interested in finding out whether the maximum (or supremum), of this function at some point equals or exceeds a zero value. This is because the scaling equation can be reformulated as  $\Phi(\lambda) = 0$ . Let us now focus on the boundary point of the domain of definition  $\text{Dom}(\Phi)$ , which is  $\lambda = 0$ , and examine the limit value of the function  $\Phi(\lambda)$  as  $\lambda \rightarrow 0_+$ . In the following steps, we present only the results for clarity. If the reader is interested in the calculation procedure, please refer to [10]. For clarity, let us introduce the notation  $z = 2\sqrt{\beta\lambda}$ , so the limit under investigation takes the form

$$\lim_{\lambda \rightarrow 0_+} \sqrt{\frac{\beta}{\lambda} \frac{\mathcal{K}_{\alpha+2}(2\sqrt{\beta\lambda})}{\mathcal{K}_{\alpha+1}(2\sqrt{\beta\lambda})}} - 1 = \lim_{z \rightarrow 0_+} \frac{2\beta}{z} \frac{\mathcal{K}_{\alpha+2}(z)}{\mathcal{K}_{\alpha+1}(z)} - 1.$$

The computation of the limit depends on the value of the parameter  $\alpha$

$$\lim_{z \rightarrow 0_+} \frac{2\beta}{z} \frac{\mathcal{K}_{\alpha+2}(z)}{\mathcal{K}_{\alpha+1}(z)} - 1 = \begin{cases} +\infty, & \alpha \geq -2, \\ -\frac{\beta}{\alpha+2} - 1, & \alpha < -2. \end{cases}$$

The fact that the function approaches infinity for  $\alpha \geq -2$  means that the function  $\Phi(z)$  has a supremum in the right neighborhood of zero. The result for  $\alpha < -2$  reveals that the function from the right at zero

also takes on a finite value. Let's compute whether the value of  $\Phi(z)$  for  $z > 0$  and  $\alpha < -2$  can exceed or acquire values that approach zero for  $z \rightarrow 0_+$ . Substitute for  $\alpha < -2$

$$\begin{aligned} \Phi(0_+) &= -\frac{\beta}{\alpha+2} - 1 \stackrel{?}{>} \frac{2\beta}{z} \frac{\mathcal{H}_{\alpha+2}(z)}{\mathcal{H}_{\alpha+1}(z)} - 1 = \Phi(z), \\ &-\frac{\beta}{\alpha+2} \stackrel{?}{>} \frac{2\beta(\alpha+2)}{z(\alpha+2)} \frac{\mathcal{H}_{\alpha+2}(z)}{\mathcal{H}_{\alpha+1}(z)}, \\ &-\frac{\beta}{\alpha+2} \stackrel{?}{>} -\frac{\beta}{\alpha+2} + \underbrace{\frac{\beta \mathcal{H}_{\alpha+3}(z)}{(\alpha+2)\mathcal{H}_{\alpha+1}(z)}}_{<0}, \end{aligned}$$

which means that  $\Phi(0_+) > \Phi(z)$  and we have just shown that the supremum of  $\Phi(z)$  is, depending on  $\alpha$ , either infinity or  $-\frac{\beta}{\alpha+2} - 1$

$$\sup(\Phi)_{\alpha \geq -2} = +\infty \quad \text{and} \quad \sup(\Phi)_{\alpha < -2} = -\frac{\beta}{\alpha+2} - 1.$$

It is clear from the introduction of the notation  $z = 2\sqrt{\beta\lambda}$  that  $\sup(\Phi(z)) = \sup(\Phi(\beta, \lambda))$ , and in the following text, we will return to the variables  $\beta$  and  $\lambda$ . Thus, we try to find  $\beta$  for which condition (2.14) is satisfied and derive the form of the set  $\mathbb{B}$ . If the supremum of the function  $\Phi(\beta, \lambda)$  is less than or equal to 0, the condition will never be satisfied. Therefore, for the condition to hold,  $\sup(\Phi) > 0$ . For  $\alpha \geq -2$ , the situation is simple because

$$\sup(\Phi)_{\alpha \geq -2} = +\infty > 0 \quad \forall \beta > 0.$$

For  $\alpha < -2$ , we obtain the requirement

$$\sup(\Phi)_{\alpha < -2} = -\frac{\beta}{\alpha+2} - 1 > 0 \quad \Leftrightarrow \quad \alpha + \beta + 2 > 0.$$

So that equality (2.14) can hold for  $\alpha < -2$ , it is necessary to meet the requirement for  $\beta$ , which formulates the desired set as

$$\mathbb{B} = \left\{ \beta \in \mathbb{R}^+ : \alpha + \beta + 2 > 0 \right\}.$$

We have thus found a suitable set  $\mathbb{B}$  of all possible choices of  $\beta$  for which the function  $\Phi(\beta, \lambda)$  satisfies the condition (2.14). By the definition of the implicit function,  $\Phi(\beta, \lambda)$  uniquely generates the implicit function  $\lambda(\beta)$ , which means that there exists a solution to the scaling equation. In other words, in order to be able to solve the scaling equation through the parameter  $\lambda$  in practice, we must observe the so-called scaling condition in the form of

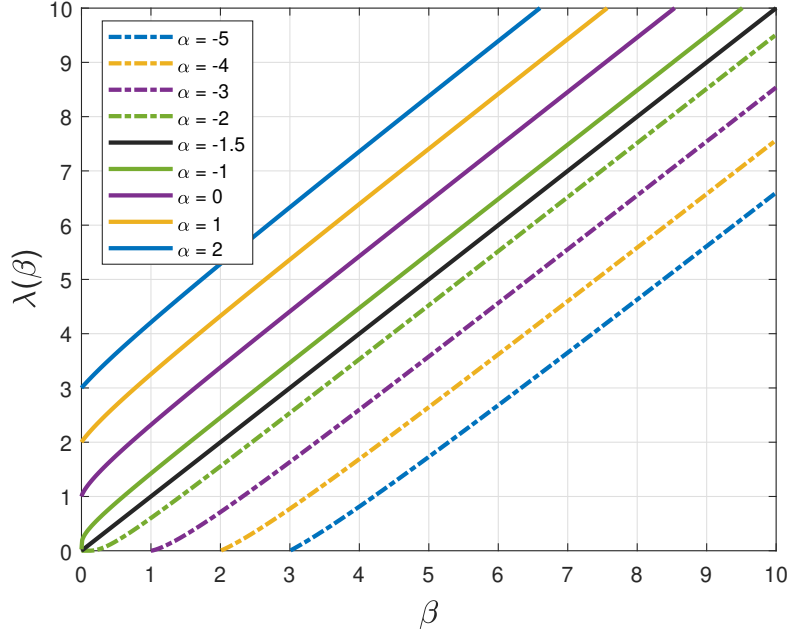
$$\alpha + \beta + 2 > 0. \tag{2.15}$$

### Properties of the scaling function $\lambda$

Let us now focus on the scaling parameter  $\lambda$  as a function  $\lambda(\beta)$  (at fixed  $\alpha \in \mathbb{R}$ ) and investigate its basic properties. For a better idea, the reader can refer to Figure 2.1, which shows examples of this scaling function calculated numerically for different values of the parameter  $\alpha$ . In the mentioned figure, let us notice the symmetry around the axis  $\lambda(\beta) = \beta$ , which is obeyed by individual pairs of parameters  $\alpha \in \left\{ -\frac{3}{2} + m, -\frac{3}{2} - m \right\}$ . We will pay more attention to this symmetry later.

A large part of the research on the approximation of the function  $\lambda(\beta)$  has already been carried out in [10] and [18], in which the asymptotic approximation was derived as

$$\lambda(\beta) = \alpha + \beta + \frac{3}{2} \quad \text{for } \alpha \in \mathbb{R} \text{ and } \beta \rightarrow +\infty.$$

Figure 2.1: Scaling function  $\lambda(\beta)$  for different values of parameter  $\alpha \in \mathbb{R}$ .

Further similarly significant statements can be proven for this approximation. The theory of implicit functions, besides verifying the existence of solutions to the scaling equation, can also help in investigating the monotonicity of the function  $\lambda(\beta)$ . Let us prove that  $\lambda(\beta)$  is an increasing function. We start from the formula for the calculation of the derivative of an implicitly defined function

$$\frac{d\lambda(\beta)}{d\beta} = -\frac{\frac{\partial\Phi(\beta,\lambda)}{\partial\beta}}{\frac{\partial\Phi(\beta,\lambda)}{\partial\lambda}}. \quad (2.16)$$

Let us list the mentioned partial derivatives here

$$\begin{aligned} \frac{\partial\Phi(\beta,\lambda)}{\partial\beta} &= \frac{\frac{\mathcal{H}_{\alpha+1}(2\sqrt{\beta\lambda})\mathcal{H}_{\alpha+2}(2\sqrt{\beta\lambda})}{2\sqrt{\beta\lambda}} + \mathcal{H}_{\alpha+1}(2\sqrt{\beta\lambda})\mathcal{H}'_{\alpha+2}(2\sqrt{\beta\lambda}) - \mathcal{H}'_{\alpha+1}(2\sqrt{\beta\lambda})\mathcal{H}_{\alpha+2}(2\sqrt{\beta\lambda})}{\mathcal{H}_{\alpha+1}^2(2\sqrt{\beta\lambda})}, \\ \frac{\partial\Phi(\beta,\lambda)}{\partial\lambda} &= \frac{\beta \frac{\mathcal{H}_{\alpha+1}(2\sqrt{\beta\lambda})\mathcal{H}_{\alpha+2}(2\sqrt{\beta\lambda})}{2\sqrt{\beta\lambda}} + \mathcal{H}_{\alpha+1}(2\sqrt{\beta\lambda})\mathcal{H}'_{\alpha+2}(2\sqrt{\beta\lambda}) - \mathcal{H}'_{\alpha+1}(2\sqrt{\beta\lambda})\mathcal{H}_{\alpha+2}(2\sqrt{\beta\lambda})}{\mathcal{H}_{\alpha+1}^2(2\sqrt{\beta\lambda})}, \end{aligned} \quad (2.17)$$

where  $\mathcal{H}'_{\alpha}(z)$  denotes the derivative  $\frac{d\mathcal{H}_{\alpha}(z)}{dz}$ , and let us examine whether the derivative (2.16) is positive, i.e., whether

$$\frac{d\lambda(\beta)}{d\beta} = -\frac{\frac{\partial\Phi(\beta,\lambda)}{\partial\beta}}{\frac{\partial\Phi(\beta,\lambda)}{\partial\lambda}} \stackrel{?}{>} 0.$$

By substituting the derivatives (2.17) into the formula (2.16), we obtain the inequality

$$-\frac{\lambda \frac{\mathcal{H}_{\alpha+1}(2\sqrt{\beta\lambda})\mathcal{H}_{\alpha+2}(2\sqrt{\beta\lambda})}{2\sqrt{\beta\lambda}} + \mathcal{H}_{\alpha+1}(2\sqrt{\beta\lambda})\mathcal{H}'_{\alpha+2}(2\sqrt{\beta\lambda}) - \mathcal{H}'_{\alpha+1}(2\sqrt{\beta\lambda})\mathcal{H}_{\alpha+2}(2\sqrt{\beta\lambda})}{\beta \frac{\mathcal{H}_{\alpha+1}(2\sqrt{\beta\lambda})\mathcal{H}_{\alpha+2}(2\sqrt{\beta\lambda})}{2\sqrt{\beta\lambda}} + \mathcal{H}_{\alpha+1}(2\sqrt{\beta\lambda})\mathcal{H}'_{\alpha+2}(2\sqrt{\beta\lambda}) - \mathcal{H}'_{\alpha+1}(2\sqrt{\beta\lambda})\mathcal{H}_{\alpha+2}(2\sqrt{\beta\lambda})} \stackrel{?}{>} 0,$$

which can be further modified using the properties of the Macdonalds function (2.5) to the form

$$\frac{[\alpha + 1] \frac{\mathcal{K}_{\alpha+1}(2\sqrt{\beta\lambda})\mathcal{K}_{\alpha+2}(2\sqrt{\beta\lambda})}{\sqrt{\beta\lambda}} + \mathcal{K}_{\alpha+1}^2(2\sqrt{\beta\lambda}) - \mathcal{K}_{\alpha+2}^2(2\sqrt{\beta\lambda})}{[\alpha + 2] \frac{\mathcal{K}_{\alpha+1}(2\sqrt{\beta\lambda})\mathcal{K}_{\alpha+2}(2\sqrt{\beta\lambda})}{\sqrt{\beta\lambda}} - \mathcal{K}_{\alpha+1}^2(2\sqrt{\beta\lambda}) + \mathcal{K}_{\alpha+2}^2(2\sqrt{\beta\lambda})} \stackrel{?}{>} 0. \quad (2.18)$$

Now, using equation (2.9) and slightly modified inequality (2.18), we arrive at the inequality

$$\frac{\alpha + \beta - \lambda + 1}{\alpha + \beta - \lambda + 2} \stackrel{?}{<} 0. \quad (2.19)$$

Thus, the monotonicity of the function  $\lambda(\beta)$  is proven since the resulting fraction (2.19) contains conditions (2.11) and (2.12), from which the inequality (2.19) follows automatically, and the proof is thereby completed. For completeness, we add that if  $\lambda(\beta)$  is an increasing function, then the inverse function  $\beta(\lambda)$  is also increasing.

Another useful piece of information are the limits for the beginnings of the function  $\lambda(\beta)$ . If we start with the limit when  $\beta \rightarrow 0_+$ , then we notice that for such a case, the Generalized Inverse Gaussian distribution (2.1) takes the form of a Gamma distribution

$$f_{\Gamma}(x) = A\Theta(x)x^{\alpha}e^{-\lambda x},$$

where the parameter  $\alpha$  is restricted to the interval  $(-1, +\infty)$ . For the Gamma distribution, it is easy to compute the value of the scaling parameter, since we can easily express the normalization constant  $A$  and the scaling constant  $\lambda$  from the equations  $\mu_0(f_{\Gamma}) = \mu_1(f_{\Gamma}) = 1$  as follows

$$\text{normalization constant } A = \frac{\lambda^{\alpha+1}}{\Gamma(\alpha+1)},$$

$$\text{scaling constant } \lambda = \alpha + 1.$$

Based on these findings, it is apparent that the scaling function  $\lambda(\beta)$  for the GIG distribution must satisfy

$$\lim_{\beta \rightarrow 0_+} \lambda(\beta) = \alpha + 1, \quad \alpha > -1.$$

Alternatively, we can determine the value of this limit for  $\alpha \in \langle -2, -1 \rangle$  using a slightly different approach. We know that the following limit holds

$$\lim_{z \rightarrow 0_+} \frac{z \mathcal{K}_{a+1}(z)}{\mathcal{K}_a(z)} = \begin{cases} 2a & \text{for } a > 0, \\ 0 & \text{for } a \leq 0. \end{cases} \quad (2.20)$$

Starting from the form (2.13) of the scaling equation

$$\begin{aligned} \sqrt{\frac{\beta}{\lambda(\beta)}} \frac{\mathcal{K}_{\alpha+2}(2\sqrt{\beta\lambda(\beta)})}{\mathcal{K}_{\alpha+1}(2\sqrt{\beta\lambda(\beta)})} &= 1 & \Big| \cdot \frac{2\lambda(\beta)}{2} \\ \frac{\sqrt{2\beta\lambda(\beta)}}{2} \frac{\mathcal{K}_{\alpha+2}(2\sqrt{\beta\lambda(\beta)})}{\mathcal{K}_{\alpha+1}(2\sqrt{\beta\lambda(\beta)})} &= \lambda(\beta), \end{aligned}$$

after taking the limit as  $\beta \rightarrow 0_+$  for  $\alpha \in \langle -2, -1 \rangle$ , we obtain

$$\lim_{\beta \rightarrow 0_+} \frac{\sqrt{2\beta\lambda(\beta)}}{2} \frac{\mathcal{K}_{\alpha+2}(2\sqrt{\beta\lambda(\beta)})}{\mathcal{K}_{\alpha+1}(2\sqrt{\beta\lambda(\beta)})} \stackrel{(2.20)}{=} 0 = \lim_{\beta \rightarrow 0_+} \lambda(\beta),$$



from which we derive

$$\lim_{\beta \rightarrow 0_+} \lambda(\beta) = 0, \quad \alpha \in \langle -2, -1 \rangle. \quad (2.21)$$

Let us also describe the limit behavior of  $\lambda(\beta)$  for the remaining cases of  $\alpha < -2$ . To investigate the limit  $\lim_{\beta \rightarrow -\alpha-2} \lambda(\beta)$  at the boundary of the scaling condition for the remaining cases of  $\alpha < -2$ , we again start from the assumption that the scaling equation still holds, i.e.,

$$\lim_{\lambda \rightarrow 0_+} \sqrt{\frac{\beta(\lambda)}{\lambda} \frac{\mathcal{H}_{\alpha+2}(2\sqrt{\beta(\lambda)\lambda})}{\mathcal{H}_{\alpha+1}(2\sqrt{\beta(\lambda)\lambda})}} \stackrel{(2.13)}{=} \lim_{\lambda \rightarrow 0_+} 1 = 1.$$

Let us focus on the calculation of the limit given on the left-hand side. First, we use the symmetry of Macdonald functions (2.5), which converts negative orders to positive ones. Then, since  $\lambda \rightarrow 0_+$  and  $\beta(\lambda)$  is increasing, we can use the approximation (2.6) of the Macdonald function for small argument. Thus, we have

$$\begin{aligned} \lim_{\lambda \rightarrow 0_+} \sqrt{\frac{\beta(\lambda)}{\lambda} \frac{\mathcal{H}_{\alpha+2}(2\sqrt{\beta(\lambda)\lambda})}{\mathcal{H}_{\alpha+1}(2\sqrt{\beta(\lambda)\lambda})}} &\stackrel{(2.5)}{=} \lim_{\lambda \rightarrow 0_+} \sqrt{\frac{\beta(\lambda)}{\lambda} \frac{\mathcal{H}_{-\alpha-2}(2\sqrt{\beta(\lambda)\lambda})}{\mathcal{H}_{-\alpha-1}(2\sqrt{\beta(\lambda)\lambda})}} = \\ &\stackrel{(2.6)}{=} \lim_{\lambda \rightarrow 0_+} \frac{\beta(\lambda)}{-\alpha-2} \frac{[1 + \frac{2\beta(\lambda)\lambda}{-2\alpha-5}]^{-\alpha-\frac{5}{2}}}{[1 + \frac{2\beta(\lambda)\lambda}{-2\alpha-3}]^{-\alpha-\frac{3}{2}}} = \\ &= \lim_{\lambda \rightarrow 0_+} \frac{\beta(\lambda)}{-\alpha-2} \cdot \lim_{\lambda \rightarrow 0_+} \frac{[1 + \frac{2\beta(\lambda)\lambda}{-2\alpha-5}]^{-\alpha-\frac{5}{2}}}{[1 + \frac{2\beta(\lambda)\lambda}{-2\alpha-3}]^{-\alpha-\frac{3}{2}}} = \\ &= \frac{\lim_{\lambda \rightarrow 0_+} \beta(\lambda)}{-\alpha-2} \cdot 1 \stackrel{!}{=} 1. \end{aligned}$$

So in order for the scaling condition to be satisfied even in the limit case, it is necessary to have

$$\frac{\lim_{\lambda \rightarrow 0_+} \beta(\lambda)}{-\alpha-2} \stackrel{!}{=} 1 \quad \Leftrightarrow \quad \lim_{\lambda \rightarrow 0_+} \beta(\lambda) = -\alpha-2 \quad \Leftrightarrow \quad \lim_{\beta \rightarrow -\alpha-2} \lambda(\beta) = 0,$$

thus we have shown that indeed

$$\lim_{\beta \rightarrow -\alpha-2} \lambda(\beta) = 0, \quad \alpha < -2.$$

Combining the results that we know from equations (2.11) and (2.12) with the information that  $\lambda(\beta)$  is an increasing function, we obtain the area for  $\lambda(\beta)$  which we call the scaling area (see Figure 2.2).

In this chapter, we have learned much more about  $\lambda(\beta)$ . Another useful fact is that  $\lambda(\beta)$  adheres to its asymptote  $\alpha + \beta + \frac{3}{2}$ . At the same time, we have solved the limiting behavior for  $\beta \rightarrow 0_+$  and  $\beta \rightarrow -\alpha-2$  in the previous procedure. By combining this information, we can determine for each  $\lambda(\beta)$ , depending on the value of the parameter  $\alpha$ , whether it has a convex or concave shape, and based on this information, narrow down the scaling area to the region where the upper or lower bound is replaced by the asymptote.

Based on these considerations, we know that  $\lambda(\beta)$  is

concave if  $\alpha > -\frac{3}{2}$ , and its narrowed scaling area is  $\alpha + \beta + 1 < \lambda(\beta) < \alpha + \beta + \frac{3}{2}$ ,

linear if  $\alpha = -\frac{3}{2}$ ,

convex if  $\alpha < -\frac{3}{2}$ , and its narrowed scaling area is  $\alpha + \beta + \frac{3}{2} < \lambda(\beta) < \alpha + \beta + 2$ .

Example of the scaling, resp. narrowed scaling area is available in the Figure 2.2, resp. Figure 2.3.

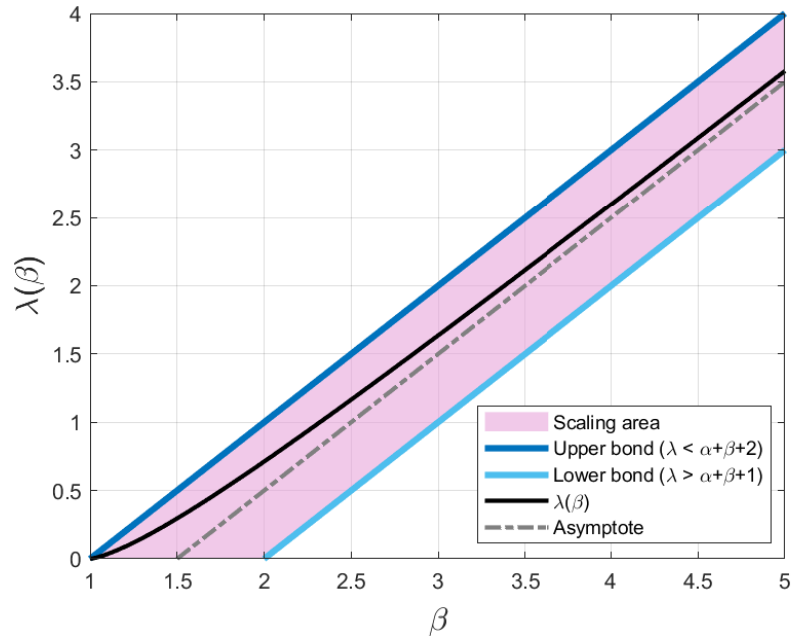


Figure 2.2: Example of scaling area for  $\lambda(\beta)$ , where  $\alpha = -3$ .

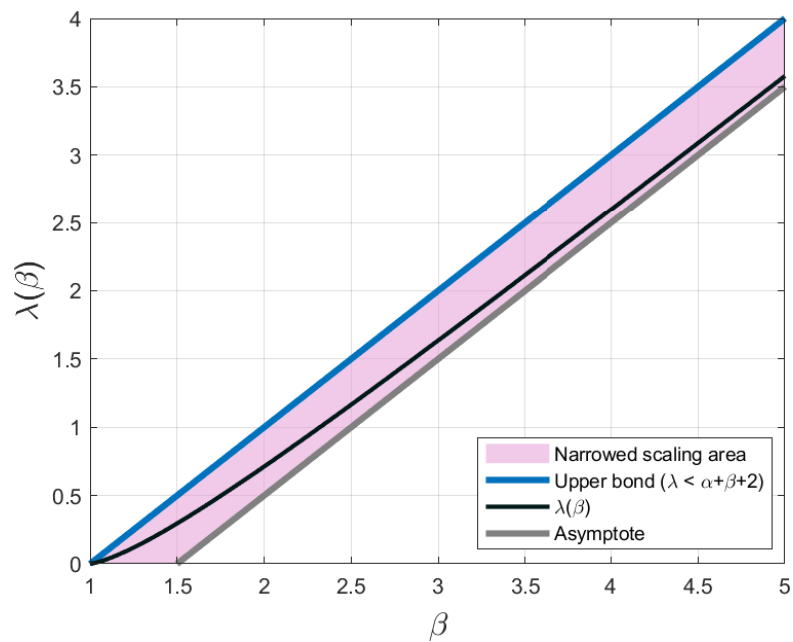


Figure 2.3: Example of narrowed scaling area for  $\lambda(\beta)$ , where  $\alpha = -3$ .

## 2.4.2 Scaling via the parameter $\beta$

### Existence of the scaling equation solution

Notice that, in addition to deeper properties related to the parameter  $\lambda$ , the previous chapter also reveals a strong interdependence between the parameters  $\beta$  and  $\lambda$ . Merely by looking at Figure 2.1, the reader may wonder if an alternative way to scaling via the parameter  $\lambda$  is scaling via the parameter  $\beta$ . For this section, assume that the scaling parameter is  $\beta > 0$ . Let us investigate the behavior of the function  $\beta(\alpha, \lambda)$  implicitly defined by equation (2.13), and consider the function  $\Phi : \mathbb{R}^2 \rightarrow \mathbb{R}$  with a fixed parameter  $\alpha$ , defined by

$$\Phi(\beta, \lambda) = \sqrt{\frac{\beta}{\lambda} \frac{\mathcal{H}_{\alpha+2}(2\sqrt{\beta\lambda})}{\mathcal{H}_{\alpha+1}(2\sqrt{\beta\lambda})}} - 1.$$

Now, let us slightly modify this problem and search for a suitable set  $\mathbb{L}$  of all possible choices of  $\lambda$ , for which the function  $\Phi$  satisfies  $\Phi(\beta, \lambda) = 0$ . Similar to the previous chapter, let us view this function as a function of a single variable

$$\Phi(\beta) = \sqrt{\frac{\beta}{\lambda} \frac{\mathcal{H}_{\alpha+2}(2\sqrt{\beta\lambda})}{\mathcal{H}_{\alpha+1}(2\sqrt{\beta\lambda})}} - 1$$

with the parameter  $\lambda > 0$ , and examine its behavior. For clarity, let us again denote  $z = 2\sqrt{\beta\lambda}$  and examine the situation for the extreme value  $\beta \rightarrow 0_+$  of the domain of  $\text{Dom}(\Phi) = (0, +\infty)$

$$\lim_{\beta \rightarrow 0_+} \sqrt{\frac{\beta}{\lambda} \frac{\mathcal{H}_{\alpha+2}(2\sqrt{\beta\lambda})}{\mathcal{H}_{\alpha+1}(2\sqrt{\beta\lambda})}} - 1 = \lim_{z \rightarrow 0_+} \frac{z}{2\lambda} \frac{\mathcal{H}_{\alpha+2}(z)}{\mathcal{H}_{\alpha+1}(z)} - 1.$$

The calculation of the limit can be divided according to the value of the parameter  $\alpha$ :

$$\lim_{z \rightarrow 0_+} \frac{z}{2\lambda} \frac{\mathcal{H}_{\alpha+2}(z)}{\mathcal{H}_{\alpha+1}(z)} - 1 = \begin{cases} \frac{\alpha+1}{\lambda} - 1, & \alpha > -1, \\ -1, & \alpha \leq -1. \end{cases}$$

Since  $\text{Ran}(\Phi) = \langle -1, +\infty \rangle$ , we know from the limit results for  $\alpha \leq -1$  that  $\Phi(z)$  takes its minimum at zero. However, the result for  $\alpha > -1$  suggests that the value of this limit can also be a positive non-zero number, which would mean that the condition  $\Phi(\beta, \lambda) = 0$  cannot be fulfilled. Let us check the monotonicity of the function  $\Phi(z)$  for this case by comparing the limit value of the function  $\Phi(z)$  at the point 0 with all other points  $z > 0$  for  $\alpha < -1$ .

$$\begin{aligned} \Phi(0_+) &= \frac{\alpha+1}{\lambda} - 1 \stackrel{?}{<} \frac{z}{2\lambda} \frac{\mathcal{H}_{\alpha+2}(z)}{\mathcal{H}_{\alpha+1}(z)} - 1 = \Phi(z), \\ \frac{\alpha+1}{\lambda} &\stackrel{?}{<} \frac{z(\alpha+1)}{2\lambda(\alpha+1)} \frac{\mathcal{H}_{\alpha+2}(z)}{\mathcal{H}_{\alpha+1}(z)} \stackrel{(2.5)}{=} \frac{\alpha+1}{\lambda} \frac{\frac{2(\alpha+1)}{z} \mathcal{H}_{\alpha+1}(z) + \mathcal{H}_{\alpha}(z)}{\mathcal{H}_{\alpha+1}(z)}, \\ \frac{\alpha+1}{\lambda} &< \frac{\alpha+1}{\lambda} + \underbrace{\frac{z\mathcal{H}_{\alpha}(z)}{2\lambda\mathcal{H}_{\alpha+1}(z)}}_{>0}. \end{aligned}$$

From the last equation, it is apparent that for  $\alpha > -1$ . No other value of  $\Phi(z)$  for  $z > 0$  can be lower than the value of  $\Phi(0_+)$ . Therefore, if we use the same reasoning as in the section on the existence of solutions to the equation in terms of  $\lambda(\beta)$ , in order for the condition  $\Phi(\beta, \lambda) = 0$  to be satisfied, it must necessarily be true that

$$\inf(\Phi) < 0. \tag{2.22}$$

We can certainly satisfy the condition (2.22) without any problem for  $\alpha \leq -1$ , since we have already found that

$$\inf_{\alpha \leq -1}(\Phi) = -1 < 0.$$

However, for  $\alpha > -1$ , we discover a new, additional, and complementary condition of GIG distribution scalability in the form of

$$\inf_{\alpha > -1}(\Phi) = \frac{\alpha + 1}{\lambda} - 1 < 0 \quad \Leftrightarrow \quad \frac{\alpha + 1}{\lambda} < 1 \quad \Leftrightarrow \quad \alpha - \lambda + 1 < 0. \quad (2.23)$$

This result means that the scaling parameter of the Generalized Inverse Gaussian distribution is

the parameter  $\lambda$  if the condition  $\alpha + \beta + 2 > 0$  is satisfied,

the parameter  $\beta$  if the condition  $\alpha - \lambda + 1 < 0$  is satisfied.

Therefore, we have shown that GIG is scalable for all possible combinations of parameters  $\alpha \in \mathbb{R}, \beta > 0$  and  $\lambda > 0$ . Moreover, the interdependence of parameters  $\lambda$  and  $\beta$  is not accidental and we can even express their mutual relationship in the *Theorem of symmetry of the GIG's scaling equation's solutions*.

**Theorem 2.1** (Symmetry of the Generalized Inverse Gaussian distribution scaling equations' solution). *Let  $m \in \mathbb{R}$ . Let  $g(x|\alpha, \beta, \lambda)$  denote the scaled Generalized Inverse Gaussian distribution with parameters  $\alpha \in \mathbb{R}, \beta > 0, \lambda > 0$  given by*

$$g(x|\alpha, \beta, \lambda) = \Theta(x) \frac{\left(\sqrt{\frac{\lambda}{\beta}}\right)^{\alpha+1}}{2\mathcal{K}_{\alpha+1}(2\sqrt{\beta\lambda})} x^\alpha e^{-\frac{\beta}{x}} e^{-\lambda x}.$$

*Then the solutions of the scaling equation for the functions  $g_1(x|-\frac{3}{2}+m, \beta_1, \lambda_1)$  and  $g_2(x|-\frac{3}{2}-m, \beta_2, \lambda_2)$  are symmetric  $\forall m \in \mathbb{R}$ , i.e.,  $\beta_1 = \lambda_2$  and  $\lambda_1 = \beta_2$ .*

*Proof.* Let  $m \in \mathbb{R}$ . From the assumptions of the theorem, we know that  $g_1(x|-\frac{3}{2}+m, \beta_1, \lambda_1)$  and  $g_2(x|-\frac{3}{2}-m, \beta_2, \lambda_2)$  are scaled distributions. Let us write down the corresponding forms of the scaling equations

$$\mu_1(g_1) \stackrel{(2.8)}{=} \sqrt{\frac{\beta_1}{\lambda_1}} \frac{\mathcal{K}_{\frac{1}{2}+m}(2\sqrt{\beta_1\lambda_1})}{\mathcal{K}_{-\frac{1}{2}+m}(2\sqrt{\beta_1\lambda_1})} = 1, \quad (2.24)$$

$$\mu_1(g_2) \stackrel{(2.8)}{=} \sqrt{\frac{\beta_2}{\lambda_2}} \frac{\mathcal{K}_{\frac{1}{2}-m}(2\sqrt{\beta_2\lambda_2})}{\mathcal{K}_{-\frac{1}{2}-m}(2\sqrt{\beta_2\lambda_2})} = 1. \quad (2.25)$$

Equation (2.25) can be further simplified using properties of the Macdonald function.

$$1 = \sqrt{\frac{\beta_2}{\lambda_2}} \frac{\mathcal{K}_{\frac{1}{2}-m}(2\sqrt{\beta_2\lambda_2})}{\mathcal{K}_{-\frac{1}{2}-m}(2\sqrt{\beta_2\lambda_2})} \stackrel{(2.5)}{=} \sqrt{\frac{\beta_2}{\lambda_2}} \frac{\mathcal{K}_{-\frac{1}{2}+m}(2\sqrt{\beta_2\lambda_2})}{\mathcal{K}_{\frac{1}{2}+m}(2\sqrt{\beta_2\lambda_2})} \quad \Big| \cdot \sqrt{\frac{\lambda_2}{\beta_2}} \frac{\mathcal{K}_{\frac{1}{2}+m}(2\sqrt{\beta_2\lambda_2})}{\mathcal{K}_{-\frac{1}{2}+m}(2\sqrt{\beta_2\lambda_2})},$$

$$\sqrt{\frac{\lambda_2}{\beta_2}} \frac{\mathcal{K}_{\frac{1}{2}+m}(2\sqrt{\beta_2\lambda_2})}{\mathcal{K}_{-\frac{1}{2}+m}(2\sqrt{\beta_2\lambda_2})} = 1. \quad (2.26)$$

We have arrived at two expressions (2.24) and (2.26) that necessarily must be equal to each other, because we assume scaled distributions  $g_1$  and  $g_2$ , therefore

$$\sqrt{\frac{\beta_1}{\lambda_1}} \frac{\mathcal{K}_{\frac{1}{2}+m}(2\sqrt{\beta_1\lambda_1})}{\mathcal{K}_{-\frac{1}{2}+m}(2\sqrt{\beta_1\lambda_1})} = \sqrt{\frac{\lambda_2}{\beta_2}} \frac{\mathcal{K}_{\frac{1}{2}+m}(2\sqrt{\beta_2\lambda_2})}{\mathcal{K}_{-\frac{1}{2}+m}(2\sqrt{\beta_2\lambda_2})}. \quad (2.27)$$

However, for equation (2.27) to hold, it must necessarily be that  $\beta_1 = \lambda_2$  and  $\lambda_1 = \beta_2$ . This completes the proof.  $\square$

### Properties of the scaling function $\beta$

Based on the mentioned symmetry theorem 2.1 and the discovered scaling condition, the reader will certainly not be surprised by Figure 2.4, which is significantly similar to Figure 2.1 as expected.

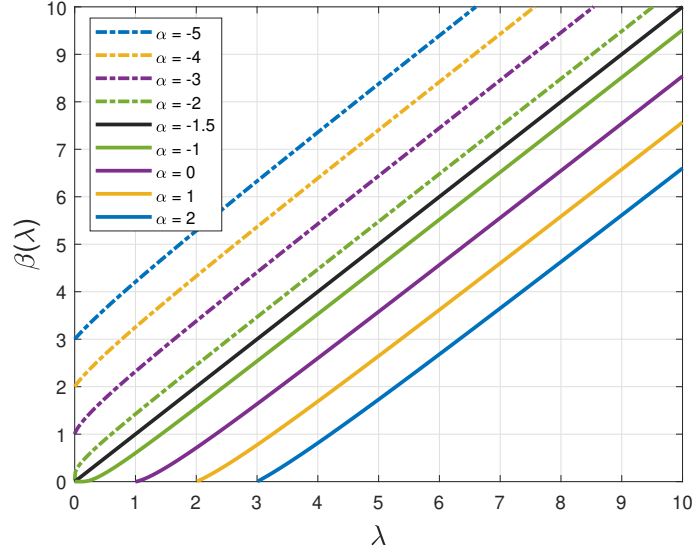


Figure 2.4: Scaling function  $\beta(\lambda)$  for different values of parameter  $\alpha \in \mathbb{R}$ .

From the mutual symmetry around the axis  $\lambda = \beta$ , we can easily determine the asymptote for  $\lambda \rightarrow +\infty$ , which will be in the form

$$\beta(\lambda) = \lambda - \alpha - \frac{3}{2} \quad \text{pro } \alpha \in \mathbb{R} \text{ a } \lambda \rightarrow +\infty.$$

Let us also mention the fact that  $\beta(\lambda)$  is an increasing function. This fact has already been proven in the proof of the monotonicity of  $\lambda(\beta)$  since they are inverse functions, and therefore, the increasing monotonicity of  $\lambda(\beta)$  implies the increasing monotonicity of  $\beta(\lambda)$ . Of course, the limit behavior at the origin of the coordinate system is analogous to the previous task, i.e.,

$$\lim_{\lambda \rightarrow 0_+} \beta_\alpha(\lambda) = -\alpha - 2 \quad \text{for } \alpha < -2,$$

$$\lim_{\lambda \rightarrow 0_+} \beta_\alpha(\lambda) = 0 \quad \text{for } \alpha \in \langle -2, -1 \rangle,$$

$$\lim_{\lambda \rightarrow \alpha+1} \beta_\alpha(\lambda) = 0 \quad \text{for } \alpha > -1.$$

Furthermore, this is also related to the possibility of using the already proven relationships (2.11) and (2.12), and we can use these findings to define a scaling area for  $\beta(\lambda)$ , which is graphically shown in Figure 2.5. Based on the mentioned properties, we can conclude this subsection by providing insights allowing for narrowing down the scaling area (see Figure 2.6). The function  $\beta(\lambda)$  is

convex if  $\alpha > -\frac{3}{2}$ , and its narrowed scaling area is  $\lambda - \alpha - \frac{3}{2} < \beta(\lambda) < \lambda - \alpha - 2$ ,

linear if  $\alpha = -\frac{3}{2}$ ,

concave if  $\alpha < -\frac{3}{2}$ , and its narrowed scaling area is  $\lambda - \alpha - 1 < \beta(\lambda) < \lambda - \alpha - \frac{3}{2}$ .

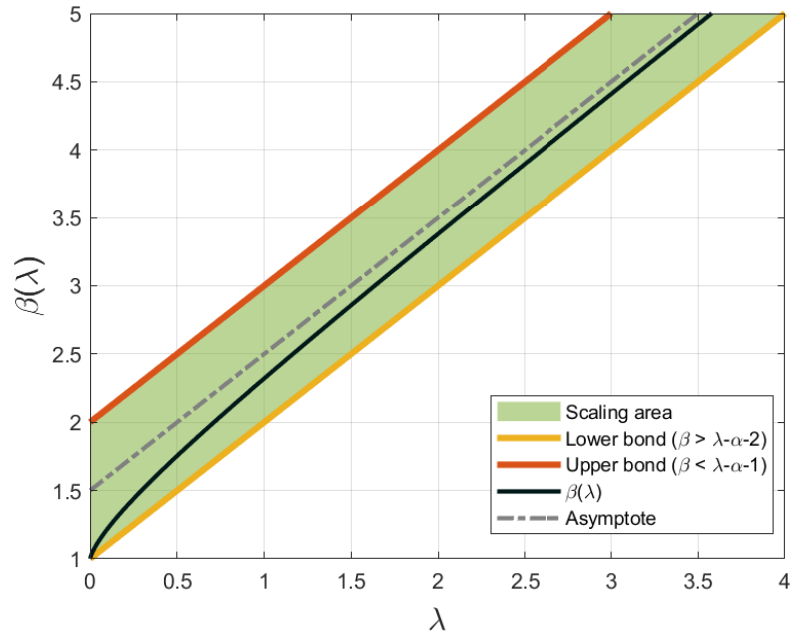


Figure 2.5: Example of scaling area for  $\beta(\lambda)$ , where  $\alpha = -3$ .

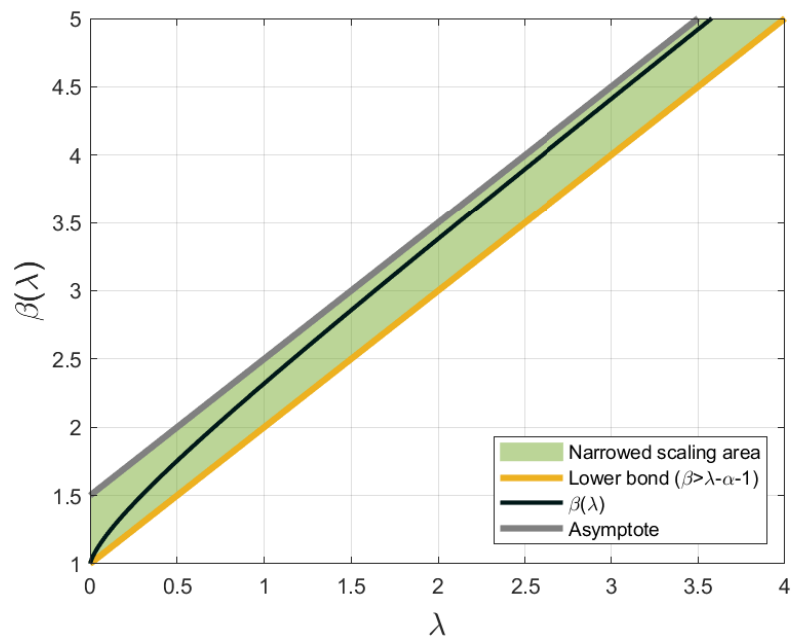


Figure 2.6: Example of narrowed scaling area for  $\beta(\lambda)$ , where  $\alpha = -3$ .

### 2.4.3 Summary of scaling results

The previous methods have examined the scaling of the Generalized Inverse Gaussian distribution for all parameter values of  $\alpha \in \mathbb{R}, \beta > 0$ , and  $\lambda > 0$ . For clarity, let us summarize the results of this chapter and comment on how these findings complement current research.

Let's start with the overview of previous research. The first work that dealt with the scaling problem was [18], but the research was focused only on non-negative values of the parameter  $\alpha$  because negative values were not attributed too much importance in the field of traffic modeling at that time. The contribution of this work is the derivation of an asymptotic approximation of the scaling function for non-negative values of the parameter  $\alpha$ . The awareness of the negative values began to change with the arrival of specific data, such as gaps between vehicles in the fast lane of a highway. These data motivated research [1], [7], and [8], which paid more attention to the negative values of  $\alpha$ . As shown in the [10], the research on the properties of the Generalized Inverse Gaussian distribution with negative values of the parameter  $\alpha$  was a symmetrical task to the study of non-negative values, and a large part of the knowledge about GIG distribution with non-negative values also applies to GIG distribution with negative values of  $\alpha$ . However, a so-called scaling condition was formulated for negative values of the parameter  $\alpha$ . In [10], which was followed by [11], it was believed that the scaling problem for parameter configurations that do not satisfy the scaling condition is not solvable, but that was in contradiction with the facts, such as the existence of all moments of the GIG distribution. Despite this factual contradiction, [11] continued to improve the approximation of the scaling function under the scaling condition, and in combination with [13], it complemented the theory regarding the properties and relationships of the scaled GIG distribution.

In this thesis, however, we tackled the scaling problem from a general perspective, without a predefined division of research into non-negative and negative values of the parameter  $\alpha$ . Removing this historically established boundary enabled us to solve the scaling problem for all parameter values and uncovered a new space for further research.

The main message of this entire chapter is that scaling of the Generalized Inverse Gaussian distribution depends on the parameter configuration. If the condition  $\alpha + \beta + 2 > 0$  holds, then the scaling parameter can be chosen as the parameter  $\lambda$ , and the scaling function  $\lambda_\alpha(\beta)$  for a fixed value of the parameter  $\alpha \in \mathbb{R}$

- is generated by the scaling equation (2.13),
- is an increasing function,
- has an asymptotic approximation of  $\lambda_\alpha(\beta) \approx \alpha + \beta + \frac{3}{2}$  as  $\beta \rightarrow +\infty$ ,
- has the following behavior at the origin of the coordinate system
  - $\lim_{\beta \rightarrow -\alpha-2} \lambda_\alpha(\beta) = 0$  for  $\alpha < -2$ ,
  - $\lim_{\beta \rightarrow 0_+} \lambda_\alpha(\beta) = 0$  for  $\alpha \in (-2, -1)$ ,
  - $\lim_{\beta \rightarrow 0_+} \lambda_\alpha(\beta) = \alpha + 1$  for  $\alpha > -1$ ,
- is, depending on the value of the parameter  $\alpha$ ,
  - concave for  $\alpha > -\frac{3}{2}$  and
    - upper-bounded  $\lambda_\alpha(\beta) < \alpha + \beta + \frac{3}{2}$ ,

- lower-bounded  $\lambda_\alpha(\beta) > \alpha + \beta + 1$ ,
- linear for  $\alpha = -\frac{3}{2}$ , where  $\lambda_\alpha(\beta) = \beta$ ,
- convex for  $\alpha < -\frac{3}{2}$  and
  - upper-bounded  $\lambda_\alpha(\beta) < \alpha + \beta + 2$ ,
  - lower-bounded  $\lambda_\alpha(\beta) > \alpha + \beta + \frac{3}{2}$ .

Furthermore, if the condition  $\alpha - \lambda + 1 < 0$  holds, then the scaling parameter can be chosen as the parameter  $\beta$ , and the scaling function  $\beta_\alpha(\lambda)$  for a fixed value of the parameter  $\alpha \in \mathbb{R}$

- is generated by the scaling equation (2.13),
- is the inverse of the function  $\lambda_\alpha(\beta)$  mentioned above,
- is an increasing function,
- has the asymptotic approximation  $\beta_\alpha(\lambda) \approx \lambda + \alpha - \frac{3}{2}$  for  $\lambda \rightarrow +\infty$ ,
- behaves as follows at the origin of the coordinate system:
  - $\lim_{\lambda \rightarrow 0_+} \beta_\alpha(\lambda) = -\alpha - 2$  for  $\alpha < -2$ ,
  - $\lim_{\lambda \rightarrow 0_+} \beta_\alpha(\lambda) = 0$  for  $\alpha \in \langle -2, -1 \rangle$ ,
  - $\lim_{\lambda \rightarrow \alpha+1} \beta_\alpha(\lambda) = 0$  for  $\alpha > -1$ ,
- is, depending on the value of the parameter  $\alpha$ ,
  - convex for  $\alpha > -\frac{3}{2}$  and
    - upper-bounded by  $\beta_\alpha(\lambda) < \lambda - \alpha - 2$ ,
    - lower-bounded by  $\beta_\alpha(\lambda) > \lambda - \alpha - \frac{3}{2}$ ,
  - linear for  $\alpha = -\frac{3}{2}$  with  $\beta_\alpha(\lambda) = \lambda$ ,
  - concave for  $\alpha < -\frac{3}{2}$  and
    - upper-bounded by  $\beta_\alpha(\lambda) < \lambda - \alpha - \frac{3}{2}$ ,
    - lower-bounded by  $\beta_\alpha(\lambda) > \lambda - \alpha - 1$ .

These two sets

$$\Lambda := \{\alpha, \beta, \lambda : \alpha \in \mathbb{R} \wedge \beta > 0 \wedge \lambda > 0 \wedge \alpha + \beta > -2\},$$

$$\Upsilon := \{\alpha, \beta, \lambda : \alpha \in \mathbb{R} \wedge \beta > 0 \wedge \lambda > 0 \wedge \alpha - \lambda < -1\},$$

defined by the aforementioned scaling conditions are not disjoint, i.e.,  $\Lambda \cap \Upsilon \neq \emptyset$ , but certainly cover the entire admissible parameter space of the GIG distribution, thus

$$\Lambda \cup \Upsilon = \{\alpha, \beta, \lambda : \alpha \in \mathbb{R} \wedge \beta > 0 \wedge \lambda > 0\}.$$



## 2.5 Compressibility of systems generated by GIG distribution

From Chapter 1, we know that one of the variables characterizing a balanced particle system is the statistical compressibility (1.4). Together with this concept, we introduced the classification of balanced particle systems in Definition 1.3 into sub-compressible, uni-compressible, and super-compressible. Let us examine this characteristic for particle systems generated by GIG distribution and try to classify them based on different values of parameters  $\alpha \in \mathbb{R}, \beta > 0$  and  $\lambda > 0$ . We emphasize that according to Definition 1.3, scaled distributions must be considered. For scaled generalized inverse Gaussian distribution, we have shown in the calculation (2.10) that

$$\chi = \text{VAR}[X] = \frac{\alpha + \beta + 2}{\lambda} - 1. \quad (2.28)$$

If we consider first the scaled Generalized Inverse Gaussian (GIG) distribution with the constraint  $\alpha \geq 0$ , then we have already shown in the previous text that it is a generator of (scaled) balanced particle systems with a repulsive generator, and we know that these systems are always sub-compressible, i.e.,  $\chi < 1$ .

Let us further consider  $\alpha < 0$  and recall the relationships between the parameters of the scaled GIG distribution (2.11) and (2.12). First, let us reveal for which parameter values the system is still sub-compressible, i.e.,

$$\chi = \frac{\alpha + \beta + 2}{\lambda} - 1 \stackrel{!}{<} 1.$$

By a simple manipulation of the expression on the left-hand side, we obtain the inequality

$$\underbrace{\alpha + \beta - \lambda + 1}_{<0} < \lambda - 1.$$

However, according to equation (2.12), we know that the largest possible value that the expression on the left-hand side can take is zero. Therefore, if

$$\lambda > 1,$$

then we can declare that it is indeed a sub-compressible particle system. Let us add that if  $\lambda = 1$ , then

$$\chi = \underbrace{\alpha + \beta + 1}_{\substack{(2.12) \\ <0}} < 1,$$

so we can extend the sub-compressibility of the system to  $\lambda \geq 1$ . For the remaining choices of parameters  $\alpha < 0, \beta > 0$  and  $\lambda \in (0, 1)$ , the study of compressibility is a more difficult task. By direct application of logical reasoning, we can still solve the compressibility for the following cases, when

$$\beta \in \langle -\alpha, +\infty \rangle:$$

$$\chi = \frac{\alpha + \beta + 2}{\lambda} - 1 = \underbrace{\frac{\alpha + \beta}{\lambda}}_{\geq 0} + \frac{1}{\lambda} + \underbrace{\frac{1}{\lambda} - 1}_{>0} > \frac{1}{\lambda} > 1,$$

$$\beta \in (0, -\alpha - 1) \wedge \lambda \in \left(\frac{1}{2}, 1\right):$$

$$\chi = \frac{\alpha + \beta + 2}{\lambda} - 1 < \frac{\alpha + (-\alpha - 1) + 2}{\frac{1}{2}} - 1 = 1.$$

For the remaining parameter values, we have not yet been able to classify the corresponding systems.

## Chapter 3

# Estimation of GIG-distributed data

A thorough research of the properties of the Generalized Inverse Gaussian (GIG) distribution offers possibilities for improving methods and procedures that are commonly used in practice when working with GIG-distributed data. In this thesis, we have chosen methods for point estimation of parameters as the area for the application of the discovered properties. We will consider three basic methods for parameter estimation:

Method of Moments (MM),

Minimum Distance Estimator (MDE),

Maximum Likelihood Estimator (MLE).

For the correctness of the following text, let us consider a probability space  $(\Omega, \mathcal{F}, \mathcal{P})$ , where  $\Omega$  is the set of all possible outcomes called sample space,  $\sigma$ -algebra  $\mathcal{F}$  is a collection of all the events called event space, and  $\mathcal{P}$  is a probability measure. Furthermore, let us denote by  $f_\theta \in \mathcal{F}$  a distribution with parameters  $\theta$  from the parameter space  $\Theta \subset \mathbb{R}^k$ . Using this distribution, we generate a random variable  $X \sim f_\theta$ . We then refer to an independent random sample  $\mathbf{X}$  as a tuple of  $n$  independent random variables  $(X_1, \dots, X_n)$  with the same distribution  $f_\theta$ .

The task of estimation methods is to estimate the parameterization of the assumed distribution  $f_{\hat{\theta}}$  based on real data  $(x_1, x_2, \dots)$ , i.e., the realization of the random sample  $\mathbf{X}$ , by finding estimates  $\hat{\theta}$  for the parameters  $\theta$ .

### 3.1 Methods for point estimation of parameters

#### 3.1.1 Method of Moments (MM)

The method of moments is based on the use of the general moments of the distribution  $\mu_n(f_\theta)$ ,  $n \in \mathbb{N}$ , from which it is possible to construct a system of moment equations (denoted as  $ME_q$ ). The advantage of this method is that it takes into account all the data from the sample, as the method consists in estimating the parameters  $\hat{\theta}$  of the distribution so that the sample moments of the random variable correspond to the moments of the theoretical distribution with these parameters  $\theta$ . To create the system of equations, we need to introduce a regular and injective mapping on the chosen class of densities

$$\boldsymbol{\mu}(\theta) = (\mu_1(\theta), \dots, \mu_s(\theta)) : \mathbb{R}^k \rightarrow \mathbb{R}^s,$$

for which there exists an inverse mapping  $\boldsymbol{\mu}^{-1}$  in the given class. This mapping  $\boldsymbol{\mu}(\theta)$  is called the moment subcode of the distribution  $f$  with parameters  $\theta$  of length  $s$  and is defined by the equation

$$\mu_r = \mu_r(\theta) = \mathbf{E}[X^r], \quad r \in \hat{s}.$$

Using the moment subcode  $\boldsymbol{\mu}(\theta)$ , we can introduce the moment estimate  $\hat{\theta}_M$  of the parameter  $\theta \in \mathbb{R}^k$  as

$$\hat{\theta}_M := \hat{\theta}_M(\mathbf{X}) = \boldsymbol{\mu}^{-1}(m'_1(\mathbf{X}), \dots, m'_k(\mathbf{X})),$$

where  $m'_r = \frac{1}{n} \sum_{i=1}^n X_i^r$  represents the  $r$ -th sample moment. The estimate  $\hat{\theta}_M$  is the solution to the  $\text{ME}_q$  equations of the form

$$\mu_r(\theta) = m'_r(\mathbf{X}) \quad \forall r \in \hat{s}. \quad (3.1)$$

If the system of  $\text{ME}_q$  equations is not uniquely solvable, or if one of the moments does not depend on  $\theta$ , we can add an additional equation in the form of  $\mu_{s+1}(\theta) = m'_{s+1}(\mathbf{X})$ . In this method, we can also alternatively use the central moments  $m_r(\mathbf{X})$ , where  $\mu_r(\theta) = \mathbf{E}[X - \mathbf{E}[X]]^r$ .

In [10], we have already applied the method of moments to the GIG distribution and arrived at the following estimates of parameters:

$$\begin{aligned} \hat{\alpha}_M &= \frac{4n \left[ \sum_{i=1}^n X_i^3 \right]^2 - 6 \sum_{i=1}^n X_i \sum_{i=1}^n X_i^2 \sum_{i=1}^n X_i^3 - 3n \sum_{i=1}^n X_i^2 \sum_{i=1}^n X_i^4 + 3 \left[ \sum_{i=1}^n X_i^2 \right]^3 + 2 \left[ \sum_{i=1}^n X_i \right]^2 \sum_{i=1}^n X_i^4}{n \sum_{i=1}^n X_i^2 \sum_{i=1}^n X_i^4 - \left[ \sum_{i=1}^n X_i^2 \right]^3 - \left[ \sum_{i=1}^n X_i \right]^2 \sum_{i=1}^n X_i^4 - n \left[ \sum_{i=1}^n X_i^3 \right]^2 + 2 \sum_{i=1}^n X_i \sum_{i=1}^n X_i^2 \sum_{i=1}^n X_i^3}, \\ \hat{\beta}_M &= \frac{1}{n} \hat{\lambda}_M \sum_{i=1}^n X_i^2 - \frac{1}{n} (\hat{\alpha}_M + 2) \sum_{i=1}^n X_i, \\ \hat{\lambda}_M &= \frac{n(\hat{\alpha}_M + 3) \sum_{i=1}^n X_i^2 - (\hat{\alpha}_M + 2) \left[ \sum_{i=1}^n X_i \right]^2}{n \sum_{i=1}^n X_i^3 - \sum_{i=1}^n X_i \sum_{i=1}^n X_i^2}. \end{aligned}$$

Thanks to this result, we are able to determine the parameter values of the distribution solely based on data, without using any numerical heuristics.

### 3.1.2 Minimum Distance Estimator (MDE)

The minimum distance estimator is particularly suitable for finding consistent estimates, i.e., estimates that become more accurate as the amount of data increases. Its principle is based on minimizing the distance between a parametrized distribution function and the empirical distribution function obtained from the data. If we have independent random variables with the same distribution  $X_1, \dots, X_n \sim f_\theta$ , we introduce the empirical distribution function  $F_{\theta,n}(x)$  as

$$F_{\theta,n}(x) = \frac{1}{n} \sum_{i=1}^n \mathbb{I}_{(-\infty, x)}(X_i),$$

where  $\mathbb{I}$  denotes the indicator function. We can also understand it as, for each  $x_i$ ,  $F_{\theta,n}(x_i)$  is the number of elements less than or equal to  $x_i$  divided by the total number of elements. Therefore, let  $X_1, \dots, X_n$  be a random sample from the distribution  $f_\theta(x)$ ,  $\theta \in \Theta \subset \mathbb{R}^k$ , and  $F_{\theta,n}(x)$  be the empirical distribution function. If there exists an estimate  $\hat{\theta} = \hat{\theta}(X_1, \dots, X_n)$  such that

$$\mathbf{d}[F_{\hat{\theta}}(x), F_{\hat{\theta},n}(x)] = \inf_{\theta \in \Theta} \{\mathbf{d}[F_\theta(x), F_{\theta,n}(x)]\},$$

we call it an estimate with minimum distance. The mapping  $d[\cdot, \cdot]$  from the class of functions to the space of real numbers is understood as a general functional metric<sup>1</sup> that satisfies the axioms of a metric on suitable function spaces. In this task, we will use the Kolmogorov distance defined for functions  $F, G : \mathbb{R} \rightarrow \mathbb{R}$  as

$$d_K[F, G] := \sup_{x \in \mathbb{R}} |F(x) - G(x)|.$$

In the language of measured data, the computation of the estimate is given by the following equation

$$\hat{\theta} = \arg \min_{\theta \in \Theta} \max_{i=1, \dots, n} |F_{\theta}(x_i) - F_{\theta, n}(x_i)|. \quad (3.2)$$

Alternatively, the MDE can also be applied to probability densities (empirical and theoretical), but for systems with smaller ranges of data samples, this method is not suitable since the choice of the division of the  $x$ -axis (binning) affects its results in an undesirable manner.

### 3.1.3 Maximum Likelihood Estimator (MLE)

This method aims to maximize the joint probability density with respect to a parameter contained in the proposed distribution. This means that the goal of this method is to maximize the probability of observed data. If we have independent random variables  $X_1, \dots, X_n$  with the same distribution  $f_{\theta}(x)$ , we introduce the likelihood function  $L(\theta)$  by

$$L(\theta) = \prod_{i=1}^n f_{\theta}(x_i)$$

and the logarithmic likelihood function

$$\ell(\theta) = \ln L(\theta) = \sum_{i=1}^n \ln f_{\theta}(x_i).$$

In practice, the logarithmic likelihood function is more often used to compute the maximum likelihood estimate (MLE), since the sum makes it easier to perform the necessary derivatives. The maximum likelihood estimate is then defined as

$$\hat{\theta}_{MLE}(\mathbf{X}) = \arg \sup_{\theta \in \Theta} L(\theta) = \arg \sup_{\theta \in \Theta} \ell(\theta), \quad (3.3)$$

provided that  $\hat{\theta}_{MLE}$  is Borel measurable, unique, and depends on  $\mathbf{X}$ . Therefore, finding the maximum likelihood estimate is the task of investigating the maximum of the (logarithmic) likelihood function. The general procedure is to set up a system of likelihood equations (denoted by  $LE_q$ )

$$\frac{\partial \ell(\vartheta_1, \dots, \vartheta_s)}{\partial \vartheta_i} = 0 \quad \forall i \in \hat{s},$$

where  $\vartheta_1, \dots, \vartheta_s$  are parameters from the set  $\theta$  of the  $f_{\theta}$  distribution with exactly  $s$  parameters. By solving these equations, we obtain estimates  $(\hat{\vartheta}_1, \dots, \hat{\vartheta}_s) = \hat{\theta}_{MLE}$ .

<sup>1</sup>Metric on a set  $\mathbb{S}$  is a function  $d : \mathbb{S} \times \mathbb{S} \rightarrow \mathbb{R}$  that satisfies the following three axioms for all  $x, y, z \in \mathbb{S}$ :

- Non-negativity:  $d[x, y] \geq 0$ , and  $d[x, y] = 0$  if and only if  $x = y$ .
- Symmetry:  $d[x, y] = d[y, x]$ .
- Triangle inequality:  $d[x, y] \leq d[x, z] + d[z, y]$ .

For the Generalized Inverse Gaussian distribution, the logarithmic likelihood function has the following form:

$$\ell(\alpha, \beta, \lambda) = \frac{n(\alpha + 1)}{2} [\ln \lambda - \ln \beta] - n \ln 2 - n \ln \mathcal{K}_{\alpha+1}(2\sqrt{\beta\lambda}) - \lambda \sum_{i=0}^n x_i - \beta \sum_{i=1}^n \frac{1}{x_i} + \alpha \sum_{i=1}^n \ln x_i.$$

The corresponding system of likelihood equations is

$$\begin{aligned} \frac{\partial \ell(\alpha, \beta, \lambda)}{\partial \alpha} &= \frac{n}{2} [\ln \lambda - \ln \beta] - n \frac{\frac{\partial}{\partial \alpha} \mathcal{K}_{\alpha+1}(2\sqrt{\beta\lambda})}{\mathcal{K}_{\alpha+1}(2\sqrt{\beta\lambda})} + \sum_{i=1}^n \ln x_i = 0, \\ \frac{\partial \ell(\alpha, \beta, \lambda)}{\partial \beta} &= -\frac{n(\alpha + 1)}{2\beta} - n \frac{\sqrt{\frac{\lambda}{\beta}} \mathcal{K}'_{\alpha+1}(2\sqrt{\beta\lambda})}{\mathcal{K}_{\alpha+1}(2\sqrt{\beta\lambda})} - \sum_{i=1}^n \frac{1}{x_i} = 0, \\ \frac{\partial \ell(\alpha, \beta, \lambda)}{\partial \lambda} &= \frac{n(\alpha + 1)}{2\lambda} - n \frac{\sqrt{\frac{\beta}{\lambda}} \mathcal{K}'_{\alpha+1}(2\sqrt{\beta\lambda})}{\mathcal{K}_{\alpha+1}(2\sqrt{\beta\lambda})} - \sum_{i=1}^n x_i = 0. \end{aligned}$$

Clearly, finding an analytical solution to this system is not a trivial task and it is therefore appropriate to solve this problem numerically.

### 3.1.4 Proposal for improving estimation methods

The minimum distance estimator and the maximum likelihood estimator are in practice dependent on numerical methods when working with data, and unlike the method of moments, the resulting estimates may not always have the same values and may differ due to the randomness brought by the use of numerical methods or heuristics.

Therefore, the first improvement that arises based on theoretical knowledge is the relationships between the parameters for scaled GIG data (2.11) and (2.12), i.e. the inequalities

$$\alpha + \beta - \lambda + 2 > 0 \quad \text{and} \quad \alpha + \beta - \lambda + 1 < 0.$$

Based on these two seemingly simple inequalities, we are able to define an area where we expect values of the GIG distribution parameters. This idea can provide algorithms with information on whether they are searching for parameters in the proper sub-area.

The second, equally important improvement is based on the knowledge presented in [14] utilizing the properties of the stochastic compressibility of the GIG distribution (2.28)

$$\chi = \text{VAR}[X] = \frac{\alpha + \beta + 2}{\lambda} - 1.$$

When working with real data, it is an easy task to obtain the variance of the data  $\text{VAR}[X]$ , which allows us to use the aforementioned formula to reformulate the estimation problem. We can express the estimate of the parameter  $\hat{\alpha}$  using the variance of the data and the estimates of the remaining two parameters  $\hat{\beta}$  and  $\hat{\lambda}$

$$\hat{\alpha} = [\text{VAR}[X] + 1]\hat{\lambda} - \hat{\beta} - 2.$$

In the application, the estimation method does not search for estimates of three parameters, but only two, reducing the problem's complexity.

Since the method of moments estimates are given by explicit computation from data, the mentioned procedures cannot be applied to this method. However, these ideas can be implemented for the minimum distance estimator and the maximum likelihood estimator. These modified versions of the methods are referred to as the assisted minimum distance estimator (AMDE) and the assisted maximum likelihood estimator (AMLE).

## 3.2 Testing of estimation methods

The last part of this thesis is devoted to implementing and comparing classical and assisted methods. Our goal is to investigate whether the proposed improvements have led to a statistically significant decrease in the error rate of the method or whether the effect of assistance has not been manifested. Simplified pseudocodes describing the implementation of estimation methods are attached in the Appendix. We implemented the estimators in the MATLAB environment, version R2020b.

### 3.2.1 Experiment design

We tested the MDE, MLE, AMDE, and AMLE methods on scaled synthetic data generated using a random number generator from the Generalized Inverse Gaussian distribution with the parameters

$$\alpha = -2,$$

$$\beta = 4,$$

$$\lambda = 3.5290,$$

and mean  $E[X] \doteq 1$  and variance  $\text{VAR}[X] \doteq 0.1334$ . This generator was constructed according to [2] and is freely available (see [17]). In addition to comparing the results based on the used method, we also examined the effects of contamination and sample size.

#### 3.2.1.1 $2^k$ factorial design

The  $2^k$  factorial design without replications was used for the experiment. A  $2^k$  factorial design is a type of experimental design commonly used in statistical analysis. In this design,  $k$  independent variables are manipulated, each with two levels (usually labeled as -1 and +1), to create a set of experimental conditions. The design is called "factorial" because the levels of each independent variable are combined with the levels of the other independent variables to create a factorial set of conditions. The purpose of a  $2^k$  factorial design is to study the main effects of each independent variable and the interactions between them. The main effect of an independent variable refers to the effect of that variable alone, while an interaction refers to the effect of the combination of two or more independent variables. The advantage of the  $2^k$  factorial design is that it allows for the efficient study of multiple independent variables and their interactions in a relatively small number of experimental conditions. However, this design also has limitations, including the assumption that the effects of the independent variables are linear and that there are no higher-order interactions between the independent variables. More details on this experimental design can be found in [12].

The experiment in this thesis involves a total of  $k = 6$  factors, hence  $2^6 = 64$  measurements. In order to verify the assumption of linearity, it is also necessary to generate data that are located in the center of the intervals of individual numerical variables. These additional measurements are called center-points and are labeled as level 0.

The experiment therefore consists of the following settings:

- A) The estimation method used:
- 1: minimum distance estimator,
  - +1: maximum likelihood estimator.
- B) The use of assistance introduced in Section 3.1.4:
- 1: without assistance, it is a classical version of the methods listed in A),
  - +1: with assistance, it is an assisted version of the methods listed in A).
- C) The size of the generated data sample:
- 1: 500 data points:  $E[X] \doteq 0.9770$ ,
  - 0 : 2,750 data points:  $E[X] \doteq 1.0043$ ,
  - +1: 5,000 data points:  $E[X] \doteq 1.0059$ .
- D) The percentage of data contamination<sup>2</sup> taken with respect to the total sample size:
- 1: 0%,
  - 0 : 5%,
  - +1: 10%.
- E) The distribution (source) from which the data used for contamination originate:
- 1: uniform with expected value  $\mu$ ,
  - +1: exponential with expected value  $\mu$ .
- F) The expected value of the distribution from which the data used for contamination originate:
- 1: the same, i.e.,  $\mu = E[X] = 1$ ,
  - +1: different, with the chosen different value  $\mu = E[X] = 3$ .

In this experiment, we observe the maximum absolute error (denoted MAE) and the mean squared error (denoted MSE) as the target variables, see Table 3.1. At the same time, we store information about which parameter values were estimated in each measurement. The individual factors and their levels are summarized more clearly once more in Table 3.2.

	target variables	formula
MAE	maximum absolute error	$MAE = \max( f_{\alpha,\beta,\lambda}(x) - f_{\hat{\alpha},\hat{\beta},\hat{\lambda}}(x) )$
MSE	mean squared error	$MSE = \text{mean}((f_{\alpha,\beta,\lambda}(x) - f_{\hat{\alpha},\hat{\beta},\hat{\lambda}}(x))^2)$

Table 3.1: Target variables used in the  $2^6$  factorial design.

<sup>2</sup>Note that if the contamination level is 0%, factors E and F are irrelevant for the measurements.

	factor variables	variable type	level -1	level 0	level +1
A	estimation method	categorical	MDE	none	MLE
B	assistance used	categorical	no	none	yes
C	sample size	numerical	500	2,750	5,000
D	contamination	numerical	0%	5%	10%
E	source distribution of the contamination	categorical	uniform	none	exponential
F	expected value of the contamination distribution	categorical	same ( $\mu = 1$ )	none	different ( $\mu = 3$ )

Table 3.2: Factors used in the  $2^6$  factorial design.

### 3.2.2 Evaluation of the experiment

#### 3.2.2.1 Analysis of measured data

Before evaluating the results, let's first analyze the data we have collected. Let's consider the data without center-points. Even from basic descriptive analysis, we can gain interesting insights that can later be confirmed (or rejected) by statistical evaluation of the experiment. We performed this analysis of the results and the subsequent evaluation of the experiment in the language R, version 4.0.2. The Tables 3.13, 3.14 and 3.15 containing the measured data are available at the end of the thesis in the Appendix. In the Figure 3.1, we have prepared simple illustration to demonstrate the meaning of maximum absolute error and mean squared error in the estimation context.

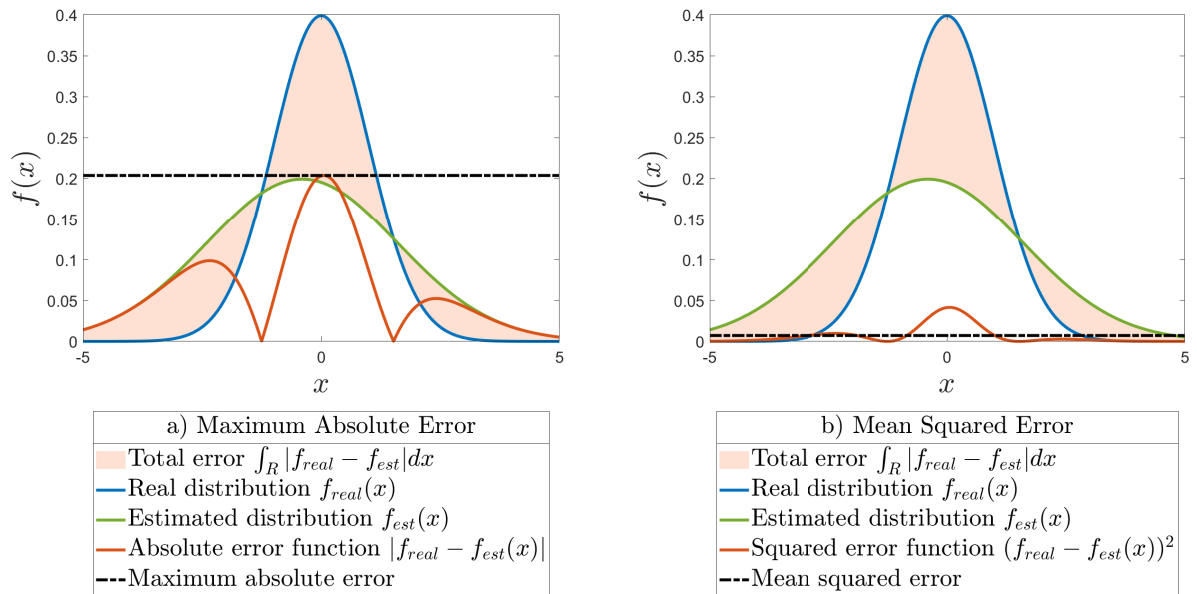


Figure 3.1: Illustrative example of the meaning behind a) maximum absolute error (MAE) and b) mean squared error (MSE).



First, let's look at the distribution of the estimated parameters  $\hat{\alpha}, \hat{\beta}, \hat{\lambda}$  when considering uncontaminated data, i.e., when factor D was set to a value of 0%, and let's distinguish between the individual methods. Recall that the original configuration of the parameters is  $\alpha = -2, \beta = 4$ , and  $\lambda = 3.5290$ . Table 3.3 shows the distribution of the parameters using minimum, mean, median, and maximum. Overall, the estimates for the parameter  $\alpha$  of the classical and assisted minimum distance methods came out negative in mean and median, while both maximum likelihood methods tended to positive values. A pleasant finding is that all methods have at least minimal estimates of the parameter  $\alpha$  negative, but only the assisted minimum distance method was able to get closest to the original value of -2. An interesting phenomenon is that in all cases, the statistics for estimates of the parameter  $\beta$  came out lower than for the estimates of the parameter  $\lambda$ , while in the original configuration,  $\beta = 4 > \lambda = 3.5290$ .

method	parameter	min	mean	median	max
MDE	$\hat{\alpha}$	-0.714	-0.200	-0.247	0.216
	$\hat{\beta}$	2.666	2.920	2.940	3.178
	$\hat{\lambda}$	3.564	4.117	4.004	4.662
AMDE	$\hat{\alpha}$	-2.223	-1.087	-1.087	0.050
	$\hat{\beta}$	3.020	3.785	3.785	4.549
	$\hat{\lambda}$	3.919	4.189	4.189	4.459
MLE	$\hat{\alpha}$	-1.596	1.162	1.071	3.751
	$\hat{\beta}$	1.719	2.716	2.692	3.751
	$\hat{\lambda}$	3.618	5.277	5.214	7.230
AMLE	$\hat{\alpha}$	-1.581	0.894	0.894	3.369
	$\hat{\beta}$	2.085	2.922	2.922	3.760
	$\hat{\lambda}$	3.675	5.214	5.214	6.752

Table 3.3: The distribution of estimated parameter's values.

Next, let's examine the data in terms of the maximum absolute error (MAE). In Figure 3.2, the MAE histogram is shown, with errors measured with and without contamination (factor D) distinguished by color. It is not surprising that the variance of MAE for contaminated data is visibly larger than for uncontaminated data. More detailed look at performance of each estimation method can be seen in Figure 3.3. The influences of individual factors on the maximum absolute error can be observed in the boxplots in Figure 3.4. Based on these boxplots, we expect that the effects of factors A, C, or D could be confirmed as significant by the experiment.

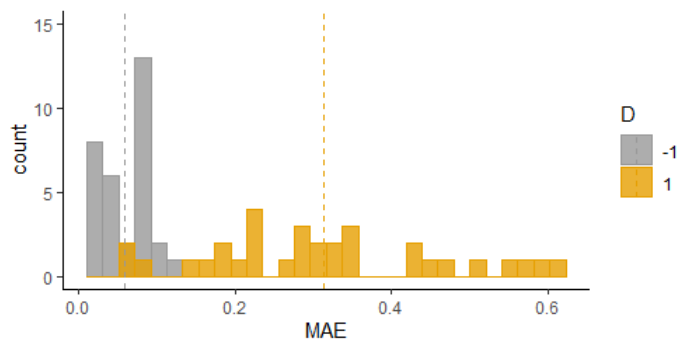


Figure 3.2: Histogram of maximum absolute error based on level of contamination.

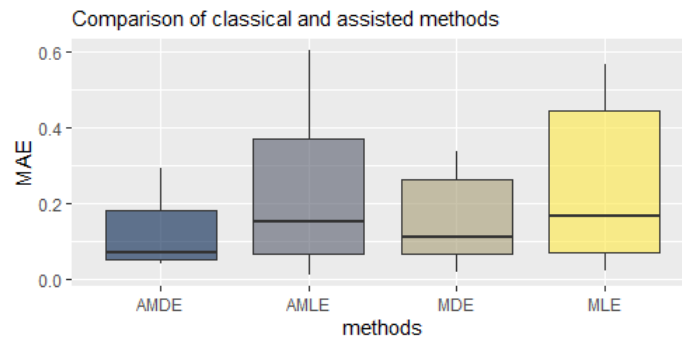


Figure 3.3: Boxplot comparing MAE for each estimation method.

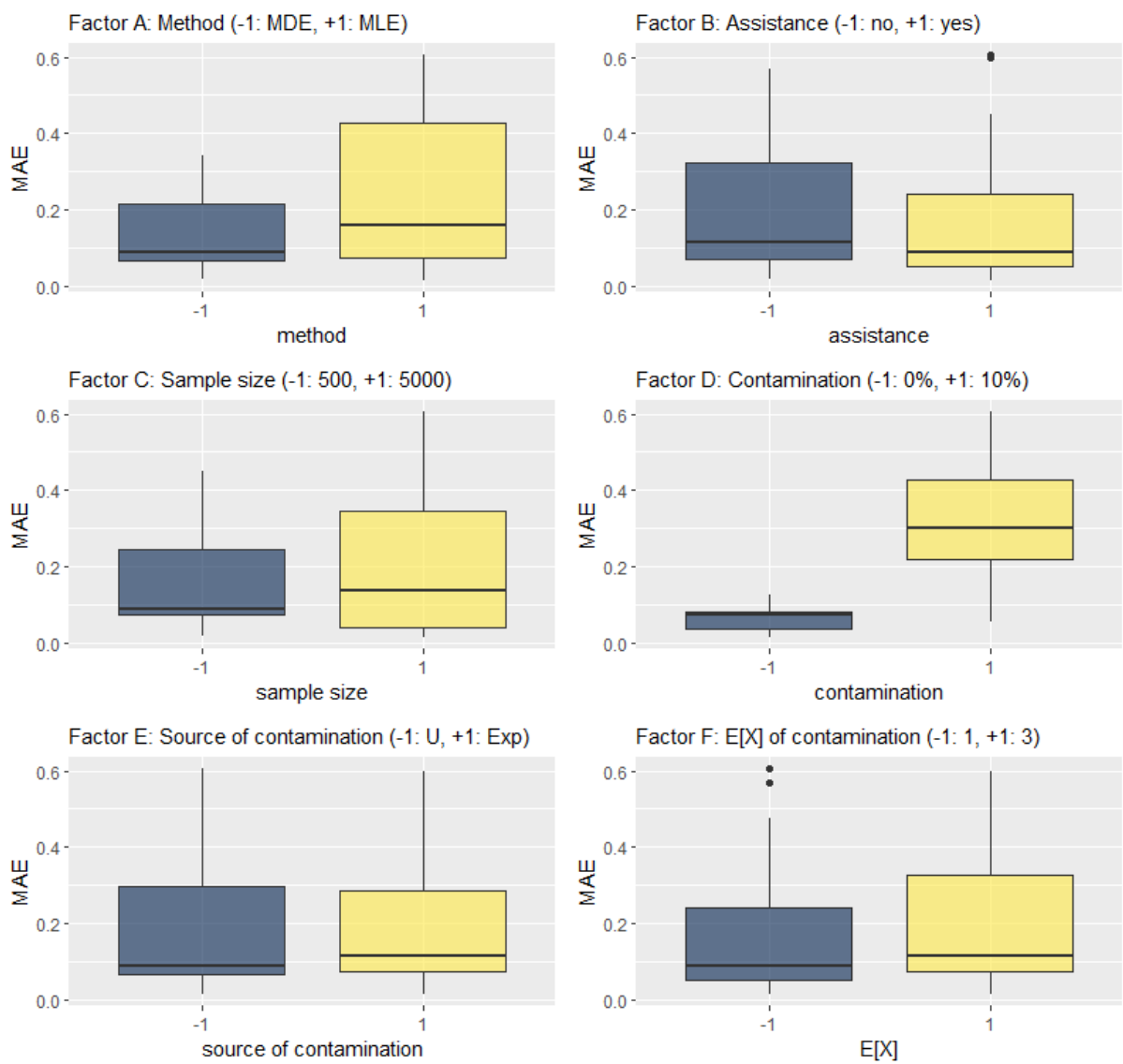


Figure 3.4: Boxplots of maximum absolute error for each factor.

Similarly, we can also examine the data from the perspective of the mean squared error (MSE). Like in the case of MAE, Figure 3.5 shows a histogram of the MSE values, clearly showing a difference in the variability of MSE for contaminated and uncontaminated data. In the following Figure 3.6, a comparison of each method based on the distribution of MSE can be seen. Based on the boxplots in Figures 3.7, we observe a difference within the levels of factor D, but for the other factors, we do not observe such significant differences. However, based on visualizations, we cannot declare the differences to be statistically significant, so in the next section, we will move on to the analysis of the  $2^k$  factorial design through linear regression.

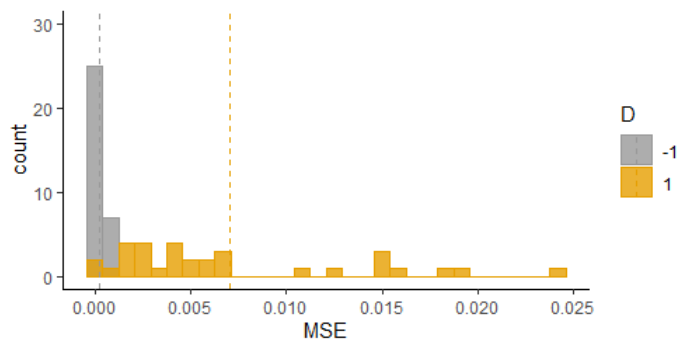


Figure 3.5: Histogram of mean squared error based on level of contamination.

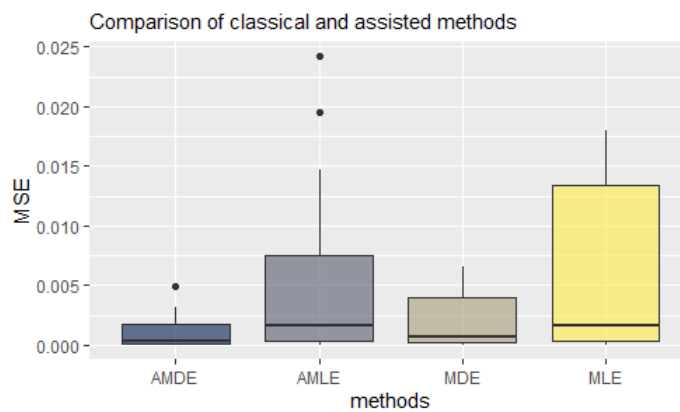


Figure 3.6: Boxplot comparing MSE for each estimation method.

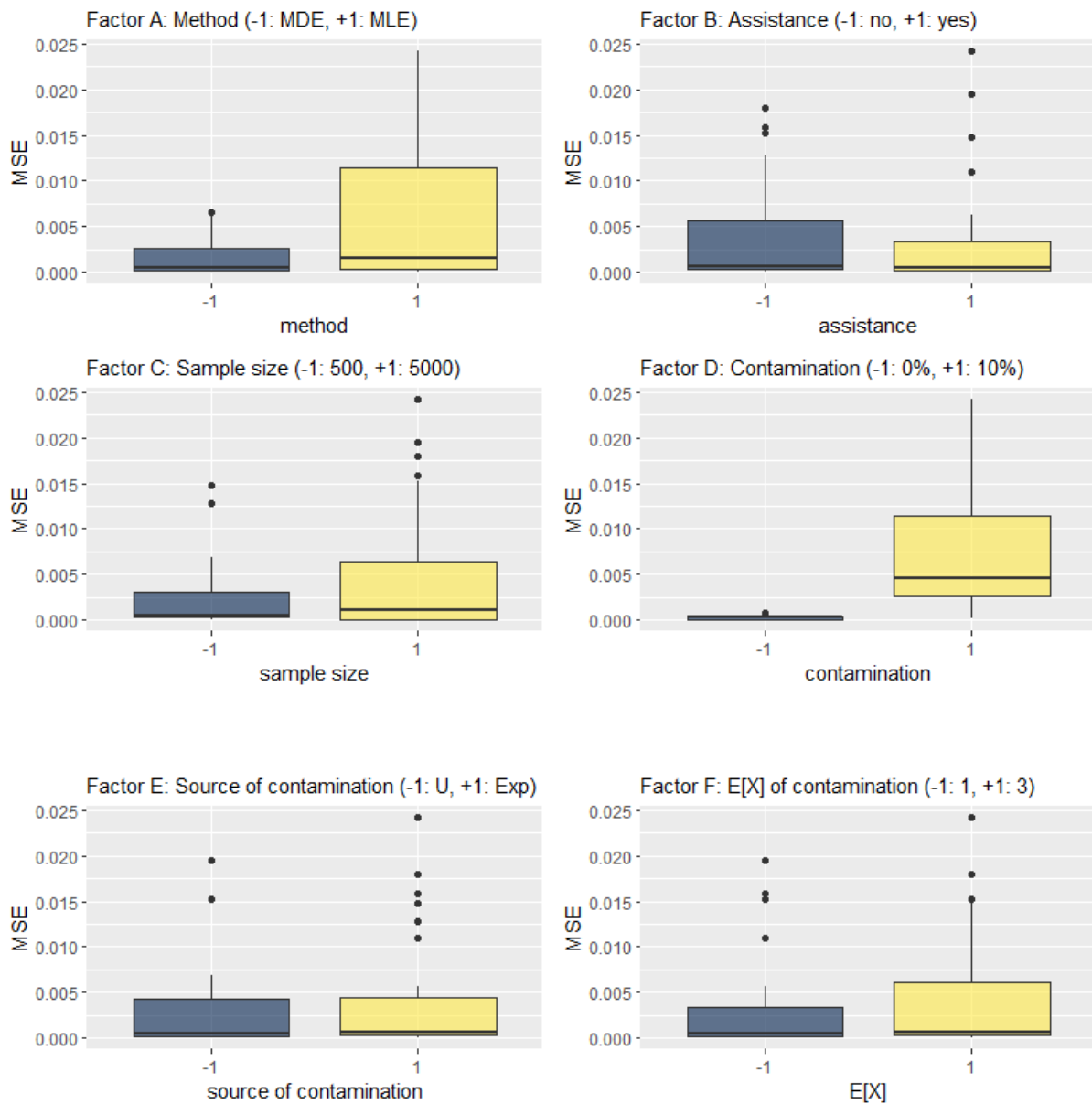


Figure 3.7: Boxplots of mean squared error for each factor.

### 3.2.2.2 Influence of the factors on Maximum Absolute Error (MAE)

The reason why we choose a  $2^k$  factorial design for the experiment is its undemanding interpretation. A prerequisite for using a  $2^k$  factorial design is linearity within the effects. In case there is curvature present in the data, it is appropriate for data interpretation to choose more complex models that capture it. However, our aim in this chapter is not to construct a model for describing the error of estimation methods. It only serves as a tool for revealing the significance of individual factors, especially the proposed assistance of estimation methods. For this purpose, we formulated two linear regression models.

Linear regression is a statistical method used to model the relationship between explanatory variables (in our case factors A, B, C, D, E, and F) and a single target variable (MAE or MSE), assuming that this relationship is linear. The aim of linear regression is to find the best linear function describing this relationship. Such a model can be written in the form

$$Y = w_0 + w_1x_1 + w_2x_2 + \cdots + w_mx_m + \varepsilon,$$

where

$Y$  is the explained (target) variable,

$x_1, \dots, x_m$  are  $m$  independent explanatory variables,

$w_0$  is the intercept and  $\vec{w} = (w_1, \dots, w_m)$  is the vector of sought coefficients,

$\varepsilon$  is random noise, which represents the unexplained variation in the explained variable that cannot be explained by the independent explanatory variables.

Let's start with the model for the maximum absolute error MAE. In the first step, we constructed a model in which all factors and double interactions between them were considered as explanatory variables. Other interactions were not included in this basic model, as if we named all combinations of factors, the number of degrees of freedom would be zero, and the model would become the data itself, which is undesirable. Even in this basic model, which is described in Table 3.4, we observe a statistically significant influence of factors A, C, and D in terms of  $p$ -value (column  $\text{Pr}(>|t|)$ ) at a significance level of  $\alpha = 0.05$ . Recall that a  $p$ -value is a measure of the strength of evidence against the null hypothesis, and its value is compared to the so-called significance level  $\alpha$ . Therefore, for example, if we choose a significance level of  $\alpha = 0.1$ , then we reject the null hypothesis for  $p\text{-value} < 0.1$ , in other words, there is strong evidence against the null hypothesis in the data. For this reason, it is a general motivation in the model to consider variables with low  $p$ -values. Within this general model, we can also plot the Main Effects plot (Figure 3.8), which clearly illustrates the influence of individual levels of factors on the maximum absolute error.

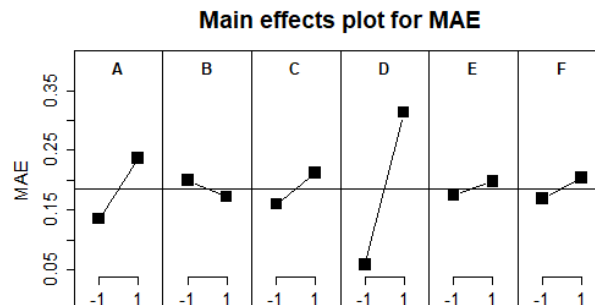


Figure 3.8: Main effects plot visualizes the effect of a factor on the target variable MAE.

	Estimate	Std. Error	t value	Pr(> t )
(Intercept)	0.1859	0.0082	22.75	0.0000
A1	0.0505	0.0082	6.18	0.0000
B1	-0.0137	0.0082	-1.67	0.1021
C1	0.0263	0.0082	3.22	0.0025
D1	0.1271	0.0082	15.56	0.0000
E1	0.0121	0.0082	1.48	0.1467
F1	0.0174	0.0082	2.13	0.0390
A1:B1	0.0050	0.0082	0.61	0.5449
A1:C1	0.0061	0.0082	0.75	0.4592
A1:D1	0.0531	0.0082	6.50	0.0000
A1:E1	0.0025	0.0082	0.30	0.7637
A1:F1	-0.0038	0.0082	-0.47	0.6415
B1:C1	-0.0049	0.0082	-0.59	0.5557
B1:D1	-0.0084	0.0082	-1.02	0.3116
B1:E1	-0.0067	0.0082	-0.81	0.4199
B1:F1	-0.0080	0.0082	-0.98	0.3311
C1:D1	0.0376	0.0082	4.60	0.0000
C1:E1	-0.0033	0.0082	-0.40	0.6925
C1:F1	-0.0059	0.0082	-0.72	0.4728
D1:E1	0.0090	0.0082	1.10	0.2782
D1:F1	0.0120	0.0082	1.47	0.1492
E1:F1	-0.0014	0.0082	-0.17	0.8638
$R^2 =$	0.8985			
$R^2_{adj} =$	0.8478			

Table 3.4: Linear Regression model:  $\text{lm}(\text{MAE} \sim (\text{A} + \text{B} + \text{C} + \text{D} + \text{E} + \text{F})^2)$ 

From the basic overview in Table 3.4, it is clear that most of the interactions and probably some of the factors are not essential for the model. Therefore, we further conduct the so-called step-wise regression, considering only significant variables (Table 3.5). Notice that in this new model, the  $R^2$  value has decreased, which is a statistic representing the proportion of the total variation in the dependent variable that is explained by the regression model. However,  $R^2$  values can be misleading when a model has multiple variables and little amount of data, so we also monitor  $R^2_{adj}$ , which is a modified version of the  $R^2$  statistic that takes into account the number of independent variables in a linear regression model. Thus, by removing insignificant variables, we have slightly reduced the quality of the model in terms of  $R^2$ , but improved its performance in terms of  $R^2_{adj}$ , and by keeping only a few selected factors, we have simplified the interpretation of the results. At the same time, if we compare these two models using the ANOVA test (Table 3.6), the resulting  $p$ -value=0.7106 indicates that there is no significant difference between the models, so removing the variables has not affected the quality of the model. It should be noted that the ANOVA test for two linear models uses the F-test, which compares the differences between the quadratic deviations of two models and determines whether these differences are statistically significant. We have thus obtained a model<sup>3</sup> (rounded) as follows

$$\text{MAE} = 0.186 + 0.051A - 0.014B + 0.026C + 0.127D + 0.017F + 0.053AD + 0.038CD,$$

<sup>3</sup>Note that the signs + or - of individual coefficients in the model represent whether the factor contributes to an increase or decrease in the maximum absolute error.

which shows the significant influence (at the significance level  $\alpha = 0.05$ ) of factors A, C, D, and F, and the interactions of factors A:D and C:D. These findings confirm our assumptions, and based on this model, we can confirm that the maximum absolute error value is related to the chosen estimation method, sample size, contamination level, and mean value of contamination data. If we were more benevolent, we could also declare factor B (assistance) as a significant factor at a significance level of  $\alpha = 0.1$ .

	Estimate	Std. Error	t value	Pr(> t )
(Intercept)	0.1859	0.0079	23.49	0.0000
A1	0.0505	0.0079	6.38	0.0000
B1	-0.0137	0.0079	-1.73	0.0900
C1	0.0263	0.0079	3.32	0.0016
D1	0.1271	0.0079	16.06	0.0000
F1	0.0174	0.0079	2.20	0.0320
A1:D1	0.0531	0.0079	6.71	0.0000
C1:D1	0.0376	0.0079	4.75	0.0000
$R^2 =$	0.8731			
$R^2_{adj} =$	0.8572			

Table 3.5: Linear Regression model:  $\text{lm}(\text{MAE} \sim \text{A} + \text{B} + \text{C} + \text{D} + \text{F} + \text{A} : \text{D} + \text{C} : \text{D})$

	ResDf	RSS	Df	SumOfSq	F	Pr(>F)
$\text{MAE} \sim (\text{A} + \text{B} + \text{C} + \text{D} + \text{E} + \text{F})^2$	42	0.18				
$\text{MAE} \sim \text{A} + \text{B} + \text{C} + \text{D} + \text{F} + \text{A} : \text{D} + \text{C} : \text{D}$	56	0.22	-14	-0.05	0.75	0.7106

Table 3.6: Comparison of two developed models for MAE using ANOVA test.

### 3.2.2.3 Influence of the factors on Mean squared Error (MSE)

Similar to constructing models for MAE, we also build a model for mean squared error. We start with a model containing all factors including double interactions as shown in Table 3.7 and in Figure 3.9 present related Main Effects plot.

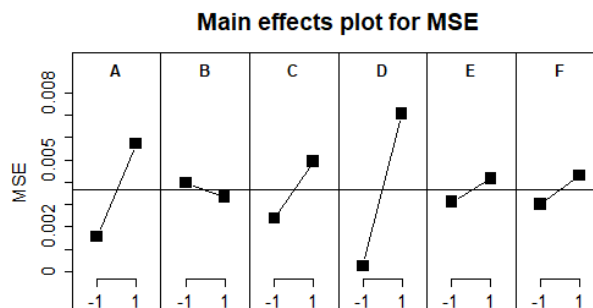


Figure 3.9: Main effects plot visualizes the effect of a factor on the target variable MSE.

	Estimate	Std. Error	t value	Pr(> t )
(Intercept)	0.0036	0.0004	10.26	0.0000
A1	0.0021	0.0004	5.84	0.0000
B1	-0.0003	0.0004	-0.89	0.3785
C1	0.0013	0.0004	3.58	0.0009
D1	0.0034	0.0004	9.58	0.0000
E1	0.0005	0.0004	1.45	0.1534
F1	0.0006	0.0004	1.82	0.0759
A1:B1	0.0001	0.0004	0.39	0.7005
A1:C1	0.0009	0.0004	2.45	0.0186
A1:D1	0.0021	0.0004	5.84	0.0000
A1:E1	0.0004	0.0004	1.25	0.2174
A1:F1	0.0002	0.0004	0.46	0.6507
B1:C1	-0.0000	0.0004	-0.04	0.9702
B1:D1	-0.0003	0.0004	-0.83	0.4113
B1:E1	0.0001	0.0004	0.17	0.8681
B1:F1	-0.0002	0.0004	-0.42	0.6744
C1:D1	0.0013	0.0004	3.79	0.0005
C1:E1	-0.0001	0.0004	-0.18	0.8551
C1:F1	-0.0003	0.0004	-0.73	0.4675
D1:E1	0.0005	0.0004	1.38	0.1734
D1:F1	0.0006	0.0004	1.72	0.0922
E1:F1	0.0004	0.0004	1.17	0.2487
$R^2 =$	0.8327			
$R^2_{adj} =$	0.7490			

Table 3.7: Linear Regression model:  $\text{lm}(\text{MSE} \sim (\text{A} + \text{B} + \text{C} + \text{D} + \text{E} + \text{F})^2)$

Based on the model in Table 3.7, we observe that factors A, C, and D have a significant impact. Using step-wise regression, we can eliminate insignificant variables and arrive at a simplified model in Table 3.8. By removing insignificant variables, we have slightly decreased the  $R^2$  statistic in favor of  $R^2_{adj}$ . The most significant factors in the model at a significance level of  $\alpha = 0.05$  are A, C, D, and the interactions A:C, A:D, and C:D. With a more benevolent approach, we can also consider factor F and the interaction D:F as significant. Note that the factor of assistance is not essential for the model describing MSE. We will use the ANOVA test (Table 3.9) to verify whether we significantly influenced the model quality by removing variables. However, with a  $p$ -value of 0.7169, we can conclude that there is no significant difference between the models, and we can consider the final model for MSE as

$$MSE = 0.004 + 0.002A + 0.001C + 0.003D + 0.001F + 0.001AC + 0.002AD + 0.001CD + 0.001DF.$$



	Estimate	Std. Error	t value	Pr(> t )
(Intercept)	0.0036	0.0003	10.60	0.0000
A1	0.0021	0.0003	6.03	0.0000
C1	0.0013	0.0003	3.69	0.0005
D1	0.0034	0.0003	9.90	0.0000
F1	0.0006	0.0003	1.88	0.0655
A1:C1	0.0009	0.0003	2.53	0.0143
A1:D1	0.0021	0.0003	6.03	0.0000
C1:D1	0.0013	0.0003	3.91	0.0003
D1:F1	0.0006	0.0003	1.78	0.0807
$R^2 =$	0.7945			
$R^2_{adj} =$	0.7646			

Table 3.8: *Linear Regression model:  $\ln(\text{MSE} \sim A + C + D + F + A : C + A : D + C : D + D : F)$*

	ResDf	RSS	Df	SumOfSq	F	Pr(>F)
$\text{MSE} \sim (A + B + C + D + E + F)^2$	42	0.00				
$\text{MSE} \sim A + C + D + F + A : C + A : D + C : D + D : F$	55	0.00	-13	-0.00	0.74	0.7169

Table 3.9: *Comparison of two developed models for MSE using ANOVA test.*

### 3.2.2.4 Verification of Linearity Assumption

Throughout the entire procedure, linearity in the effect of factors was assumed. At this point, it is important to mention that the failure to meet the linearity assumption does not invalidate the conclusions drawn, but calls for caution in interpreting the resulting models. Any possible presence of curvature can be detected, for example, by comparing the average value of the target variables without center-points and then the average value of the target variables measured at the center-points. If the reader looks at Table 3.10, there is a small difference in the average values for both MAE and MSE, but we are unable to determine whether this difference is significant. To do this, we can once again build linear regression models. In the general linear model for maximum absolute error in Table 3.11, or mean squared error in Table 3.12, we observe that the curvature represented by the variable `iscube(data)` is not significant. Therefore, we can declare curvature is not present and the assumption of linearity in the effects is satisfied.

	experiment data	center points
average MAE	0.1859	0.2027
average MSE	0.0036	0.0030

Table 3.10: *Average values of target variables in experiment data and center points.*

	Estimate	Std. Error	t value	Pr(> t )
(Intercept)	0.2027	0.0155	13.08	0.0000
A	0.0524	0.0069	7.56	0.0000
B	-0.0191	0.0069	-2.76	0.0078
C	0.0263	0.0077	3.39	0.0013
D	0.1271	0.0077	16.40	0.0000
E	0.0117	0.0069	1.68	0.0978
F	0.0151	0.0069	2.17	0.0339
iscube(data)TRUE	-0.0169	0.0173	-0.97	0.3349
A:B	0.0009	0.0069	0.13	0.9000
A:C	0.0061	0.0077	0.79	0.4342
A:D	0.0531	0.0077	6.85	0.0000
A:E	0.0049	0.0069	0.71	0.4788
A:F	-0.0075	0.0069	-1.09	0.2809
B:C	-0.0049	0.0077	-0.63	0.5337
B:D	-0.0084	0.0077	-1.08	0.2848
B:E	-0.0087	0.0069	-1.26	0.2145
B:F	-0.0080	0.0069	-1.16	0.2508
C:D	0.0376	0.0077	4.85	0.0000
C:E	-0.0033	0.0077	-0.42	0.6762
C:F	-0.0059	0.0077	-0.76	0.4482
D:E	0.0090	0.0077	1.16	0.2517
D:F	0.0120	0.0077	1.55	0.1269
E:F	-0.0038	0.0069	-0.55	0.5858

Table 3.11: *Linear regression*  $\text{lm}(\text{MAE} \sim (\text{A} + \text{B} + \text{C} + \text{D} + \text{E} + \text{F})^2 + \text{iscube}(\text{data}))$

	Estimate	Std. Error	t value	Pr(> t )
(Intercept)	0.0030	0.0007	4.53	0.0000
A	0.0020	0.0003	6.77	0.0000
B	-0.0005	0.0003	-1.68	0.0987
C	0.0013	0.0003	3.85	0.0003
D	0.0034	0.0003	10.32	0.0000
E	0.0005	0.0003	1.73	0.0894
F	0.0005	0.0003	1.73	0.0889
iscube(data)TRUE	0.0007	0.0007	0.89	0.3757
A:B	-0.0000	0.0003	-0.14	0.8888
A:C	0.0009	0.0003	2.64	0.0108
A:D	0.0021	0.0003	6.28	0.0000
A:E	0.0005	0.0003	1.59	0.1177
A:F	0.0000	0.0003	0.12	0.9052
B:C	-0.0000	0.0003	-0.04	0.9679
B:D	-0.0003	0.0003	-0.89	0.3753
B:E	-0.0001	0.0003	-0.21	0.8378
B:F	-0.0002	0.0003	-0.53	0.5996
C:D	0.0013	0.0003	4.08	0.0001
C:E	-0.0001	0.0003	-0.20	0.8438
C:F	-0.0003	0.0003	-0.79	0.4331
D:E	0.0005	0.0003	1.49	0.1414
D:F	0.0006	0.0003	1.86	0.0687
E:F	0.0003	0.0003	0.96	0.3430

Table 3.12: *Linear regression*  $\text{lm}(\text{MSE} \sim (\text{A} + \text{B} + \text{C} + \text{D} + \text{E} + \text{F})^2 + \text{iscube}(\text{data}))$

### 3.2.3 Summary of estimation methods testing

The aim of this chapter was to experimentally verify whether straightforwardly applied relationships found in Chapter 2 and specified in the Section 3.1.4 could improve existing methods for point estimates of parameters. To conduct the experiment, a  $2^k$  factorial design was chosen. The general advantage of this experimental design is the saving of time and resources, as it allows for valid statistical comparisons with a relatively low number of measurements, which, however, must be performed independently of each other and with a pre-defined setting. The only assumption for the use of this design is linearity within the effects of individual factors. In this work, the experiment took the form of a  $2^6$  factorial design, including 64 measurements, and an additional 16 measurements at the center points, which serve to verify the linearity assumption. The selected factors were the type of estimation method (MDE/MLE), assistance (yes/no), size of generated data (500/5,000), level of contamination (0%/10%), source of contaminated data (uniform/exponential distribution), and mean of contaminated data (same/different).

Before evaluating the experiment itself, we conducted a descriptive analysis of the measured data. We compared the distributions of estimated parameters (Table 3.3), from which we can state that the estimates were shifted from the original configuration. A positive fact was that all methods at least allowed for the negativity of the parameter  $\alpha$ , the assisted minimum distance estimator was even closest to the actual value of the parameter  $\alpha$  in the minimum. Furthermore, we monitored the histograms and boxplots of the maximum absolute error and mean squared error, respectively, from which we obtained preliminary information about what dependencies we could expect within the experiment.

To evaluate the experiment, we advantageously used linear regression, from which it is easy to determine the statistical significance of the effects of individual factors. We constructed two models, the first for the maximum absolute error (Table 3.5), and the second for the mean squared error (Table 3.8). Both models show that the maximum absolute and mean squared errors are significantly influenced (at the significance level of  $\alpha = 0.05$ ) by factors A (used method), C (data size), D (level of data contamination), and F (mean of contaminated data). Thus, it was statistically shown that the minimum distance estimator is more suitable than the maximum likelihood estimator, and that contamination together with the mean of contaminated data has a negative impact on the maximum absolute or mean squared error. Surprisingly, the results of both models (for MAE and MSE) also suggested that estimation methods performed better on a smaller data sample. The explanation for this unexpected behavior may be the setting of the maximum number of iterations in the internal parameter of the functions, which could lead to premature termination of the process with a large amount of data. However, we do not consider the use of this limitation inappropriate, as it is in our interest that the calculation finishes in a relatively reasonable time, but it is appropriate to mention this limitation in the context of this result.

As for the assistance factor, the conclusion of the experiment is negative. Assistance did not prove itself as significant, only in the model for the maximum absolute error can it be stated that, when choosing a more benevolent significance level of  $\alpha = 0.1$ , assistance contributed to reducing MAE.

# Conclusion

We have come to the conclusion of this thesis. Let us review in the following paragraphs the main contributions of each chapter and provide a brief discussion on the possibilities for future research.

In the first chapter, the reader was introduced to the theoretical background of mathematical traffic modeling. Necessary concepts such as the class of balanced densities  $\mathcal{B}$ , headways  $\mathcal{R}$ , multi-headways  $\mathcal{X}$ , interval frequencies  $\mathcal{N}_L$ , and the balanced particle system (Definition 1.2) were introduced. One of the characteristics of the particle system is its stochastic rigidity  $\Delta(L)$ , closely related to the concept of stochastic compressibility  $\chi$ , which is obtained using the variance of headways in the balanced particle system. Based on stochastic compressibility, Definition 1.3 introduced the classification of particle systems into sub-compressible, uni-compressible, and super-compressible.

The second part of the first chapter introduced the model of thermodynamic traffic gas. To describe the expected behavior of particles (drivers), the force interaction was applied to this model. In this thesis, we expected the particles (drivers) to exhibit behavior that prevents collisions and overtaking, causes the disappearance of mutual influence between particles with increasing distance, and ensures smooth traffic flow. As for the range of interactions between particles, we only consider a short-ranged system in which only neighboring particles interact with each other, i.e., a driver reacts to the behavior of the driver in front of and behind him/her. We focused on deriving the probability distribution of the gaps between particles (drivers), which are called clearances. We led the reader through a complete derivation process, at the end of which we showed that the clearance distribution is described by the density (1.14).

The highlight of the first chapter is the connection between the theory of balanced particle systems and thermodynamic traffic gas, where we can use the found clearance density as a generator of the balanced particle system and formulate the Definition 1.4 of the balanced particle system with a repulsive generator, or the Definition 1.5 of the balanced particle system with a composite generator.

By choosing the potential  $\psi(x) = \frac{1}{x}$  in the density (1.16), which was used to define the balance particle system with a repulsive or composite generator, we obtained the so-called Generalized Inverse Gaussian distribution. In the second chapter, we have shown the basic properties that this distribution satisfies. We have verified its membership in the class of balanced densities and derived key relationships between the parameters (2.11) and (2.12). The main part of this chapter is further devoted to a thorough solution of the scaling problem.

The existence of the first general moment of the GIG distribution implies the solvability of the scaling equation in the form of (2.13). In the first step, we assumed that the scaling parameter is the parameter  $\lambda$ . Using the theory of implicit functions, we were able to show that this parameter can be considered as a solution to the scaling equation only if the scaling condition (2.15) is satisfied. During the investigation

of the properties of the scaling function in terms of the parameter  $\lambda$ , we observed its strong correlation with the parameter  $\beta$ . Based on this correlation, in the second step, we attempted to solve the scaling equation from the perspective of the parameter  $\beta$ . In this part, we discovered that scaling through the parameter  $\beta$  leads to another scaling condition (2.23). Furthermore, based on the observed analogy in scaling problems between the parameters  $\beta$  and  $\lambda$ , we formulated and proved the Theorem (2.1) on the symmetry of solutions of the scaling equation of the GIG distribution. This parallel approach to scaling the GIG distribution and the formulated theorem are significant advances in the research of the properties of the GIG distribution and are the most important contributions of this thesis. A detailed summary of the scaling results was provided in Section 2.4.3.

The last chapter of this thesis had an experimental character. Based on the discovered relationships between the parameters of the Generalized Inverse Gaussian distribution and the definition of stochastic compressibility, we proposed a stabilization procedure, called assistance, which aimed to reduce the error of selected estimation methods. The method of moments, the minimum distance estimator, and the maximum likelihood estimator were introduced to the reader. Based on the essence of the assistance, we implemented the proposed improvement for the minimum distance estimator and the maximum likelihood estimator. We named the improved methods as the assisted minimum distance estimator and the assisted maximum likelihood estimator.

In the experiment, we examined the effect of assistance, contamination, and sample size on the maximum absolute error and mean squared error. A  $2^6$  factorial design was chosen as the experimental design, for which were performed 80 measurements in total. First, a descriptive analysis of the measured data was performed, followed by a statistical evaluation of the experiment using linear regression, where the chosen method, assistance, sample size, contamination level, contamination source, and expected value of the contamination data were considered as explanatory variables and maximum absolute error, resp. mean squared error, as the target variable. The results of the experiment showed that the minimum distance estimator is more suitable than the maximum likelihood estimator, and that contamination together with the expected value of contaminated data has a negative impact on the maximum absolute or mean squared error. Surprisingly, the results also suggested that estimation methods performed better on a smaller data sample. The explanation for this unexpected behavior may be the setting of the maximum number of iterations in the internal parameter of the functions.

Finally, let us briefly consider the possibilities for further research. This work presented a new approach to scaling GIG distribution through the parameter  $\beta$ . Based on the theorem (2.1), further research could focus on studying the properties of GIG distributions that are connected to each other by the symmetric solution to the scaling equation. At the same time, the scaling areas found in this thesis offer space for improvement of the approximation of the scaling function  $\lambda(\beta)$ , resp.  $\beta(\lambda)$ .

# Appendix

## Chapter 1

### Calculation of stochastic rigidity for a scaled Poisson particle system

Recall that a (scaled) Poisson system is described by the probability  $P[\mathcal{N}_L = k] = \frac{L^k}{k!} e^{-L}$ . The stochastic rigidity can be calculated directly from the definition

$$\Delta_P(L) = E[\mathcal{N}_L - L]^2 = E[\mathcal{N}_L^2] - 2LE[\mathcal{N}_L] + L^2 = \underbrace{\sum_{k=1}^{+\infty} k^2 P[\mathcal{N}_L = k]}_{S_1} - 2L \underbrace{\sum_{k=1}^{+\infty} k P[\mathcal{N}_L = k]}_{S_2} + L^2. \quad (3.4)$$

To calculate the value of  $\Delta_P(L)$ , we need to evaluate the sums  $S_1$  and  $S_2$ . Let us start with the value of sum  $S_2$

$$S_2 = \sum_{k=1}^{+\infty} k P[\mathcal{N}_L = k] = \sum_{k=1}^{+\infty} k \frac{L^k}{k!} e^{-L} = L e^{-L} \sum_{k=1}^{+\infty} \frac{L^{k-1}}{(k-1)!} = L e^{-L} \sum_{k=0}^{+\infty} \frac{L^k}{k!} = \left| \sum_{k=0}^{+\infty} \frac{x^k}{k!} = e^x \right| = L. \quad (3.5)$$

To calculate the sum  $S_1$ , we can use similar reasoning

$$\begin{aligned} S_1 &= \sum_{k=1}^{+\infty} k^2 P[\mathcal{N}_L = k] = \sum_{k=1}^{+\infty} k^2 \frac{L^k}{k!} e^{-L} = L e^{-L} \sum_{k=1}^{+\infty} k \frac{L^{k-1}}{(k-1)!} = L e^{-L} \sum_{k=0}^{+\infty} (k+1) \frac{L^k}{k!} = \\ &= L \sum_{k=0}^{+\infty} k \frac{L^k}{k!} e^{-L} + L e^{-L} \sum_{k=0}^{+\infty} \frac{L^k}{k!} = L \sum_{k=1}^{+\infty} k P[\mathcal{N}_L = k] + L \stackrel{(3.5)}{=} L^2 + L. \end{aligned} \quad (3.6)$$

Thus, if we substitute the obtained results (3.5) and (3.6) into the calculation (3.4), we obtain the value of the stochastic rigidity of the scaled Poisson particle system

$$\Delta_P(L) = L^2 + L - 2L^2 + L^2 = L. \quad (3.7)$$

### Approximation of partial sum of clearance distribution for a system with general short-range potential

Let  $g(r) = \Theta(r) \frac{Z_{N-1}(L-r)}{Z_N(L)} e^{-\beta r \varphi(r)}$  be a density for the distribution of clearances  $\mathcal{R}_1, \mathcal{R}_2, \dots, \mathcal{R}_N \sim g(r)$ , where  $Z_N(L)$  denotes the partition sum of the system and  $\varphi(r)$  is any short-range potential. We will continue with the calculation that was stopped in the previous text at equation (1.10). If we denote  $f(r) = \Theta(r) e^{-\beta r \varphi(r)}$ , then the partial sum has the form

$$Z_N(L) = \int_{\mathbb{R}^N} \delta\left(L - \sum_{k=1}^N r_k\right) \prod_{k=1}^N f(r_k) d\vec{r}. \quad (3.8)$$

Let's apply Laplace transform to this equation and perform a series of adjustments

$$\begin{aligned}
\mathcal{L}[Z_N(L)](s) &= \int_{\mathbb{R}} Z_N(L) e^{-sL} dL \stackrel{(3.8)}{=} \int_{\mathbb{R}} \int_{\mathbb{R}^N} \delta\left(L - \sum_{k=1}^N r_k\right) \prod_{k=1}^N f(r_k) e^{-sL} d\vec{r} dL = \\
&= \int_{\mathbb{R}^N} \prod_{k=1}^N f(r_k) \underbrace{\int_{\mathbb{R}} \delta\left(L - \sum_{k=1}^N r_k\right) e^{-sL} dL}_{\mathcal{L}\left[\delta\left(L - \sum_{k=1}^N r_k\right)\right](s) = e^{-s \sum_{k=1}^N r_k}} d\vec{r} = \\
&= \left( \int_{\mathbb{R}} f(r) e^{-sr} dr \right)^N = (\mathcal{L}[f(r)](s))^N.
\end{aligned}$$

Let  $\mathcal{L}[f(r)](s) := F(s)$ . From the procedure, it follows that there is a relation between the Laplace transform of the partial sum  $Z_N(L)$  and the Laplace transform of the kernel  $f(r)$  given by

$$\mathcal{L}[Z_N(L)](s) = F^N(s). \quad (3.9)$$

Now, if we apply the inverse Laplace transform, we obtain the value of  $Z_N(L)$  as

$$Z_N(L) = \mathcal{L}^{-1}[F^N(s)](L) = \frac{1}{2\pi i} \int_{a-i\infty}^{a+i\infty} F^N(s) e^{sL} ds, \quad (3.10)$$

where the specific value of  $a \in \mathbb{R}$  does not matter. We plan to use the method of steepest descent, and for that purpose, we need to find the extreme point of the integrand  $F^N(s) e^{sL}$ . We take the derivation of the integrand

$$\frac{d}{ds} (F^N(s) e^{sL}) = N F^{N-1}(s) \frac{dF}{ds} e^{sL} + L e^{sL} F^N(s) \stackrel{!}{=} 0, \quad (3.11)$$

from which we obtain an equation for the stationary point  $\lambda$

$$\frac{1}{F(\lambda)} \frac{dF}{ds}(\lambda) = -\frac{L}{N}. \quad (3.12)$$

Thus, the position of the stationary point  $\lambda$  changes with the shape of the potential  $\varphi(r)$  through  $F(\lambda)$ , the length of the circle, and the number of particles on it. We can simplify this situation by choosing  $L = N$ , so equation (3.12) becomes

$$\frac{1}{F(\lambda)} \frac{dF}{ds}(\lambda) = -1. \quad (3.13)$$

To apply the method of steepest descent, we need to evaluate the value of

$$\frac{d^2 H(s)}{ds^2} = \frac{N}{F^2(s)} \left( F(s) \frac{d^2 F(s)}{ds^2} - \left( \frac{dF(s)}{ds} \right)^2 \right) \quad (3.14)$$

where  $H(s) = \ln F^N(s) = N \ln F(s)$ . Then, we can obtain an approximation

$$Z_N(L) \stackrel{(3.10)}{=} \frac{1}{2\pi i} \int_{a-i\infty}^{a+i\infty} F^N(s) e^{sL} ds \doteq \frac{F^N(\lambda) e^{\lambda L}}{\sqrt{2\pi \left| \frac{d^2 H(\lambda)}{ds^2} \right|}} = \frac{F^N(\lambda) e^{\lambda L}}{\sqrt{N}} \underbrace{\left| \frac{F^2(\lambda)}{F(\lambda) \frac{d^2 F(\lambda)}{ds^2} - \left( \frac{dF(\lambda)}{ds} \right)^2} \right|^{\frac{1}{2}}}_C = C \frac{F^N(\lambda) e^{\lambda L}}{\sqrt{N}}, \quad (3.15)$$

where the constant C includes all fixed values independent of  $L$  and  $N$ .



### The alternative equation for stationary point

Currently, we are focused on explaining the term  $F(\lambda)$  in the equation (1.13), where  $\lambda$  is the stationary point from equation (3.13). Because  $f(r) = \Theta(r)e^{-\beta_T\varphi(r)}$ , then

$$F(s) = \mathcal{L}[f(r)](s) = \int_{\mathbb{R}} \Theta(r)e^{-\beta_T\varphi(r)} e^{-rs} dr.$$

At the same time, based on Laplace transform properties, it holds

$$\frac{dF}{ds} = -\mathcal{L}[rf(r)](s). \quad (3.16)$$

By substitution of (3.16) to equation (3.13), we obtain

$$\mathcal{L}[f(r)](\lambda) = \mathcal{L}[rf(r)](\lambda),$$

i.e.,

$$\int_{\mathbb{R}} \Theta(r)e^{-\beta_T\varphi(r)} e^{-r\lambda} dr = \int_{\mathbb{R}} \Theta(r)re^{-\beta_T\varphi(r)} e^{-r\lambda} dr. \quad (3.17)$$

From this equation, we can observe two interesting facts. The first observation is that the normalization constant and the integral on the left-hand side are clearly related, with

$$A^{-1} = \int_{\mathbb{R}} \Theta(r)e^{-\beta_T\varphi(r)} e^{-r\lambda} dr = F(\lambda),$$

which after substitution to (3.17) results into

$$A \int_{\mathbb{R}} \Theta(r)re^{-\beta_T\varphi(r)} e^{-r\lambda} dr = 1.$$

This leads us to the second realization, which consists of the fact that the equation for the stationary point can also be understood as a scaling equation of distribution  $\Theta(r)e^{-\beta_T\varphi(r)} e^{-\lambda r}$ .

## Chapter 3

### Pseudo-codes of estimation methods

---

**Algorithm 1** Minimum distance estimator MDE.

---

**Input:** scaled GIG-distributed data:  $\mathbf{x}$

**Output:** parameter estimates:  $\hat{\alpha}, \hat{\beta}, \hat{\lambda}$

compute empirical distribution function  $F_n$  from  $\mathbf{x}$

**for**  $i = 1:25$  **do**

    initialize  $\alpha_0, \beta_0, \lambda_0$

    compute  $\alpha[i], \beta[i], \lambda[i]$  from  $\mathbf{x}$  using (3.2)

**if**  $\beta[i] \leq 0$  or  $\lambda[i] \leq 0$  **then**

        |  $\alpha[i], \beta[i], \lambda[i] \leftarrow \text{NaN}, \text{NaN}, \text{NaN}$

**end**

**end**

$\hat{\alpha}, \hat{\beta}, \hat{\lambda} \leftarrow \text{mean}(\alpha), \text{mean}(\beta), \text{mean}(\lambda)$

---

---

**Algorithm 2** Maximum likelihood estimator MLE.

---

**Input:** scaled GIG-distributed data:  $\mathbf{x}$

**Output:** parameter estimates:  $\hat{\alpha}, \hat{\beta}, \hat{\lambda}$

**for**  $i = 1:25$  **do**

    initialize  $\alpha_0, \beta_0, \lambda_0$

    compute  $\alpha[i], \beta[i], \lambda[i]$  from  $\mathbf{x}$  using (3.3)

**if**  $\beta[i] \leq 0$  or  $\lambda[i] \leq 0$  **then**

        |  $\alpha[i], \beta[i], \lambda[i] \leftarrow \text{NaN}, \text{NaN}, \text{NaN}$

**end**

**end**

$\hat{\alpha}, \hat{\beta}, \hat{\lambda} \leftarrow \text{mean}(\alpha), \text{mean}(\beta), \text{mean}(\lambda)$

---

---

**Algorithm 3** Assisted minimum distance estimator AMDE.

---

**Input:** scaled GIG-distributed data:  $\mathbf{x}$

**Output:** parameter estimates:  $\hat{\alpha}, \hat{\beta}, \hat{\lambda}$

compute empirical distribution function  $F_n$  from  $\mathbf{x}$

$a \leftarrow 0$

**for**  $i \leftarrow 1:25$  **do**

**while**  $a = 0$  **do**

        initialize  $\beta_0, \lambda_0$

        compute  $\beta[i], \lambda[i]$  from  $\mathbf{x}$  using (3.2)

$\alpha[i] \leftarrow (\text{var}(\mathbf{x}) + 1)\lambda[i] - \beta[i] - 2$

**if**  $\alpha[i] + \beta[i] - \lambda[i] + 2 > 0$  and  $\alpha[i] + \beta[i] - \lambda[i] + 1 < 0$  and  $\lambda[i] > 0$  and  $\beta[i] > 0$  **then**

            |  $a \leftarrow 1$

**end**

**end**

**end**

$\hat{\alpha}, \hat{\beta}, \hat{\lambda} \leftarrow \text{mean}(\alpha), \text{mean}(\beta), \text{mean}(\lambda)$

---

---

**Algorithm 4** Assisted maximum likelihood estimator AMLE.

---

**Input:** scaled GIG-distributed data:  $\mathbf{x}$ **Output:** parameter estimates:  $\hat{\alpha}, \hat{\beta}, \hat{\lambda}$ 

```
a ← 0
for i ← 1:25 do
  while a = 0 do
    initialize  $\beta_0, \lambda_0$ 
    compute  $\beta[i], \lambda[i]$  from  $\mathbf{x}$  using (3.3)
     $\alpha[i] \leftarrow (\text{var}(\mathbf{x}) + 1)\lambda[i] - \beta[i] - 2$ 
    if  $\alpha[i] + \beta[i] - \lambda[i] + 2 > 0$  and  $\alpha[i] + \beta[i] - \lambda[i] + 1 < 0$  and  $\lambda[i] > 0$  and  $\beta[i] > 0$  then
      a ← 1
    end
  end
end
end
 $\hat{\alpha}, \hat{\beta}, \hat{\lambda} \leftarrow \text{mean}(\alpha), \text{mean}(\beta), \text{mean}(\lambda)$ 
```

---

**Measured data**

#	A	B	C	D	E	F	MAE	MSE	$\hat{\alpha}$	$\hat{\beta}$	$\hat{\lambda}$
1	MDE	no	500	0%	uniform	1	0.0183	0.0000	0.0	3.2	4.7
2	MLE	no	500	0%	uniform	1	0.0744	0.0003	3.6	1.9	6.9
3	MDE	yes	500	0%	uniform	1	0.0721	0.0003	-2.2	4.5	3.9
4	MLE	yes	500	0%	uniform	1	0.0885	0.0005	3.4	2.1	6.8
5	MDE	no	5000	0%	uniform	1	0.0990	0.0005	-0.7	2.9	3.6
6	MLE	no	5000	0%	uniform	1	0.0234	0.0000	-1.6	3.8	3.6
7	MDE	yes	5000	0%	uniform	1	0.0407	0.0001	0.1	3.0	4.5
8	MLE	yes	5000	0%	uniform	1	0.0126	0.0000	-1.6	3.8	3.7
9	MDE	no	500	10%	uniform	1	0.0664	0.0002	0.0	2.8	4.2
10	MLE	no	500	10%	uniform	1	0.2333	0.0028	5.0	0.0	6.1
11	MDE	yes	500	10%	uniform	1	0.0560	0.0002	1.2	2.4	4.9
12	MLE	yes	500	10%	uniform	1	0.3060	0.0041	4.7	0.0	5.9
13	MDE	no	5000	10%	uniform	1	0.1500	0.0013	-0.2	2.4	3.5
14	MLE	no	5000	10%	uniform	1	0.4745	0.0153	2.4	0.0	3.3
15	MDE	yes	5000	10%	uniform	1	0.1593	0.0013	4.1	0.8	5.9
16	MLE	yes	5000	10%	uniform	1	0.6049	0.0195	2.5	0.0	3.9
17	MDE	no	500	0%	exponential	1	0.0272	0.0000	0.1	3.0	4.6
18	MLE	no	500	0%	exponential	1	0.0708	0.0003	3.6	1.7	6.6
19	MDE	yes	500	0%	exponential	1	0.0721	0.0003	-2.2	4.5	3.9
20	MLE	yes	500	0%	exponential	1	0.0885	0.0005	3.4	2.1	6.8
21	MDE	no	5000	0%	exponential	1	0.0762	0.0003	-0.2	2.8	4.0
22	MLE	no	5000	0%	exponential	1	0.0365	0.0001	-1.1	3.5	3.8
23	MDE	yes	5000	0%	exponential	1	0.0407	0.0001	0.1	3.0	4.5
24	MLE	yes	5000	0%	exponential	1	0.0126	0.0000	-1.6	3.8	3.7

Table 3.13: Part 1/3 of measured data.

#	A	B	C	D	E	F	MAE	MSE	$\hat{\alpha}$	$\hat{\beta}$	$\hat{\lambda}$
25	MDE	no	500	10%	exponential	1	0.2791	0.0039	-0.6	2.1	3.0
26	MLE	no	500	10%	exponential	1	0.3266	0.0056	4.2	0.0	5.3
27	MDE	yes	500	10%	exponential	1	0.1829	0.0017	-4.0	4.1	1.8
28	MLE	yes	500	10%	exponential	1	0.2177	0.0027	5.1	0.0	6.2
29	MDE	no	5000	10%	exponential	1	0.2599	0.0041	0.6	1.5	3.4
30	MLE	no	5000	10%	exponential	1	0.5695	0.0159	3.0	0.0	4.5
31	MDE	yes	5000	10%	exponential	1	0.2266	0.0031	-0.7	2.3	2.9
32	MLE	yes	5000	10%	exponential	1	0.4242	0.0110	3.1	0.0	4.2
33	MDE	no	500	0%	uniform	3	0.0297	0.0000	0.2	2.9	4.6
34	MLE	no	500	0%	uniform	3	0.0727	0.0003	3.0	2.2	6.6
35	MDE	yes	500	0%	uniform	3	0.0721	0.0003	-2.2	4.5	3.9
36	MLE	yes	500	0%	uniform	3	0.0885	0.0005	3.4	2.1	6.8
37	MDE	no	5000	0%	uniform	3	0.0683	0.0002	-0.3	3.0	4.0
38	MLE	no	5000	0%	uniform	3	0.0766	0.0003	-0.8	3.2	3.7
39	MDE	yes	5000	0%	uniform	3	0.0407	0.0001	0.1	3.0	4.5
40	MLE	yes	5000	0%	uniform	3	0.0126	0.0000	-1.6	3.8	3.7
41	MDE	no	500	10%	uniform	3	0.3207	0.0061	-0.3	1.7	2.5
42	MLE	no	500	10%	uniform	3	0.3414	0.0069	-4.5	3.5	0.3
43	MDE	yes	500	10%	uniform	3	0.1851	0.0019	-5.5	4.6	0.6
44	MLE	yes	500	10%	uniform	3	0.2825	0.0042	-12.7	10.7	0.0
45	MDE	no	5000	10%	uniform	3	0.3401	0.0066	-1.0	2.0	2.1
46	MLE	no	5000	10%	uniform	3	0.5035	0.0152	2.0	0.2	2.9
47	MDE	yes	5000	10%	uniform	3	0.2941	0.0049	-3.6	3.3	1.0
48	MLE	yes	5000	10%	uniform	3	0.3528	0.0063	-6.6	4.6	0.0
49	MDE	no	500	0%	exponential	3	0.0859	0.0004	-0.3	2.8	3.9
50	MLE	no	500	0%	exponential	3	0.0994	0.0005	3.8	2.0	7.2
51	MDE	yes	500	0%	exponential	3	0.0721	0.0003	-2.2	4.5	3.9
52	MLE	yes	500	0%	exponential	3	0.0885	0.0005	3.4	2.1	6.8
53	MDE	no	5000	0%	exponential	3	0.1259	0.0009	-0.4	2.7	3.6
54	MLE	no	5000	0%	exponential	3	0.0400	0.0001	-1.2	3.5	3.7
55	MDE	yes	5000	0%	exponential	3	0.0406	0.0001	0.0	3.0	4.5
56	MLE	yes	5000	0%	exponential	3	0.0126	0.0000	-1.6	3.8	3.7
57	MDE	no	500	10%	exponential	3	0.2137	0.0026	-0.2	2.2	3.2
58	MLE	no	500	10%	exponential	3	0.4342	0.0129	-3.6	2.6	0.4
59	MDE	yes	500	10%	exponential	3	0.0898	0.0005	-7.5	6.1	0.2
60	MLE	yes	500	10%	exponential	3	0.4499	0.0147	-3.6	2.5	0.3
61	MDE	no	5000	10%	exponential	3	0.3039	0.0053	-0.1	1.8	2.7
62	MLE	no	5000	10%	exponential	3	0.5431	0.0180	-0.2	1.0	1.6
63	MDE	yes	5000	10%	exponential	3	0.2232	0.0028	-5.6	4.5	0.3
64	MLE	yes	5000	10%	exponential	3	0.6001	0.0242	-1.8	1.3	0.6

Table 3.14: Part 2/3 of measured data.

#	A	B	C	D	E	F	MAE	MSE	$\hat{\alpha}$	$\hat{\beta}$	$\hat{\lambda}$
65	MDE	no	2750	5%	uniform	1	0.0999	0.0006	-0.6	2.8	3.6
66	MLE	no	2750	5%	uniform	1	0.3060	0.0060	4.1	0.0	6.1
67	MDE	yes	2750	5%	uniform	1	0.0973	0.0005	0.9	2.2	4.5
68	MLE	yes	2750	5%	uniform	1	0.1912	0.0021	5.5	0.0	6.5
69	MDE	no	2750	5%	exponential	1	0.1689	0.0018	-1.1	2.7	3.0
70	MLE	no	2750	5%	exponential	1	0.3449	0.0079	3.6	0.0	4.6
71	MDE	yes	2750	5%	exponential	1	0.0911	0.0006	-3.3	4.0	2.3
72	MLE	yes	2750	5%	exponential	1	0.2765	0.0048	4.4	0.0	5.3
73	MDE	no	2750	5%	uniform	3	0.2251	0.0028	-1.2	2.5	2.6
74	MLE	no	2750	5%	uniform	3	0.2363	0.0033	-6.1	4.6	0.1
75	MDE	yes	2750	5%	uniform	3	0.1667	0.0016	-4.5	4.2	1.2
76	MLE	yes	2750	5%	uniform	3	0.2189	0.0032	-5.4	4.3	0.6
77	MDE	no	2750	5%	exponential	3	0.1777	0.0018	-1.5	2.9	2.6
78	MLE	no	2750	5%	exponential	3	0.3910	0.0094	0.5	1.1	2.6
79	MDE	yes	2750	5%	exponential	3	0.1128	0.0007	-6.9	5.6	0.4
80	MLE	yes	2750	5%	exponential	3	0.1388	0.0008	-10.0	8.0	0.0

Table 3.15: Part 3/3 of measured data (center-points).

# Bibliography

- [1] Bari C. S., Chandra S., Dhamaniya A., 2022, *Service headway distribution analysis of FASTag lanes under mixed traffic conditions*, Physica A: Statistical Mechanics and its Applications, volume 604, Article 127904, ISSN 0378-4371.
- [2] Devroye L., 2014, *Random variate generation for the generalized inverse Gaussian distribution*, Statistics and Computing, Volume 24, Pages 239–246.
- [3] Georgano G.N., 1985, *Cars: Early and Vintage, 1886–1930*, London: Grange-Universal, ISBN 1-59084-491-2.
- [4] Jörgensen B., 1982, *Statistical Properties of the Generalized Inverse Gaussian Distribution*, Lecture Notes in Statistics 9, Springer, ISBN 978-1-4612-5698-4.
- [5] Krbálek M., Helbing D., 2004, *Determination of interaction potentials in freeway traffic from steady-state statistics*, Physica A: Statistical Mechanics and its Applications, Volume 333, Pages 370-378, ISSN 0378-4371.
- [6] Krbálek M., 2012, *Úlohy matematické fyziky (Problems of mathematical physics)*, Study Notes, CTU, ISBN 978-80-01-05000-2.
- [7] Krbálek M., Šeba F., 2020, *Super-Poissonian Statistics In Traffic Flow*, APLIMAT 2020 - Proceedings, Pages 930-941.
- [8] Krbálek M., Krbálková M., Šeba F., 2022, *Super-random states in vehicular traffic — Detection & explanation*, Physica A: Statistical Mechanics and its Applications, Volume 585, Article 126418, ISSN 0378-4371.
- [9] Krbálek M., Vacková J., 2022, *Matematické modelování dopravy (Mathematical traffic modeling)*, Study Notes, CTU, ISBN 978-80-01-06958-5.
- [10] Lhotáková A., 2020, *Vlastnosti distribuční rodiny GIG s negativní hodnotou parametru (Properties of distribution family GIG with negative value of parameter)*, Bachelor thesis, FNSPE CTU.
- [11] Lhotáková A., 2022, *Testování účinnosti odhadovacích metod pro GIG-distribuovaná data (Testing the efficiency of estimation methods for GIG-distributed data)*, Research project, FNSPE CTU.
- [12] Montgomery D. C., 2012, *Design and analysis of experiments — Eighth edition*, John Wiley & Sons, ISBN 978-1-118-14692-7.
- [13] Nábělek J., 2022, *Superpoissonovské stavy balančního částicového systému (Super-Poisson states of balanced particle system)*, Bachelor thesis, FNSPE CTU.

- [14] Pánek V., 2021, *Statistická kompresibilita v systémech se střednědosahovými potenciály (Statistical compressibility for systems with middle-ranged potentials)*, Research project, FNSPE CTU.
- [15] Pánek V., 2022, *Statistické vlastnosti termodynamického částicového plynu s kombinovaným potenciálem (Statistical properties of thermodynamic particle gas with combined potential)*, Master thesis, FNSPE CTU.
- [16] Setright L. J. K., 2004, *Drive On!: A Social History of the Motor Car*, Granta Books, ISBN 1-86207-698-7.
- [17] Statovic, 2017, *gigrnd(P, a, b, sampleSize)*, MATLAB Central File Exchange, retrieved 16/01/2023, <https://www.mathworks.com/matlabcentral/fileexchange/53594-gigrnd-p-a-b-samplesize>.
- [18] Vacková J., 2016, *Multi-headway statistika systémů s kombinovanými potenciály (Multi-headway statistics of systems with combined potentials)*, Research project, FNSPE CTU.